Trade-offs Between Performance, Data Rate and Transmission Delay in Networked Control Systems

Barforooshan, Mohsen

DOI (link to publication from Publisher):
10.54337/aau300042036

Publication date:
2018

Document Version
Publisher's PDF, also known as Version of record

TRADE-OFFS BETWEEN PERFORMANCE, DATA RATE AND TRANSMISSION DELAY IN NETWORKED CONTROL SYSTEMS

BY
MOHSEN BARFOROOSHAN

DISSERTATION SUBMITTED 2018

AALBORG UNIVERSITY
DENMARK

Trade-offs Between Performance, Data Rate and Transmission Delay in Networked Control Systems

Ph.D. Dissertation

Mohsen Barforooshan

Dissertation submitted August, 2018

Dissertation submitted: August, 2018

PhD supervisor: Prof. Jan Østergaard,
Aalborg University

PhD committee: Professor Rafael Wisniewski (chairman)
Aalborg University

Professor Nuno Martins
University of Maryland

Associate Professor Tobias Oechtering
KTH Royal Institute of Technology

PhD Series: Technical Faculty of IT and Design, Aalborg University

Department: Department of Electronic Systems

ISSN (online): 2446-1628
ISBN (online): 978-87-7210-257-3

Published by:
Aalborg University Press
Langagervej 2
DK – 9220 Aalborg Ø
Phone: +45 99407140
aauf@forlag.aau.dk
forlag.aau.dk

Printed in Denmark by Rosendahls, 2018

This thesis has been typeset using LaTeX 2ε.

Abstract

Nowadyas, digital data networking has taken over hardwire point-to-point communications in several real-world technological applications. This includes automatic control systems which play a key role in our everyday life. However, communication uncertainties caused by phenomena such as time delay, data rate limitation and packet dropout insert new constraints which should be addressed very carefully when analyzing and designing networked control systems (NCSs). Otherwise, those imperfections may have adverse impacts on system performance. In this thesis, we study the interaction between communication constraints and control performance in four control system setups.

In the first setup, we consider an error-free channel with a known fixed delay in the feedback path. We model coding and control on both sides of the channel by causal, but otherwise arbitrary, mappings. The considered plant is linear time-invariant (LTI) with Gaussian disturbances. We characterize the aforementioned trade-off by deriving lower and upper bounds on the minimum average data rate needed to attain a prescribed level of performance. To this end, we employ a method based on the information-theoretic aspects of causal feedback loops. We show that when the performance level is fixed, increasing channel delay renders the obtained lower and upper bounds greater. Therefore, meeting a specific control performance criterion in an NCS with a channel with higher delay necessitates spending higher average data rates.

In the second setup, the system is comprised of elements with the same properties as the system considered in the first case except for the fact that the channel transmission delay is randomly distributed. In this case, we use arguments which are much simpler than the ones in the previous setup with constant channel delay. We derive a lower bound on the infimum average data rate required to guarantee that the average of steady-state variance of a specific system output over all realizations of the channel delay is less than a predetermined level. We try the aforementioned simple reasoning on the special case of known constant channel delay and observe that it leads to the same comprehensive and computable upper and lower bounds as derived in our first study on the desired minimum average data rate.

In our third study, we analyze the interplay between data rate, performance

and network-induced delay from a different point of view in that the ℓ^0 norm of the control input indicates the size of the data transmitted over the channel. We consider a disturbance-free LTI plant which is fully observable. The communication channel between the controller and the actuator is subject to data packet dropouts and constant time delays. We compensate for such effects by considering a packetized predictive controller which generates a sequence of control packets and forward them to a buffer installed at the plant. In this setup, we expect the controller to produce sparse control inputs while guaranteeing closed-loop stability. In one scenario, the controller minimizes the ℓ^0 norm of control packets at each time instant with respect to an ℓ^2 constraint. In the other scenario, the corresponding optimization problem is an sparsity-promoting unconstrained $\ell^1 - \ell^2$ problem. We establish the stability conditions for both cases in the presence of channel delay. We show that when the channel delay increases, the stability is achieved but with degraded performance and larger packet sizes.

Our fourth study revolves around the trade-offs between performance and sparsity of control inputs in uncertain linear systems. In particular, the problem is designing a finite sequence of control inputs with minimum ℓ^1 norm in such a way that a finite-horizon linear-quadratic regulator (LQR) cost keeps bounded from above by a certain value. We show that such problem can be relaxed to a second-order cone programmings for certain plants, plants with discrete uncertainties and plants with polytopic uncertainties. We show by simulation that performances close to optimal standard LQR cost can be achieved by sparse control inputs.

Resumé

I dag har digitale datanetværk erstattet analoge og kablet punkt-til-punkt kommunikation for langt de fleste teknologiske applikationer. Dette omfatter automatiske kontrolsystemer, som spiller en central rolle i vores hverdag. Kommunikations usikkerheder forårsaget af tidsforsinkelser, data rate begrænsninger og pakkeudfald fører imidlertid til nye begrænsninger, som bør behandles meget omhyggeligt ifbm. analyse og design af netværksbaserede kontrolsystemer (NCSs) da det ellers kan have negative konsekvenser for systemets performance. I denne afhandling studerer vi samspillet mellem kommunikations begrænsninger og kontrol performance for fire forskellige kontrolsystemopsætninger.

I den første opsætning, fokuserer vi på en fejlfri kanal med en given konstant forsinkelse i tilbagekoblingsvejen. Vi modellerer kodnings- og kontrolkomponenterne på begge sider af kanalen ved kausale, men ellers vilkårlige funktioner. Det system som styres, er lineært og tidsinvariant med Gaussiske eksterne signaler. Vi karakteriserer førnævnte trade-off ved at udlede nedre og øvre grænser for den minimale gennemsnitlige data rate, der er nødvendig for at opnå et givent performance niveau. Til dette formål anvender vi en metode baseret på informationsteoretiske aspekter af kausale tilbagekoblingsløkker. Vi viser, at når performance niveauet holdes fast og kanalforsinkelsen øges, så øges også den mindste gennemsnitlige påkrævede data rate. Dette medfører at hvis forsinkelsen øges så skal data raten også øges for at opretholde en ønsket kontrolperformance.

I den anden opsætning består systemet af elementer med samme egenskaber som det system, der tages i betragtning i det første tilfælde bortset fra at transmissionsforsinkelsen i kanalen er stokastisk. I dette tilfælde benytter vi argumenter som er simplere end de argumenter vi benyttede i det forrige opsætning med konstant kanal forsinkelse. Der udledes en nedre grænse for den mindste gennemsnitlige data rate, som er nødvendig for at garantere at den gennemsnitlige steady-state varians af systemets output opfylder et performance kriterie. Vi benytter det føromtalte simple ræsonnement for tilfældet med kendt og konstant kanalforsinkelse og observerer at det fører til de samme øvre og nedre grænser som vi udledte i vores første studie omkring den gen-

nemsnitlige minimum data rate.

I den tredje opsætning, analyseres sammenspillet mellem data rate, performance og forsinkelsen i netværket, hvor ℓ^0 normen af kontrolsignalet specificerer mængden af data som skal transmitteres. Der undersøges et lineært og tidsinvariant system uden eksterne forstyrrelser (støj). Systemet er fuldt observerbart. Transmissionskanalen mellem kontrolleren og aktuatoren har pakketab og en konstant forsinkelse. Der kompenseres for disse effekter ved at bruge en pakkebaseret prediktiv kontroller, som genererer en sekvens af kontrolsignaler og sender dem til en buffer. Kontrolsignalerne er sparse men garanterer lukketsløjfe stabilitet. For at opnå dette, minimerer kontrolleren ℓ^0 normen af kontrolsignalerne til ethvert tidspunkt under den betingelse af en given performance (ℓ^2 norm) er opfyldt. Der etableres stabilitets betingelser under givne kanalforsinkelser. Det kan vises at hvis forsinkelsen i kanalen øges så stabilitet opnås dog med reduceret performance samt brug af størrer data pakker.

Den fjerde opsætning drejer sig om afvejningerne mellem performance og sparsity af kontrolsignalerne i fejlbehæftede lineære systemer. Problemet er her at designe en endelig sekvens af kontrolsignaler med en minimum ℓ^1 norm på en sådan måde, at en endelig-horisont lineær-kvadratur regulator (LQR) kostfunktion afgrænses fra oven. Vi viser, at et sådant problem kan for visse systemer og systemer med diskrete eller polytopiske usikkerheder omskrives til et SOCP problem. Vi viser gennem simuleringer, at performance nær optimal standard LQR-performance kan opnås ved brug af sparse kontrolsignaler.

Contents

List of Publications

Thesis Title:	Trade-offs Between Performance, Data Rate and Transmission Delay in Networked Control Systems
Ph.D. Student:	Mohsen Barforooshan
Supervisor:	Prof. Jan Østergaard, Aalborg University

The main body of this thesis consists of the following papers.

[A] M. Barforooshan, J. Østergaard, and M. S. Derpich, "Interplay Between Transmission Delay, Average Data Rate, and Performance in Output Feedback Control over Digital Communication Channels," in *Proceedings of the American Control Conference (ACC),* Seattle, USA, May 2017, pp. 1691–1696.

[B] M. Barforooshan, J. Østergaard, and P. A. Stavrou, "Achievable Performance of Zero-Delay Variable-Rate Coding in Rate-Constrained Networked Control Systems with Channel Delay," in *Proceedings of the 56th IEEE Annual Conference on Decision and Control (CDC),* Melbourne, AU, Dec. 2017, pp. 5991-5996.

[C] M. Barforooshan, M. S. Derpich, P. A. Stavrou, and J. Østergaard, "The Effect of Time Delay on the Average Data Rate and Performance in Networked Control Systems," *IEEE Transactions on Automatic Control,* Submitted.

[D] M. Barforooshan, M. Nagahara, and J. Østergaard, "Sparse Packetized Predictive Control Over Communication Networks with Packet Dropouts and Time Delays," Technical report, Aug. 2018.

[E] M. Kishida, M. Barforooshan, and M. Nagahara, "Hands-Off Control for Discrete-time Linear Systems Subject to Polytopic Uncertainties", to be published in *Proceedings of the 7th IFAC Workshop on Distributed Estimation and Control in Networked Systems (NECSYS),* Groningen, Netherlands, Aug. 2018.

Preface

This thesis reports the results of research conducted as a PhD study at the Department of Electronic Systems at Aalborg University from September 2015 to September 2018. The thesis is submitted to the Technical Doctoral School of IT and Design at Aalborg University in partial fulfillment of the requirements for the degree of Doctor of Philosophy. The corresponding PhD project received funding from VILLUM FONDEN Young Investigator Programme, under grant agreement No. 19005.

This thesis is about trade-offs between control performance and communication constraints in networked control systems. The work encompasses two research directions. One studies the infimum data rate required to attain a prescribed quadratic performance level in an NCS with channel-induced delay by using the information-theoretic properties of causal feedback loops. The other utilizes arguments in hands-off control in two setups. One is a packetized predictive control system closed over a channel subject to time delay and data packet dropouts where conditions for stabilizing the system by sparse control inputs are derived. The other is the LQR-constrained ℓ^1-optimal control of linear uncertain systems.

I would like to thank VILLUM FONDEN for providing this PhD project with financial support. I would also like to thank Aalborg University for granting me an environment perfectly suited for research activities. My biggest thanks go to my PhD supervisor Jan Østergaard for guiding me step by step throughout the PhD study. His constructive advices, useful criticisms, and encouraging positivity played a key role in removing the obstacles along the path to the project goals. I would like to thank Milan S. Derpich and Photios A. Stavrou for their brilliant suggestions and valuable reviews on the papers. I feel very grateful to Masaki Nagahra from the University of Kitakyushu for his incredible hospitality during my study abroad at Japan. Finally, I should emphasize that this thesis is dedicated to my family and my confidants to whom I owe big times.

Mohsen Barforooshan
Aalborg University, Friday 31st August, 2018

Part I

Introduction

Introduction

1 Introduction

1.1 Notation

We denote by $\mathbb{R}$, $\mathbb{R}^+$ and $\mathbb{R}_0^+$ the sets of real numbers, strictly positive real numbers and nonnegative real numbers, respectively. The set of natural numbers is symbolized by $\mathbb{N}$ based on which we define the set $\mathbb{N}_0$ as $\mathbb{N}_0 \triangleq \mathbb{N} \cup \{0\}$. Operators for expectation, natural logarithm and magnitude are $\mathbf{E}$, log and $|.|$, respectively. In most of the cases, the time index of considered signals is denoted by k which is an integer belonging to $\mathbb{N}_0$. Moreover, the transpose of the matrix (vector) M is represented by M^T. We denote the ℓ^1 and the ℓ^2 norm of the vector $z = [z_1, \ldots, z_n]^T \in \mathbb{R}^n$ by $\|z\|_1$ and $\|z\|_2$, and define them as $\|z\|_1 \triangleq |z_1| + \cdots + |z_n|$ and $\|z\|_2 \triangleq \sqrt{z^T z}$, respectively. We also denote the support set of the vector z by $supp(z)$ and define it as $supp(z) \triangleq \{i : z_i \neq 0\}$ based upon which the ℓ^0 norm of z is defined through $\|z\|_0 \triangleq |supp(z)|$ where $|supp(z)|$ is the cardinality of the set $supp(z)$. Hence, ℓ^0 norm of a vector is actually the number of its non-zero elements. In the case where $\beta(k)$ denotes the k-th sample of a discrete-time signal, we refer to β^k as shorthand for $\beta(0), \ldots, \beta(k)$. In addition, α^k is defined as $\alpha^k \triangleq \alpha(0) \times \cdots \times \alpha(k)$ for the time-dependent set $\alpha(i), i \in \mathbb{N}_0$. However, if ϕ is a fixed time-invariant set, then $\phi^k \triangleq \phi \times \cdots \times \phi$ (k times).

Consider v and q as two random variables each of which with known marginal and joint probability distribution functions (PDFs). Functions $f(v)$, $f(q)$ and $f(v, q)$ denote the marginal PDF of v, the marginal PDF of q, and their joint PDF, respectively. We say that $\mathbf{E}_v(.)$ is the operator for the expectation with respect to the distribution of v and $f(v|q)$ represents the conditional PDF of v given q. The differential entropy of v and the conditional differential entropy of v given q are defined as $h(v) \triangleq -\mathbf{E}_v(\log f(v))$ and $h(v|q) \triangleq -\mathbf{E}_{v,q}(\log f(v|q))$, respectively. Finally, by $I(v; q)$, we denote the mutual information between v and q which is defined as $I(v; q) \triangleq -\mathbf{E}_{v,q}(\log(f(v)f(q)/f(v, q)))$.

1.2 Networked Control Systems, Data Rate and Transmission Delay

The advent and rapid development of communications, network and computer technologies revolutionized signal transmission means through replacing conventional wired point-to-point connections with data communication networks [1]. Stimuli for such transition include reduction in the volume, complexity and costs associated with wiring, ease and low cost of installation, maintenance and diagnosis of channel equipments, flexibility for upgradation and reliability of data transfer over long distances [2]. These advantages played also the role of sparks which ignited the idea of using data communication networks for control and automation purposes. Consequently, a new paradigm emerged in theory and applications of control named networked control systems (NCSs) [3]. Essentially, any control system wherein the information exchange among feedback loop components (plants, sensors, controllers, actuators, etc.) is carried out via a real-time data network is said to be an NCS. Throughout the literature, NCSs have been defined in various ways but the common element across all presented definitions is signal transmission between closed-loop system nodes by means of a shared network [4].

As one of the early efforts along the lines of implementing NCSs, in 1983, Bosch initiated a study program with the purpose of evaluating the feasibility of utilizing networked devices for control systems embedded in passenger cars. This led to introducing the communication protocol controller area network (CAN) in 1986 [5]. Since then, the applications of NCSs have been evolving and growing extensively. So in addition to the automotive industry, nowadays, NCSs are vastly employed in applications such as aerospace industry, remote operation and control systems (telesurgery, operation in hazardous environments,etc.), industrial automation systems (control and monitoring), large-scale distributed processes (power grids, chemical processes, etc.), and sensor networks which cover multi-agent systems, autonomous robots, control and navigation of satellites and unmanned aerial vehicles (UAVs), and intelligent transportation and traffic systems, to name a few [6, 7].

On the other hand, communication limitations in data networks appear as challenges in analysis and design of NCSs [8]. Among others, constraints caused by quantization, time delay and data packet dropout are crucial in that they have determinative effects on system stability and performance. Due to the fact that the scarcity of power and bandwidth in digital communication channels restricts the amount of information to be transferred per unit of time, quantization becomes unavoidable. Therefore, quantization and data rate limitation are two sides of the same coin in digital data transmission. Moreover, network access pattern and inherent transmission characteristics of the channel can be considered as sources of time delay in data communication networks [9]. Data rate constraints and channel transmission delay have been the center of

attention for decades in the literature of NCSs [10]. In what follows, we present a brief overview on research trends in the area of data rate-limited NCSs and NCSs subject to network-induced delays.

Data Rate Constraints in NCSs

When dealing with analysis of NCSs, ideas from control theory, communications theory and information theory are applicable. In particular, due to the communication imperfection associated with data rate-limited NCSs, these systems are studied by utilizing either control-theoretic or information-theoretic approaches. The former method mostly uses classical nonlinear control tools while the other approach is based upon investigating the information-theoretic aspects of the feedback loops. In both cases, the very basic concern is the interplay between data rate limitation and system stability. Along this line, efforts started with a series of work by D. Delchamps reported in [11–15] where it was revealed that the traditional view of modeling the quantization effect as an additive white noise is inadequate for explaining chaotic behavior of system outputs when the plant is unstable with poles of magnitude greater than 2. Following this direction, W. S. Wong and R. W. Brockett studied state estimation with coded observation in [16] and found out that there is a relationship between convergence properties of estimation and the transmission rate of observed data. More importantly, in [17], the same authors showed that a noiseless scalar linear plant can be rendered bounded by a memoryless quantizer if and only if the data rate is greater than or equal to the natural logarithm of the plant unstable pole. This result is the first version of the so-called data rate theorem. The data rate theorem revolves around the minimum data rate required for stabilizability of linear plants. Though derived for different setups using various methodologies, the minimum data rate pertaining to the data rate theorem appears as an increasing function of magnitude of plant unstable poles across all related works [18–27]. Of course boundedness was not the only notion of stability studied under data rate constraints. For instance, [20, 26, 27] propose adaptive zooming quantization schemes that with the use of memory guarantees global asymptotic stability provided that data rate meets the stabilizability requirements. Even without using memory, zooming in-zooming out quantization policy was shown to be efficient for achieving quadratic stability [28–31]. Stabilization of linear plants disturbed by known bounded signals [32], stochastic linear plants [33, 34], and stabilizability of linear plants over noisy channels [35–38] are also topics covered in the literature. Particularly, the author of [38] introduced the interesting notion of anytime capacity to establish the conditions of moment stability over binary symmetric channels for which Shannon capacity was not suitable to analyze. This insufficiency is due to the inherent long delays associated with reliable data transmission over noisy channels at rates close to the channel Shannon capacity. The stabilizability of

single-input multiple-output (SIMO), multiple-input single-output (MISO) and multiple-input multiple-output (MIMO) linear plants over channels with data rate limitations are addressed in [39], [40] and [41], respectively. More recent results in stabilization of linear plants over finite-rate communication channels are reported in [42–48]. Such a rich literature, as briefly reviewed above, testifies that system stability has been addressed well for linear plants via both control-theoretic and information-theoretic approaches.

As performance has always been a critical requirement in control of feedback systems, research on performance analysis of data rate-constrained NCSs started to proceed simultaneously with stabilization analysis. From the very beginning, researchers in this realm of study paid a great deal of attention to the trade-offs between the data rate and control performance of NCSs. One fundamental observation was that reducing the transmission rate (or channel Shannon capacity) to the minimum data rate required for stabilizability (or entropy rate of the plant) will bring about degradation in system performance [13, 33, 49]. On the contrary, using an approach rooted in control theory, [50] showed that when the plant is LTI, noiseless and fully observable with bounded initial states, it is possible to render the quantized linear-quadratic regulator (LQR) performance cost arbitrarily close to the ideal non-networked one by using encoders with memory as long as the average data rate satisfies the stabilizability requirement. Considering instantaneous data rate, [51] studied data rate-limited LQR problem for scalar plants. Similar problems were addressed in [52] and [53] for noiseless plants and plants with bounded noise, respectively. A sector bound approach was utilized in [54] to investigate H_2 and H_∞ performance under logarithmic quantization. Robustness of system regularity, as a performance measure, against time-varying data rate constraints was studied in [55]. Authors of [56, 57] compared the interplay between system performance, quantizer complexity and the contraction rate (the ratio between the volumes of the starting and target sets for system states) across different stabilizing quantized controllers. Model predictive control (MPC) was analyzed in [41] for a system in which a multivariable plant, sensors, a centralized controller and actuators are networked via a data rate-constrained communication channel. As a fundamental result, [58] showed that the optimal linear-quadratic-Gaussian (LQG) cost under vector quantization is attained by a scheme where an encoder-controller estimates the states from the measurements, calculates the control input based on such estimation, quantizes the obtained continuous control command sequentially and send the symbols to a decoder-controller part that applies the the control input to the plant. Other early results on data rate-limited state estimation utilizing the control theoretic method can be found in [59–61]. Recently, conditions for certainty equivalence, separation between the design of coder and that of controller, and dual effect have been derived in [62] for an NCS subject to data rate and finite-horizon linear quadratic (LQ) performance constraints. Furthermore, [63] proposes

an adaptive backstepping approach that ensures attaining a certain level of tracking performance for uncertain nonlinear systems with data rate-limited channels on the control path.

Information-theoretic arguments have proved to be strong tools for performance analysis of data rate-limited NCSs. An initial step in using such a method was taken in [64] where the LQG control of partially observed linear systems under data rate constraints was investigated. The article [64] showed that the optimal LQG cost is yielded by estimation and control schemes for which separation principle holds if the observation noise is the only process to be encoded and transmitted over the channel. In [65], minimizing closed-loop LQ costs over memoryless noisy channels was studied. For such a problem and in the case of LTI plants, [65] proposed a joint design for coding via an iterative procedure and established separation principle and certainty equivalence conditions. Optimal stochastic control of nonlinear plants over noisy data rate-constrained channels was considered in [66] where an implicit characterization for the optimal scheme was presented. Finding the minimum data rate required to guarantee achieving a certain level of performance is another concern in the performance study of data rate-limited NCSs. As pointed out in [10], the well-known Shannon's rate-distortion theory for digital communications deals with a similar problem [67, 68]. However, the causal rate-distortion problem is often studied for open-loop communication systems for which optimal coding schemes necessitate long delays [69, 70]. So, the corresponding results cannot be directly applied to feedback control loops. Notwithstanding, inspired by the idea of causal rate-distortion function, [71] derived an analytic expression for the minimum data rate needed to assure that an LQG cost keeps bounded from above by a certain value in a setup where a linear fully observable plant is controlled over a noisy channel with data rate limitations. Moreover, [71] suggested a sequential coding scheme that renders the certainty equivalence and separation principle valid for the system. Compared to the data rate requirement for stabilization, the exact value of minimum data rate guaranteeing performance levels is not easy to obtain, specially when the plant is partially observable. In such cases, bounds on the desired minimal data rate are derived. For instance, [72] established lower bounds on minimum data rates required to achieve three different notions of convergence in state estimation over noiseless data rate-limited channels. Inspired by [49, 73, 74], deriving lower and upper bounds on the infimum average data rate which is necessary for attaining a quadratic performance level was investigated in [75–77]. The NCSs considered in these works are comprised of LTI plants with Gaussian system and observation noises, causal but otherwise arbitrary coders and controllers, and noiseless delay-free digital communication channels between encoding and decoding sections. While the design approach proposed in [75, 76] was a second-stage one, coding and control are designed jointly in [77]. Particularly, in [77], the concept of directed information rate [78, 79] plays a key role in obtaining the lower

bound in that the infimum directed information rate over a scheme comprised of LTI filters and an additive white Gaussian noise (AWGN) channel with feedback subject to a specific quadratic performance constraint gives a lower bound on the infimum data rate guaranteeing the same performance over the main arbitrary scheme. The article [77] showed that the lower bound characterized in this way is the dual solution of a convex SNR-constrained optimal control problem [80]. For the upper bound problem, [77] proposed using entropy-coded dithered quantizers (ECDQs) [81] that give any admissible performance level with operational average data rates which are at most roughly 1.254 bits per sample greater than the associated lower bound. Recently, along the lines of [75–77], the minimum directed information rates required for meeting LQG performance criteria are calculated in [82] based on a semidefinite programming (SDP) approach for MIMO fully observable plants controlled over noiseless binary channels. In turn, authors of [83] analyze the LQR problem over delay-free data rate-limited communication channels and apply Shannon's lower bound on distortion-rate function and variable-length innovation-based lattice quantization together with entropy coding in order to obtain lower and upper bounds, respectively, on the minimum mutual information needed to attain a prescribed level of LQR performance. In all the above works, the effect of channel delay has been somehow neglected while as mentioned earlier, channel transmission delay is a common phenomenon in actual communication networks which should be taken into account when it comes to control of NCSs. One of the very relevant and recent results that considers both time delay and data rate constraints in channel model and concerns performance analysis of NCSs via employing an information-theoretic approach is reported in [84]. In this paper, bounds are derived on the minimal individual data rate which is needed to achieve an individual performance level for a setup incorporating a linear plant with Gaussian exogenous inputs and a digital channel imposing random time delay. For obtaining the lower bound, [84] uses a single-shot approach while the upper bound is given based on a model predictive strategy.

One of the areas where ideas from data rate-limited control have been lately employed is packetized predictive control (PPC). In a PPC setup, the controller generates a finite-length sequence of control inputs based on a model predictive strategy and sends the whole sequence as a data packet to the actuator over a communication channel at each time instant. At the actuator node, a buffer is installed whose task is deciding what element of the most recently received packet is to be applied to the plant according to a selection logic which depends on the channel situation [85–90]. The motivation for using PPC as control policy is the robustness it brings to the system against channel uncertainties such as data packet dropouts or transmission delays [91, 92]. As one of the early results along the lines of quantized PPC, [93] studied the effect of entropy-constrained lattice quantization of control packets on mean square stability and performance of a linear disturbed plant controlled over a bit rate-limited

channel with packet dropouts. Recently, in [44, 94, 95], multiple descriptions (MDs) combined with ECDQs are utilized in PPC over a rate-limited channel and upper bounds on the operational bit rate guaranteeing a desired performance level are derived. Furthermore, the authors of [96] apply fixed-rate vector quantization with a dictionary inspired by sparse regression codes (SPARC) to the packetized predictive control of an NCS in order to evaluate the best mean-square error performance (MSE) at each operational data rate.

From the viewpoint of network resource consumption, one very advantageous control policy for NCSs is hands-off control. Basically, hands-off control is a strategy for minimizing the control effort; a requirement which is crucial in feedback control loops due to numerous environmental [97, 98], economical [99, 100] and technical [101] causes. According to this approach, the control signal is held exactly equal to zero over certain periods of time. To do so, sparsity-promoting techniques are utilized in hands-off control. Examples include works on model predictive control (MPC) [102–107], optimal control design [108–110], state estimation [111–114] and sampled-data control [115–117]. The idea of maximizing the number of time instants over which the control input is equal to zero led to the introduction of a new interesting topic in the theory of systems and control called maximum hands-off control [118, 119]. In the maximum hands-off control, the ℓ^0 norm of the control input is minimized subject to certain performance constraints. It was shown in [118, 119] that for continuous-time setups and under the assumption of normality, the ℓ^0 optimal control problem associated with maximum hands-off control can be equivalently formulated by an ℓ^1 optimization problem which is convex and much easier to analyze. For the case of continuous-time plants, [120] shows that the value function of the minimum ℓ^0 norm of the control input is continuous and strictly convex with respect to initial states in the reachable set, a property which guarantees stability of the maximum hands-off control when applied to MPC. The conditions for the equivalence between ℓ^0 and ℓ^1 optimal control in discrete-time linear systems are established in [121]. The sparsity associated with maximum hands-off control makes it very appealing for the use in NCSs in that sending zero-valued control inputs is basically equal to not using the channel and, in addition, having many zero elements in control packets means compression with low effort [115, 122–124]. Particularly, [115, 124, 125] combine maximum hands-off control with PPC and call the obtained control policy sparse PPC. In other words, the controller generates a sequence of control inputs at each time instant by minimizing finite-horizon sparsity promoting cost functions. The authors of [115, 124–126] prove that in the case where the plant is noiseless LTI and the channel between the controller and the actuator is only subject to bounded packet dropouts, the unconstrained $\ell^1 - \ell^2$ sparse PPC and ℓ^2-constrained ℓ^0 sparse PPC guarantee practical and asymptotic stability, respectively, under certain conditions.

Time Delay in NCSs

In most of the cases, time delays are known to worsen the performance of or cause instability to closed-loop control systems [127–131]. As already mentioned before, time delays are inherent characteristics of data communication networks which appear in NCSs as a result of network traffic (packets waiting for network availability before being transmitted), propagation (physical distance between components) and computation (devices processing time). In the study of NCSs, the computational delays are often neglected since they are small compared to delays caused by congestion or propagation. It is actually the application that determines the prominence of the delay source or other characteristics of the network-induced delay such as being constant or time-varying, being deterministic or stochastic, and being smaller than the sampling period or otherwise [132–135]. Various formulations have been presented to model the time delay in different NCS architectures for which different problems have been investigated with different analysis and synthesis approaches. For instance, in an early attempt, [136] proposed the augmentation method for control of discrete-time linear plants over networks with periodic delays. Moreover, [137–139] used queuing mechanisms to render the entire NCS with random delays time-invariant by reshaping the delays to deterministic time delays. Optimal stochastic control tools were utilized in [132] to study the LQG problem in NCSs subject to random delays. The stabilizability over channels with random delays was analyzed in [140, 141] based on the perturbation theory. Furthermore, [142] devised the sampling period scheduling methodology that compensates the effect of time delay on system performance by choosing the sampling period appropriately. Another relevant early endeavour was documented in [143] where event-triggered methods were employed for controlling robotic manipulators over Internet. A thorough discussion on modeling NCSs with channel time delay by delayed differential equations (DDEs) and switched systems and analyzing them by Lyapunov-based approaches are presented in [9]. Recent approaches in analysis and synthesis of NCSs with network delays are classified into two general methods: robustness and adaptation. In the former approach, the information of the time delay value at each time instant is not considered as a parameter for analysis and design. In the robustness framework, the controller is only required to be robust against the time-varying delay. As an example, conditions for stabilizability and H_∞ performance are derived in [144] for a singular cascade NCS by utilizing a method based on the selection of appropriate Lyapunov-Krasovskii functionals. Moreover, a fuzzy-model-based approach is utilized in [145] where the rules are based on the delay size. So the design approach proposed in [145] incorporates all the possible values of time delay and the resultant controller is robust over time delay variations. Other relevant instances of fuzzy-model-based control over channels with time-varying delay include [146, 147]. The conservativeness associated

with the robustness approach can be reduced by taking into account that in NCSs, signals are commonly transmitted in form of data packets which contain information revealing the time delay they have been exposed to (time stamps) and actuators can possess a certain level of intelligence. These features of NCSs are extensively used in analysis and synthesis based on the second framework, adaptation. One approach in this framework is modeling the overall NCS as a stochastic switched system. Using such a method, [148, 149] investigate the stability and H_2/H_∞ performance of Markov jump linear systems (MJLSs), respectively. Predictive control is another approach in the adaptation framework where a smart actuator selects the control input from a sequence of control packets according to a selection logic that uses the time-stamp of the received packets. Networked predictive control covers problems such as output tracking [150], nonlinear control [151] and wide-area damping control [152].

In this work, we first investigate the infimal data rate required to achieve prescribed quadratic performance levels in general NCSs with causal coding and control schemes under the effect of constant and random channel delays. Then we study hands-off control once in the sparse PPC over channels with constant time delays and once for uncertain linear systems constrained by LQR performance costs. Before going through the contributions of each paper reporting a portion of the entire research associated with this thesis, we present a brief introduction to four fundamentally relevant topics in hopes of providing a better understanding of studied problems. These topics are data rate theorem, rate-distortion theory, maximum hands-off control and packetized predictive control.

2 Rate-Distortion Theory

As pointed out in [10], the problem of finding the minimum data rate required for attaining a certain performance level in NCSs is the closed-loop version of what is sought in the Shannon's rate-distortion theory. So getting a grasp on the rate-distortion theory provides insights to the rate-performance trade-offs in NCSs. Along this line, we give a brief presentation of fundamentals of the rate-distortion theory in this section. It is well-known that describing an arbitrary real number perfectly is not possible with finite number of bits. So, any finite-length description of a discrete-time continuous random variable is a distorted version of it. The rate-distortion theory deals with the interplay between the loss and the number of bits associated with finite-alphabet representation of a random source. The loss is quantified with a measure of distance between the random variable and its representation called distortion measure. The very basic question here is as follows: "provided that the distribution of the source and the distortion measure is known, what is the minimum rate required to attain a prescribed distortion?". The properties of the answer to the latter

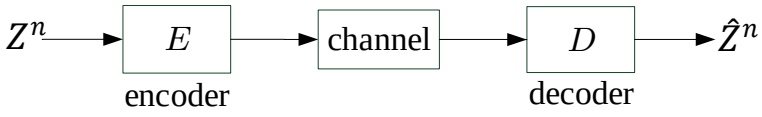

Fig. 1: A typical rate-distortion setting

question is given by the rate-distortion function which we formalize in what follows.

Consider the coding scheme of Fig. 1 where $Z^n = [z_1, \ldots, z_n]^T$ is an i.i.d random sequence which denotes the source of information. Without loss of generality, we suppose that for every $i \in \{1, \ldots, n\}$, z_i is a discrete random variable with probability mass function (PMF) $p(z)$ and finite support set $\mathcal{Z}$, i.e. $z \in \mathcal{Z}$. The encoder is assumed to assign nR bits for representing the source sequence by the symbol $E_n(Z^n) \in \{1, ..., 2^{nR}\}$. The channel is error-free and instantaneous (without delay). On the other end of the channel, the decoder task is to reconstruct the source based on the received symbol. The decoder gives $\hat{Z}^n = [\hat{z}_1, \ldots, \hat{z}_n]^T$, where $\hat{z}_i \in \hat{\mathcal{Z}}$ for every $i \in \{1, \ldots, n\}$, as an approximation of Z^n based on $\hat{Z}^n = D_n(E_n(Z^n))$. The arbitrary mappings $E_n : \mathcal{Z}^n \mapsto \{1, ..., 2^{nR}\}$ and $D_n : \{1, ..., 2^{nR}\} \mapsto \hat{\mathcal{Z}}^n$ define a $(2^{nR}, n)$-rate distortion code. We also define the distortion between the source sequence Z^n and its reconstruction $\hat{Z}^n$ as

$$d(Z^n, \hat{Z}^n) = \frac{1}{n} \sum_{i=1}^{n} d(z_i, \hat{z}_i), \tag{1}$$

where $d : \mathcal{Z}^n \times \hat{\mathcal{Z}}^n \mapsto \mathbb{R}_0^+$ is a function that specifies the mismatch between z_i and $\hat{z}_i$, for every $i \in \{1, \ldots, n\}$ and called distortion function. Depending on the application, the distortion function can be characterized in different ways. For instance, one very common distortion function is the squared difference between the source and the reconstruction which in our case is formulated as $d(z_i, \hat{z}_i) = (z_i - \hat{z}_i)^2$, $\forall i \in \{1, \ldots, n\}$. Note that in (1), the distortion between two sequences is the average of the distortion associated with each pair of corresponding elements. For the $(2^{nR}, n)$-rate distortion code related to the scheme of Fig. 1, we define the distortion as the average of the distortion between Z^n and $\hat{Z}^n$ with respect to the distribution of Z^n. Such notion of distortion is denoted by D and formulated as

$$D = \sum_{Z^n} p(Z^n) d(Z^n, D_n(E_n(Z^n))). \tag{2}$$

According to the definition provided in (2), the achievability of a rate-distortion pair (D, R) is defined as follows:

Definition 2.1
We call a rate-distortion pair (R, D) achievable if there exists (E_n, D_n), denoting a sequence of $(2^{nR}, n)$-rate distortion codes, that satisfies

$$\lim_{n\to\infty} \sum_{Z^n} p(Z^n) d(Z^n, D_n(E_n(Z^n))) \leq D.$$

We call the closure for the set of all achievable rate-distortion pairs (R, D) the rate-distortion region for the source Z^n. Now, we are in the position to define the rate-distortion function.

Definition 2.2
For a specific distortion D, the rate-distortion function $R(D)$ is the infimum rate R over all achievable pairs (R, D) associated with D located inside the rate-distortion region of the source.

A concept similar to the rate-distortion function is presented by information rate-distortion function.

Definition 2.3
For a source Y with the distortion measure $d(Y, \hat{Y})$, the information rate-distortion function $R^{(I)}(D)$ is defined as

$$R^{(I)}(D) = \min_{p(\hat{Y}|Y):\sum_{(Y,\hat{Y})} p(Y)p(\hat{Y}|Y)d(Y,\hat{Y})\leq D} I(Y;\hat{Y}), \tag{3}$$

where $I(Y;\hat{Y})$ denotes the mutual information between Y and $\hat{Y}$. Moreover, the optimization in (3) is carried out with respect to all conditional distributions $p(\hat{Y}|Y)$ that are associated with joint distributions $p(Y, \hat{Y})$ satisfying the expected distortion constraint.

It can be implied from (3) that the information rate-distortion function provides a more mathematically treatable formulation for the minimum data rate required for achieving a particular distortion than the classical rate-distortion function. More interestingly, the information rate-distortion function is equal to rate-distortion function. This result is formalized in the following theorem:

Theorem 2.1
[153, Theorem 10.2.1] For the source sequence Z^n with i.i.d samples each possessing the distribution $p(z)$ and with the distortion function $d(Z^n, \hat{Z}^n)$, the following holds:

$$R^{(I)}(D) = R(D),$$

where $R^{(I)}(D)$ is defined as in (3).

The information rate-distortion function can be calculated for several sources with different distortion measures. For instance, assume that $n = 1$ and Z^1 is a scalar source which has a normal distribution with mean 0 and variance σ^2, i.e.

$Z^1 \sim \mathcal{N}(0, \sigma^2)$. Moreover, assume that the distortion measure is mean-squared error. Then, the rate-distortion function is given by

$$R(D) = \begin{cases} \frac{1}{2} \log \frac{\sigma^2}{D}, & 0 < D \leq \sigma^2 \\ 0, & D > \sigma^2. \end{cases}$$

It is a well-known result in the rate-distortion theory that coding all samples of a sequence together into one description is more efficient in the sense of rate-distortion function than describing each element separately. This holds even in the case where the elements of a sequence are independent. Therefore, in an open-loop communication system, it is favorable to wait for more samples to send a joint description. However, it means long delays in data transmission which is not appreciated in a lot of applications such as closed-loop feedback systems. This actually sheds a light on one aspect of rate-performance trade-offs in NCSs; block coding comes with the price of control performance degradation.

3 Data Rate Theorem

In this section, we present a brief explanation for the data rate theorem in data rate-limited NCSs. Like every other control setup, stability is a very fundamental requirement in NCSs. In particular, when studying stabilization of data rate-limited NCSs, this question naturally arises that what is the minimum data rate that assures stability?. The answer to this question for LTI plants is stated as a theorem referred to as data rate theorem. According to this theorem, it is not possible to render the response of an unstable LTI plant bounded with a causal coding and control scheme in the feedback path unless the data rate exceeds the sum of the logarithm of the absolute value of the unstable plant poles. As already pointed out before, the data rate theorem is shown to be valid for both deterministic and stochastic LTI plants controlled over various types of communication channels under different notions of stability. Here, we consider a setup which is similar to the system taken into account in the data rate-limited control part of this thesis. For such a setting, we briefly explain the data rate theorem quantitatively in what follows.

Consider the NCS of Fig. 2 where the plant P is discrete-time, LTI, noisy and partially observable with dynamics described as follows:

$$\begin{aligned} x(k+1) &= Ax(k) + Bu(k) + w(k) \\ y(k) &= Cx(k) + n(k) \end{aligned}$$

where $x(k) \in \mathbb{R}^{n_x}$ and $u(k) \in \mathbb{R}^p$ represent the plant states and control input for all $k \in \mathbb{N}_0$, respectively. Moreover, $w(k) \in \mathbb{R}^{n_x}$ and $n(k) \in \mathbb{R}^m$ are process and observation noises, respectively. Assume that the pair (A, B) is reachable

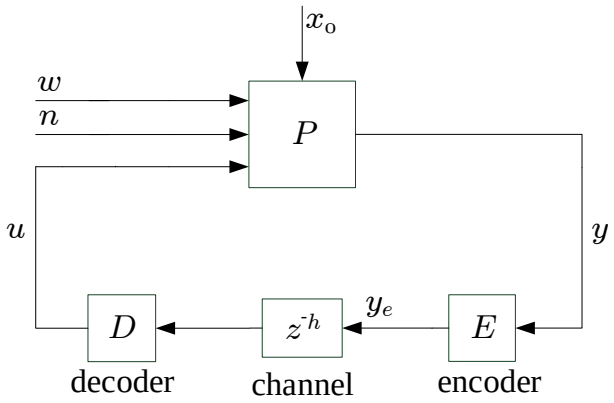

Fig. 2: The general NCS architecture for which data rate theorem is studied

and (A, C) is an observable pair. Furthermore, at each time instant $k \in \mathbb{N}_0$, the noises $w(k)$ and $n(k)$ are random variables that together with the initial states $x(0)$ compose a mutually independent triplet. Another assumption is the existence of a $\varrho > 0$ in such a way that $2+\varrho$-th absolute moments of $w(k)$, $n(k)$ and $x(0)$ are uniformly bounded for every $k \in \mathbb{N}_0$. In addition, at each time instant $k \in \mathbb{N}_0$, the random variable associated with the process noise $w(k)$ is assumed to have a probability distribution which is absolutely continuous as a function of Lebesgue measure γ on $\mathbb{R}^{n_x}$. It should be pointed out that noises w and n are not restricted to be Gaussian. In the NCS of Fig. 2, the plant and the controller are connected via a digital communication channel. Therefore, every observation y needs to be quantized before being sent, as a binary symbol, over the channel. Such a task is carried out by the encoder E according to the following dynamics:

$$y_e(k) = \mathcal{E}_k(y^k, y_e^{k-1}), \tag{4}$$

where $\mathcal{E}_k : \mathbb{R}^{m\times(k+1)} \times \mathcal{Y}_e^{k-1} \mapsto \mathcal{Y}_e(k)$ denotes a causal, but otherwise arbitrary, mapping and $\mathcal{Y}_e(k)$ is a countable set of binary words at each time instant $k \in \mathbb{N}_0$. Note that the encoder uses the entire past and current value of the observation and the past symbols to produce the new symbol. The channel between the encoder and the controller is error-free but induces h steps of delay. The average data rate over this channel is defined as

$$\mathcal{R} \triangleq \lim_{k\to\infty} \frac{1}{k} \sum_{l=0}^{k-1} \log_2 \mathcal{L}(l),$$

where $\mathcal{L}(k)$ symbolizes the size of the binary word $y_e(k)$ at any time instant $k \in \mathbb{N}_0$. On the receiver side of the channel, the controller generates the control input as follows:

$$u(k) = \mathcal{D}_k(y_e^{k-h}), \tag{5}$$

in which $\mathcal{D}_k : \mathcal{Y}_e^{k-h} \mapsto \mathbb{R}^p$ is a causal, but otherwise arbitrary, mapping. It can be implied from the structure of the channel that no data is received by the controller at the first h time steps. For this interval, let assume that the control input is set a priori. So, the value of $u(k)$ is known for every $k \in \{0, \ldots, h-1\}$.

The aim is analyzing the stabilizability of the overall NCS described above. Therefore, we first need to clarify what notion of stability we are interested in. We consider mean square stability as the stability notion. The NCS of Fig. 2 is called mean square stable if the plant states keep bounded at each time instant based on

$$\sup_{k \in \mathbb{N}_0} \mathbf{E}(x(k))^2 < \infty, \tag{6}$$

where $\mathbf{E}(.)$ is the expectation operator. Now we are in the position to state the data rate theorem

Theorem 3.1

[33, Theorem 2.1] Consider the NCS of Fig. 2 with conditions and assumptions as specified above. Then for any coder-controller pair satisfying (4) and (5) and rendering the feedback system of Fig. 2 mean square stable, the following holds:

$$\mathcal{R} > H \triangleq \sum_{j=1}^{n_{up}} \log_2 |\lambda_j|, \tag{7}$$

where $\lambda_1, \ldots, \lambda_{n_{up}}$ are eigenvalues of A lying on or outside the unit circle, i.e., plant unstable poles. Moreover, the mean square norm on the left-hand side of (6) approaches to ∞ as the average data rate R gets close to H from above. The inequality in (7) is a sufficient condition for mean square stability as well. In other words, for any $R > H$, one can find a causal coder-controller with dynamics described by (4) and (5) that stabilizes the NCS of Fig. 2 in the mean square sense.

Note that in the considered setup, causality is the only restriction assumed for the encoder and controller; a characteristic which is very inherent for feedback loops. Moreover, the distributions of process and observation noises are mildly constrained. So, the version of data rate theorem expressed in Theorem 3.1 covers several cases of controlling LTI stochastic plants over data rate-limited channels. Furthermore, it can be implied from right-hand side of (7) that stabilizability is neither affected by the channel delay h nor by noise distributions. This is caused by the weakness of considered stability notion. This together with the fact that imposing communication constraints on the path from controller to the plant would not change the minimum average data

rate required for mean square stability is discussed in [40]. In addition, remark that no causal encoder-controller pair can bring mean square stability to the NCS of Fig. 2 with an average data rate lower than H. Moreover, the performance degradation caused by approaching the data rate to H is independent of coding and control schemes. Therefore, reducing the average data rate R of any stabilizing coder-controller pair towards the minimum data rate required for stabilizability derived in (7) makes the expected value of the states squared norm arbitrarily large.

4 Maximum Hands-Off Control

This section discusses a general discrete-time maximum hands-off control setup briefly. We previously stated that the maximum hands-off control maximizes the total time interval over which the control input amounts to zero while guarantees meeting certain performance or stability requirements for the overall closed-loop system. Saving energy through reducing fuel and electricity consumption, avoiding pollution via lowering toxic emissions, conserving communication network resources by less expenditure of transmission rate and reduction in noise and vibration are among the main motivations for developing theory and applications of maximum hands-off control. Due to its environmental-friendly properties, maximum hands-off control is also known as green control [154]. In the maximum hands-off control, the ℓ^0 norm of the control input is to be minimized subject to certain performance constraints. Due to the lack of convexity and continuity for the cost function, the ℓ^0-optimization problem is difficult to solve. However, such problem is equivalent to the convex ℓ^1-optimization under certain conditions. In other words, given these conditions, ℓ^0 and ℓ^1-optimization problems are interchangeable in the sense that they give an identical minimal value with the same solution. The discontinuity associated with bang-off-bang feature of ℓ^1 norm minimization can be resolved by $\ell^1 - \ell^2$ relaxation. Though $\ell^1 - \ell^2$-optimization problem is not necessarily solved by the sparsest minimizer, its solution has certain sparsity properties. In what follows, we briefly show how this chain of observations is applied to a general maximum hands-off control system.

Consider a discrete-time plant whose dynamics is described by

$$x(k+1) = f(x(k)) + \sum_{l=1}^{p} h_l(x(k))u_l(k), \qquad k \in \mathbb{N}_0, \tag{8}$$

where $x(k) \in \mathbb{R}^{n_x}$ represents plant states and the scalar signals $u_1(k), \ldots, u_p(k)$ specify the plant control input as $u(k) = [u_1(k), \ldots, u_p(k)]^T$ at each time instant $k \in \mathbb{N}_0$. Functions $f : \mathbb{R}^{n_x} \mapsto \mathbb{R}^{n_x}$ and $h_l : \mathbb{R}^{n_x} \mapsto \mathbb{R}$, $l = 1, \ldots, p$, are arbitrary (possibly nonlinear) time-invariant continuous functions with continuous first derivatives with respect to their arguments. The plant is controlled

according to a maximum hands-off control law which is required to drive the plant states to the origin within a limited time duration by producing as many zero control inputs as possible. let us denote the final time instant by N. So, as the first requirement, $\{u(0), \ldots, u(N-1)\}$ should be designed in such a way that $x(N)$ satisfies $x(N) = \rho$ for given initial states $x(0) = \theta$. Let impose the following typical constraint on the component with largest magnitude of each control input over $[0, N-1]$:

$$\max_l |u_l(k)| < 1, k = 1, \ldots, N-1. \tag{9}$$

The constraint in (9) together with the foreshadowed requirement on the terminal states $x(N)$ define the sequence $\{u(0), \ldots, u(N-1)\}$ as admissible control if it is bounded as in (9) and applying it to the plant (8) with $x(0) = \rho$ results in $x(N) = 0$. We denote by $\mathbb{U}(N, \rho)$ as the set of all admissible controls. Suppose that N is large enough to guarantee that $\mathbb{U}(N, \rho)$ is non-empty. The problem of discrete-time maximum hands-off control (ℓ^0-optimal control) is to find the admissible control with minimum ℓ^0 norm. Such optimal control sequence is denoted by $u^*_{\ell^0}$ and defined as

$$u^*_{\ell^0} \triangleq \arg \min_{u \in \mathbb{U}(N,\rho)} \frac{1}{N} \sum_{l=1}^{p} \nu_l \|u_l\|_0, \tag{10}$$

where $\|q\|_0$ indicates the number of non-zeros elements for $q \in \mathbb{R}^N$. As already pointed out, the optimization problem associated with ℓ^0-optimal control problem can be equivalent to the one related to ℓ^1-optimal control problem. The final goal in the latter problem is to obtain $u^*_{\ell^1}$ defined as

$$u^*_{\ell^1} \triangleq \arg \min_{u \in \mathbb{U}(N,\rho)} \frac{1}{N} \sum_{l=1}^{p} \nu_l \|u_l\|_1, \tag{11}$$

where

$$\|u_l\|_1 = \sum_{k=0}^{N-1} |u_l(k)|, \qquad l = 1, \ldots, p.$$

The question here is that what are the conditions for equivalence between maximum hands-off control and ℓ^1-optimal control?. To answer this, defining the concept of normality in a discrete-time ℓ^1-optimal control setup is needed. We call a discrete-time ℓ^1-optimal control problem normal if the following holds:

$$|N \nu_l^{-1} h_l(x^*(k)^T) p^*(k+1)| \neq 1, \tag{12}$$

where $k = 0, \ldots, N-1$. Moreover, x^* and p^* are state and costate associated with $u^*_{\ell^1}$.

Theorem 4.1
[118, Theorem 11] For the ℓ^1-optimal control problem in (11), suppose that the normality condition (12) holds. Moreover, assume that the sets of the solutions for the ℓ^0-optimal control in (10) and ℓ^1-optimal control are denoted by $\mathbb{U}_0^*$ and $\mathbb{U}_1^*$, respectively. Then $\mathbb{U}_0^* = \mathbb{U}_1^*$.

It is well-known that the solutions to the ℓ^1-optimal control problem possess bang-off-bang property meaning that the value of the corresponding optimal control input changes sharply between limited number of levels over time. Such hard switching might not be tolerable by actuation units in some applications. One way to overcome this undesirable discontinuity, while obtaining a sufficiently sparse control input, is modifying the cost function associated with ℓ^1-optimal control by adding a weighted version of the ℓ^2 norm of the control input to it. The resultant problem is called $\ell^1-\ell^2$-optimal control problem for which a solution is formulated as

$$u^*_{\ell^1-\ell^1} = \arg \min_{u\in\mathbb{U}(N,\rho)} \frac{1}{N}\sum_{l=1}^{p} \nu_l \|u_l\|_1 + \frac{\varphi_l}{2}\|u_l\|_2^2, \tag{13}$$

where

$$\|u_l\|_2^2 = \sum_{k=0}^{N-1} |u_l(k)|^2$$

and $\varphi_l > 0$ and $\nu_l > 0$ for $l = 1, \ldots, p$. For the continuous-time $\ell^1-\ell^2$-optimal control problem, it is shown in [118] that the optimal solution is continuous with respect to time. Moreover, [118] shows that the weighting parameters associated with ℓ^1 and ℓ^2 norms (similar to ν_l and φ_l in (13)) determine the trade-off between smoothness and sparsity of the $\ell^1-\ell^2$-optimal control input in that as the parameter weighting the ℓ^1 norm goes to 0, the solution to the continuous $\ell^1-\ell^2$-optimal control problem will converge to the ℓ^2-optimal control input. On the other hand, as the parameter related the squared ℓ^2 norm goes to zero, the $\ell^1-\ell^2$-optimal control input will converge to ℓ^1-optimal control input. Nevertheless, to the best of our knowledge, similar theoretical results regarding the discrete-time $\ell^1-\ell^2$-optimal control have not been established yet in the literature. However, [124] demonstrates via simulation that discrete-time $\ell^1-\ell^2$-optimal control problem can indeed have sparse solutions but it comes with the price of performance degradation. Intuitively speaking, the structure of the $\ell^1-\ell^2$-optimization problem associated with (13) gives similar insights about the continuity and sparsity of $\ell^1-\ell^2$-optimal control in a discrete-time setup.

5 Packetized Predictive Control

In this section, we provide a short and general description of PPC systems. As already mentioned before, the packetized predictive controller is actually

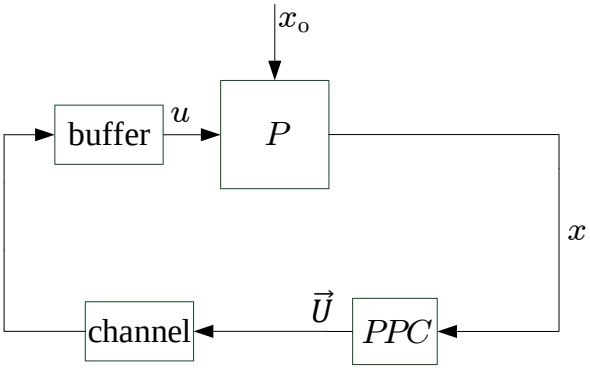

Fig. 3: A typical PPC system

a model predictive controller that instead of sending one control input to the actuator, transmits a sequence including a limited number of tentative future control inputs. We also mentioned previously that the core motivation behind employing this control strategy in NCSs is to attain robustness versus channel imperfections such as packet dropouts or time delays. In a PPC setup, there is often a buffer available at the plant side which stores received packets so as to apply their elements as control inputs at the time of arrival and later on when there will be no packet received. In what follows, we elaborate on the description of PPC mechanisms in a more quantitative manner.

Consider the general structure of Fig. 3 which depicts the architecture of an NCS incorporating a plant, a packetized predictive controller, a communication channel and a buffer. The plant is described by the following general state-space model:

$$x(k+1) = f(x(k), u(k)), \qquad k \in \mathbb{N}_0,$$

where $x(k) \in \mathcal{X} \subseteq \mathbb{R}^{n_x}$ and $u(k) \in \mathcal{U} \subseteq \mathbb{R}^p$ denote plant states and the control input, respectively. The sets $\mathcal{X}$ and $\mathcal{U}$ contain the origin and impose constraints (e.g. performance-related constraints) on x and u. Moreover, $f : \mathbb{R}^{n_x} \times \mathbb{R}^p \mapsto \mathbb{R}^{n_x}$ is an arbitrary (possibly nonlinear) time-invariant function. Let us assume complete observability for the plant and ideal communications for the uplink channel (the channel between the sensor and the controller). So, the controller is provided with full access to a version of plant states which is not corrupted. Since the controller in the NCS of Fig. 3 is a packetized predictive controller and such controller works based on an MPC strategy, it uses the received plant states $x(k)$ to minimize the following general finite-horizon

cost function:

$$J(x(k), \vec{U}(k)) = T(x^{'})(k+N)) + \sum_{i=0}^{N-1} S(x^{'}(k+i), u^{'}(k+i)). \tag{14}$$

where $x^{'}(k+i)$ predicts $x(k+i)$ based on the following recursion:

$$x^{'}(k+i+1) = f(x^{'}(k+i), u^{'}(k+i)), \qquad x^{'}(k) = x(k). \tag{15}$$

for any $i \in \{1, \ldots, N\}$ and any $k \in \mathbb{N}_0$. So, $\{x^{'}(j)\}_{j=k+1}^{k+N}$ denotes a prediction of plant states at the upcoming N time steps, $\{x(j)\}_{j=k+1}^{k+N}$, and N is the horizon length for this prediction. Moreover, complying with the constraint on plant states, $x^{'}(j)$ is constrained as $x^{'}(j) \in \mathcal{X}$ for all $j \in \{k+1, \ldots, k+N\}$. The argument $\vec{U}(k)$ of the cost function J is defined as

$$\vec{U}(k) \triangleq [u^{'}(k), \ldots, u^{'}(k+N-1)]^T.$$

Actually, $\vec{U}(k)$ is comprised of all decision variables for the problem of minimizing $J(x(k), \vec{U}(k))$ at time instant $k \in \mathbb{N}_0$. So, every $\vec{U}(k)$ in the feasible set of the latter optimization problem is a candidate for the packet which encompasses tentative future control inputs. Since every control input of the plant belongs to the set $\mathcal{U}$, $u^{'}(j)$ is constrained as $u^{'}(j) \in \mathcal{U}$ for any $j \in \{k, \ldots, k+N-1\}$. The functions T and S in (14) are called terminal cost and stage cost, respectively, for which the following assumptions are typically considered:

$$\begin{aligned} &T(0) = 0, \qquad T(x) \geq 0, \quad \forall x \in \mathcal{X} \\ &S(0,0) = 0, \qquad S(x,u) \geq \gamma(\|x(k)\|), \quad \forall x \in \mathcal{X}, \forall u \in \mathcal{U}, \end{aligned}$$

where the function $\gamma : \mathbb{R}^+ \mapsto \mathbb{R}^+$ is continuous, nondecreasing and possesses the properties $\gamma(0) = 0$ and $\gamma(\ell) > 0$, $\forall \ell > 0$. As already mentioned before, in PPC, the sequence of tentative future control inputs that characterizes the control packet is obtained by minimizing the finite-horizon cost function J defined as in (14). Therefore, at each time instant $k \in \mathbb{N}_0$, the desired control input sequence, say $\vec{U}^*(k)$, is calculated as

$$\vec{U}^*(k) = \arg \min_{\vec{U}(k) \in \mathbb{U}} J(x(k), \vec{U}(k)), \tag{16}$$

where $\mathbb{U}$ represents the set of all admissible solutions for the optimization problem associated with (16) which is solved by the packetized predictive controller at each time instant $k \in \mathbb{N}_0$. To emphasize that $\vec{U}^*(k)$ is comprised of the tentative control inputs for time k to $k+N-1$ which are constructed based on predictions at time k, we express $\vec{U}^*(k)$ as follows:

$$\vec{U}^*(k) = [u(k;k), \ldots, u(k+N-1;k)]^T,$$

where $u(k+j-1;k) = u^{'}(k+j-1)$ for every $j \in \{1,\ldots,N\}$. According to (15), the states $x(k)$ and the matrix $\vec{U}^*(k)$ determine the predictions of future states generated at time k which we specify by

$$\vec{x}^*(k) = [x(k+1;k),\ldots,x(k+N;k)]^T,$$

where $x(k+j;k) = x^{'}(k+j)$ for all $j \in \{1,\ldots,N\}$. Moreover, the optimization problem pertaining to (16) gives the following optimal value function

$$V(x(k)) = \min_{\vec{U}(k)\in\mathbb{U}} J(x(k),\vec{U}(k)).$$

The PPC unit in Fig. 3 forwards the sequence $\vec{U}^*(k)$ as a data packet to the actuator over the communication channel. Such data transmission could be subject to various faults induced by the communication channel. For instance, the channel could impose bounded data packet dropouts. In this case, it is not guaranteed that every control packet generated at the controller reaches the plant. So, one selection strategy for the buffer installed at the actuator could be storing every newly received packet over the existing one and using the elements of the new packet in a receding manner until the arrival of the next control packet. The channel could also induce time delay on the packets. The selection logic of the buffer in this case could be prioritizing the received packet which has been produced at the most recent time instant and applying its elements as control input till the arrival of a packet which is associated with a more recent time instant.

6 Summary of Contributions

We study the performance of data rate-constrained NCSs over channels with time delays, sparse PPC over channels with time delays and packet dropouts, and hands-off control subject to LQR constraints for plants with polytopic uncertainties. The research associated with these problems is reported in five papers which constitute the main body of this thesis. In what follows, we summarize the contributions of each paper.

6.1 Paper A-Interplay Between Transmission Delay, Average Data Rate, and Performance in Output Feedback Control over Digital Communication Channels

In this paper, we derive a lower bound on the infimum average data rate required to assure that the steady-state variance of a plant output keeps bounded. The considered plant is LTI, disturbed by Gaussian noises and with Gaussian initial states. The plant has single control input and single sensor output which

is transmitted to an encoder-controller pair modeled by a causal, but otherwise arbitrary, function. This encoder-controller maps the measurement output into a binary word and sends the word to a decoder-controller over an error-free channel that induces a known constant delay. The decoder-controller, also represented by an arbitrarily causal mapping, generates the control input. We formulate the aforementioned desired infimum data rate and derive a lower bound on it based on an information-theoretic method. This method takes advantage of the Gaussianity of the system exogenous inputs and the considered notion of stability which is being strongly asymptotically wide-sense stationary (SAWSS) to derive information inequalities involving average data rate, the directed information rate across the channel and the power spectral densities of channel signals. We derive such fundamental information inequalities under the network-induced delays which lead to a lower bound given by the infimum directed information rate over a scheme comprised of LTI filters and an additive white Gaussian (AWGN) channel with feedback and delay. We show that this lower bound is calculated by solving a convex SNR-constrained optimal control problem. We analyze this SNR-constrained problem by introducing an auxiliary equivalent problem and compute the lower bound for different values of channel delay. The results show that for a fixed performance level, a greater delay necessitates a larger lower bound on the infimal required average data rate.

6.2 Paper B-Achievable Performance of Zero-Delay Variable-Rate Coding in Rate-Constrained Networked Control Systems with Channel Delay

In this paper, we investigate how to approximate the coding and control schemes giving the lower bound in the paper A with actual implementable schemes and evaluate how close the resultant actual average data rates are to their corresponding lower bounds. So, we consider the same NCS architecture as in the paper A and study the upper bound problem. In other words, we derive an upper bound on the infimum average data rate required to attain a quadratic performance level in an NCS comprised of a noisy LTI plant, an arbitrary coding and control scheme and a delay-free channel with known constant delay. We propose entropy-coded dithered quantizer (ECDQ)-based linear coding schemes that by using the LTI filters associated with the lower bound together with subtractively dithered uniform scalar quantizers and entropy coders, guarantee achieving admissible performance levels with data rates that are at most (approximately) 1.254 bits/sample higher than the corresponding lower bounds. We show how to design such schemes and simulate a candidate system applying the designed ECDQ-based linear schemes for different values of the channel delay. The results demonstrate that the achieved operation data rates are considerably lower than the upper bound. Moreover, the upper bound and the

achieved average data rates are increasing functions of channel delay. In other words, in order to attain a fixed performance level, one should increase the required actual data rate as the channel delay grows.

6.3 Paper C-The Effect of Time Delay on the Average Data Rate and Performance in Networked Control Systems

In this paper, we consider the same system structure as in paper A and paper B except for the fact that the channel is single-input multiple output (SIMO) and imposes random time delay on transmitted data. In such an NCS, the steady-state variance of the output and the average data rate are random variables depending on the realization of the channel delay for every coding and control scheme rendering the system SAWSS. We consider the mean of those random variables with respect to the distribution of the channel delay as notions for data rate and performance. We derive a lower bound on the infimum average data rate guaranteeing that the average steady-state variance of a system output over all channel delay realizations is bounded from above by a predetermined value. Using the idea of information inequalities involving the average directed information rate and the defined average data rate, we obtain a lower bound on the infimal desired data rate stated as the average of a function of the power spectral densities of feedback path signals over all possible realizations of the delay. The proof approach for this derivation is much simpler and shorter than the one for similar results in paper A. We utilize this simple approach for the study of rate-performance trade-offs in the special case of a known constant channel delay and rederive the results of paper A and paper B. Moreover, we show in the constant delay case that changing the position of the time delay in the feedback loop can have neutral effect on the values of system signals if side the information changes as well.

6.4 Paper D-Sparse Packetized Predictive Control Over Communication Networks with Packet Dropouts and Time Delays

In this paper, we investigate the sparse PPC over a channel with known constant time delay and bounded packet dropouts. This channel links the controller to the actuator of a noiseless LTI plant. The plant is fully observable and an uncorrupted version of its states is received at the controller at each time instant. So unlike the actuation path, the plant and controller exchange data over an ideal communication channel in the measurement path. We analyze two sparse PPC strategies; unconstrained ℓ^1-ℓ^2 PPC and ℓ^2-constrained ℓ^0 PPC. In the former scenario, the controller solves a limited number of finite-horizon

unconstrained ℓ^1-ℓ^2 sparsity-promoting optimization problems each taking a prediction of future states as input. In the latter regime, the control packets are solutions to a limited number of finite-horizon ℓ^2-constrained ℓ^0 sparsity-promoting optimization problems. Upon arrival of a packet sequence at the smart actuator, the actuator selects the control packet associated with the precise approximation of the current states. We propose efficient methods for solving the aforementioned optimization problems and establish conditions of practical stability and asymptotic stability for unconstrained ℓ^1-ℓ^2 sparse PPC and ℓ^2-constrained ℓ^0 sparse PPC, respectively, in the presence of channel delay. We also show that in both setup, in order to maintain system stability, increasing channel delay necessitates increasing the number of control packets to be produced at each time instant. We simulate an example system using ℓ^1-ℓ^2 sparse PPC and ℓ^2-constrained ℓ^0 sparse PPC and show that the system has the expected stability properties.

6.5 Paper E-Hands-Off Control for Discrete-Time Linear Systems subject to Polytopic Uncertainties

This paper studies the hands-off control subject to finite-horizon linear-quadratic regulator (LQR) performance constraints. The aim is minimizing the ℓ^1 norm of the control input while making sure that an LQR cost keeps bounded from above by a prescribed value over a certain time duration. We investigate this problem for three types of linear discrete-time noiseless plants; deterministic plants, uncertain plants with discrete uncertainties, uncertain plants with polytopic uncertainties. In the first two cases, deterministic plants and uncertain plants with discrete uncertainties, we show that the overall optimization problems pertaining to the hands-off control strategies can be expressed as second-order cone programmings. In the last case, uncertain plants with polytopic uncertainties, we show that the corresponding LQR-constrained ℓ^1 optimization problem is relaxed to a second-order cone programming by deriving an upper bound on the LQR cost function. We consider a real-world plant model with polytopic uncertainty and show through simulation that the controller designed based on the proposed LQR-constrained hands-off strategy leads to a performance fairly close to the standard LQR performance but with sparser control inputs.

7 Conclusions and Future Research

Generally speaking, the research reported in this thesis deals with two topics: data rate-constrained NCSs and hands-off control. The work associated with the former topic was about the trade-offs between data rate, time delay and control performance in data rate-constrained NCSs. In particular, we derived

bounds on the ifimum average data rate needed to guarantee achieving a certain level of quadratic performance in an NCS comprised of a discrete-time noisy LTI plant with Gaussian initial states and disturbance, a causal but otherwise arbitrary coding and control scheme and an error-free communication channel with time delay that makes the connection between the encoder and the decoder. We considered two channel model; one imposing a known constant delay and the other inducing random time delay. In the constant delay case, we showed that for any admissible performance level, a lower bound on the corresponding desired infimum data rate is given by minimizing the SNR, constrained by the same performance requirement, over an scheme comprised of LTI pre- and post- filters and an AWGN channel with feedback and delay. To prove this, we used two different approaches, though they are both based on the concept of directed information rate across channels with delay. We also proposed ECDQ-based linear coding schemes that give any admissible performance level with an average data rate which is at most (approximately) 1.254 bits/sample greater than the corresponding lower bound. We also showed that moving the delay block around the system can lead to equivalent systems if side information is allowed to change. We illustrated through simulation that all the derived bounds and empirical data rates are increasing with respect to the channel delay. In other words, attaining a certain performance level requires higher data rate if the channel delay is higher. For the case of random channel delay, we considered the mean of average data rate and steady-state output variance over all possible realizations of the delay as notions of rate and performance, respectively. Considering these notions, we established a lower bound on the minimum data rate required to guarantee that the performance measure is bounded. We showed that this lower bound is stated in terms of average power spectral densities of feedback path signals over all possible realizations of the channel time delay.

We studied hands-off control in two settings. In one, the controller generates a limited number of control packets at each time instant once based on unconstrained ℓ^1-ℓ^2 and once based on ℓ^2-constrained ℓ^0 finite-horizon sparsity-promoting optimization problems. We considered a noiseless fully observable LTI plant whose actuator is connected to the packetized predictive controllers via a communication link imposing bounded packet dropouts and constant time delay. We showed that unconstrained ℓ^1-ℓ^2 and ℓ^2-constrained ℓ^0 sparse PPC policies render the overall closed-loop system bounded and asymptotically stable, respectively, under certain conditions. We showed that in the considered setup, increasing channel delay means increasing the number of packets generated by the controller at each time instant. So achieving stability over channels with higher delays comes with the price of sending more packets at each time instant and also performance degradation. We demonstrated through simulation that the proposed unconstrained ℓ^1-ℓ^2 and ℓ^2-constrained ℓ^0 sparse PPC strategies indeed bring practical and asymptotic stability to the system. The

other setup where we used hands-off control is the control of a linear discrete-time plant based on minimizing the ℓ^1 norm of the control input subject to an LQR performance constraint. We analyzed this control problem for three cases: the plant being certain, the plant being subject to discrete uncertainties and the plant having polytopic uncertainties. We showed for the first two cases that the corresponding LQR-constrained ℓ^1-norm optimization problems can be expressed as second-order cone programming. For the case of polytopic uncertainty in the plant model, we derived an upper bound on the corresponding LQR cost which leads to relaxing the related ℓ^1-norm optimization problem to a second-order cone programming. Simulating the proposed method for a practical plant demonstrated that the obtained control input is much sparser than the one associated with standard finite-horizon LQR control while the resultant performance is close to the standard LQR performance.

In the work on data rate-constrained NCSs, we approximated the infimum average data rate that guarantees attaining a certain level of performance by deriving bounds on it. Though the established bounds are fairly tight, an exact analytic expression similar to ones obtained in data rate theorem is still missing for the latter infimum required data rate. If obtained, such an expression will give a much better understanding of data rate-performance-time delay trade-offs in NCSs. So one possibility for future research will be investigating a closed-form solution for the problem of finding the foreshadowed desired data rate. One approach could be analyzing the Karush–Kuhn–Tucker (KKT) conditions for the corresponding optimization problem. In our research on data rate-limited NCSs, we also considered plants with single control input and single sensor output which is not the case in several real-world applications. Therefore, deriving bounds in the case of plants having multiple control inputs and multiple measurement outputs could be a possible direction for future work. In this case, we hypothesize that the same approach as for the case with single control input and sensor output can be used but the challenging factor would be the correlation between signals which should be taken care of carefully. Future research may also be concerned with studying the effect of vector quantization, instead of symbol-by-symbol coding, on the interplay between data rate, channel delay and performance in the considered data rate-constrained NCS.

In the work on sparse PPC over channels with constant delay, we showed that the number of control packets to be generated by the controller at each time instant is upper bounded by a finite value which is an exponential function of the delay. This means that for large channel delays, the controller might produce a massive number of packets. Besides the huge load of computational effort which is required in this case, the channel bandwidth might not be adequate for reliable transmission of such long packet sequences. Hence, efficient quantization and coding of control packets in sparse PPC with channel delay could be one topic for future research. Using multiple descriptions is

one candidate idea for reducing the rate of data transmission. Finally, in the LQR-constrained ℓ^1-optimal control of uncertain systems, we derived an upper bound on the LQR cost and use this bound as the performance measure. So if such a measure is bounded from above by a given value, then the original LQR cost for every pair of state and input matrices inside the considered polytope will be upper bounded by that value. However, the conservativeness resulted form this approach was not evaluated. Analyzing such conservativeness for the purpose of proposing other methods to attain sparser control inputs than the ones given by our approach for a fixed LQR cost could be carried out in the future research.

References

[1] Y. Tipsuwan and M.-Y. Chow, "Control methodologies in networked control systems," *Control engineering practice*, vol. 11, no. 10, pp. 1099–1111, 2003.

[2] X. M. Zhang, Q. L. Han, and X. Yu, "Survey on recent advances in networked control systems," *IEEE Transactions on Industrial Informatics*, vol. 12, no. 5, pp. 1740–1752, Oct. 2016.

[3] P. F. Hokayem and C. T. Abdallah, "Inherent issues in networked control systems: a survey," in *Proceedings of the 2004 American Control Conference (ACC)*, vol. 6, Jun. 2004, pp. 4897–4902.

[4] R. A. Gupta and M. Y. Chow, "Networked control system: Overview and research trends," *IEEE Transactions on Industrial Electronics*, vol. 57, no. 7, pp. 2527–2535, Jul. 2010.

[5] J. Baillieul and P. J. Antsaklis, "Control and communication challenges in networked real-time systems," *Proceedings of the IEEE*, vol. 95, no. 1, pp. 9–28, Jan. 2007.

[6] L. Zhang, H. Gao, and O. Kaynak, "Network-induced constraints in networked control systems—a survey," *IEEE Transactions on Industrial Informatics*, vol. 9, no. 1, pp. 403–416, Feb. 2013.

[7] A. S. Matveev and A. V. Savkin, *Estimation and control over communication networks*. Springer Science & Business Media, 2009.

[8] X. Tang and J. Yu, "Networked control system: survey and directions," in *International Conference on Life System Modeling and Simulation*. Springer, 2007, pp. 473–481.

[9] J. P. Hespanha, P. Naghshtabrizi, and Y. Xu, "A survey of recent results in networked control systems," *Proceedings of the IEEE*, vol. 95, no. 1, pp. 138–162, Jan. 2007.

[10] G. N. Nair, F. Fagnani, S. Zampieri, and R. J. Evans, "Feedback control under data rate constraints: An overview," *Proceedings of the IEEE*, vol. 95, no. 1, pp. 108–137, Jan. 2007.

[11] D. F. Delchamps, "The 'stabilization' of linear systems with quantized feedback," in *Proceedings of the 27th IEEE Conference on Decision and Control (CDC)*, vol. 1, Dec. 1988, pp. 405–410.

[12] ——, "Controlling the flow of information in feedback systems with measurement quantization," in *Proceedings of the 28th IEEE Conference on Decision and Control (CDC)*, no. 3, Dec. 1989, pp. 2355–2360.

[13] ——, "Some chaotic consequences of quantization in digital filters and digital control systems," in *IEEE International Symposium on Circuits and Systems,*, no. 1, May 1989, pp. 602–605.

[14] ——, "Extracting state information from a quantized output record," *Systems & Control Letters*, vol. 13, no. 5, pp. 365–372, 1989.

[15] ——, "Stabilizing a linear system with quantized state feedback," *IEEE Transactions on Automatic Control*, vol. 35, no. 8, pp. 916–924, Aug. 1990.

[16] W. S. Wong and R. W. Brockett, "Systems with finite communication bandwidth constraints. i. state estimation problems," *IEEE Transactions on Automatic Control*, vol. 42, no. 9, pp. 1294–1299, Sept. 1997.

[17] ——, "Systems with finite communication bandwidth constraints. ii. stabilization with limited information feedback," *IEEE Transactions on Automatic Control*, vol. 44, no. 5, pp. 1049–1053, May 1999.

[18] J. Baillieul, "Feedback designs for controlling device arrays with communication channel bandwidth constraints," in *ARO workshop on smart structures*. University Park PA, 1999, pp. 16–18.

[19] ——, "Feedback coding for information-based control: operating near the data-rate limit," in *Proceedings of the 41st IEEE Conference on Decision and Control (CDC).*, vol. 3, Dec. 2002, pp. 3229–3236.

[20] R. W. Brockett and D. Liberzon, "Quantized feedback stabilization of linear systems," *IEEE Transactions on Automatic Control*, vol. 45, no. 7, pp. 1279–1289, Jul. 2000.

[21] G. N. Nair and R. J. Evans, "Stabilization with data-rate-limited feedback: Tightest attainable bounds," *Systems & Control Letters*, vol. 41, no. 1, pp. 49–56, 2000.

[22] ——, "Exponential stabilisability of finite-dimensional linear systems with limited data rates," *Automatica*, vol. 39, no. 4, pp. 585–593, 2003.

[23] S. Tatikonda, A. Sahai, and S. Mitter, "Control of lqg systems under communication constraints," in *Proceedings of the 37th IEEE Conference on Decision and Control*, vol. 1, Dec. 1998, pp. 1165–1170 vol.1.

[24] S. C. Tatikonda, "Control under communication constraints," Ph.D. dissertation, Massachusetts Institute of Technology, 2000.

[25] S. Tatikonda and S. Mitter, "Control under communication constraints," *IEEE Transactions on Automatic Control*, vol. 49, no. 7, pp. 1056–1068, Jul. 2004.

[26] D. Liberzon, "On stabilization of linear systems with limited information," *IEEE Transactions on Automatic Control*, vol. 48, no. 2, pp. 304–307, Feb. 2003.

[27] I. R. Petersen and A. V. Savkin, "Multi-rate stabilization of multivariable discrete-time linear systems via a limited capacity communication channel," in *Proceedings of the 40th IEEE Conference on Decision and Control*, vol. 1, Dec. 2001, pp. 304–309 vol.1.

[28] N. Elia and S. K. Mitter, "Stabilization of linear systems with limited information," *IEEE Transactions on Automatic Control*, vol. 46, no. 9, pp. 1384–1400, Sept. 2001.

[29] H. Ishii and B. A. Francis, *Limited data rate in control systems with networks*. Springer Science & Business Media, 2002.

[30] ——, "Quadratic stabilization of sampled-data systems with quantization," *Automatica*, vol. 39, no. 10, pp. 1793 – 1800, 2003.

[31] H. Ishii, T. Başar, and R. Tempo, "Randomized algorithms for quadratic stability of quantized sampled-data systems," *Automatica*, vol. 40, no. 5, pp. 839 – 846, 2004.

[32] D. Liberzon and D. Nešić, "Input-to-state stabilization of linear systems with quantized feedback," in *Proceedings of the 44th IEEE Conference on Decision and Control (CDC)*, Dec. 2005, pp. 8197–8202.

[33] G. Nair and R. Evans, "Stabilizability of stochastic linear systems with finite feedback data rates," *SIAM Journal on Control and Optimization*, vol. 43, no. 2, pp. 413–436, 2004.

[34] K. Tsumura and J. Maciejowski, "Stabilizability of SISO control systems under constraints of channel capacities," in *Proceedings of the 42nd IEEE International Conference on Decision and Control (CDC)*, vol. 1, Dec. 2003, pp. 193–198.

[35] S. Tatikonda and S. Mitter, "Control over noisy channels," *IEEE Transactions on Automatic Control*, vol. 49, no. 7, pp. 1196–1201, Jul. 2004.

[36] N. C. Martins, M. A. Dahleh, and N. Elia, "Feedback stabilization of uncertain systems in the presence of a direct link," *IEEE Transactions on Automatic Control*, vol. 51, no. 3, pp. 438–447, Mar. 2006.

[37] T. Simsek, R. Jain, and P. Varaiya, "Scalar estimation and control with noisy binary observations," *IEEE Transactions on Automatic Control*, vol. 49, no. 9, pp. 1598–1603, Sept. 2004.

[38] S. Sahai, "The necessity and sufficiency of anytime capacity for control over a noisy communication link," in *Proceedings of the 43rd IEEE Conference on Decision and Control (CDC)*, vol. 2, Dec. 2004, pp. 1896–1901.

[39] A. S. Matveev and A. V. Savkin, "Multirate stabilization of linear multiple sensor systems via limited capacity communication channels," *SIAM journal on control and optimization*, vol. 44, no. 2, pp. 584–617, 2005.

[40] G. N. Nair, R. J. Evans, and P. E. Caines, "Stabilising decentralised linear systems under data rate constraints," in *Proceedings of the 43rd IEEE Conference on Decision and Control (CDC)*, vol. 4, Dec. 2004, pp. 3992–3997.

[41] G. C. Goodwin, H. Haimovich, D. E. Quevedo, and J. S. Welsh, "A moving horizon approach to networked control system design," *IEEE Transactions on Automatic Control*, vol. 49, no. 9, pp. 1427–1445, Sept. 2004.

[42] D. Nešić and D. Liberzon, "A unified framework for design and analysis of networked and quantized control systems," *IEEE Transactions on Automatic Control*, vol. 54, no. 4, pp. 732–747, Apr. 2009.

[43] A. A. Zaidi, T. J. Oechtering, S. Yüksel, and M. Skoglund, "Stabilization of linear systems over gaussian networks," *IEEE Transactions on Automatic Control*, vol. 59, no. 9, pp. 2369–2384, Sept. 2014.

[44] J. Østergaard and D. Quevedo, "Multiple descriptions for packetized predictive control," *EURASIP Journal on Advances in Signal Processing*, vol. 2016, no. 1, p. 45, Apr. 2016.

[45] M. F. Lupu, M. Sun, F. Wang, and Z. Mao, "Information-transmission rates in manual control of unstable systems with time delays," *IEEE Transactions on Biomedical Engineering*, vol. 62, no. 1, pp. 342–351, Jan. 2015.

[46] S. Wen and G. Guo, "Minimum data rate for exponential stability of networked control systems with medium access constraints," *International Journal of Control, Automation and Systems*, vol. 16, no. 2, pp. 717–725, 2018.

[47] K. Okano and H. Ishii, "Stabilization of uncertain systems with finite data rates and markovian packet losses," *IEEE Transactions on Control of Network Systems*, vol. 1, no. 4, pp. 298–307, Dec. 2014.

[48] Q. Ling, "A sufficient bit rate condition for mean-square stabilisation of linear systems over multiple lossy networks," *IET Control Theory & Applications*, vol. 10, no. 13, pp. 1531–1538, 2016.

[49] N. C. Martins and M. A. Dahleh, "Fundamental limitations of performance in the presence of finite capacity feedback," in *Proceedings of the 2005 American Control Conference (ACC)*, vol. 1, Jun. 2005, pp. 79–86.

[50] A. V. Savkin, "Analysis and synthesis of networked control systems: Topological entropy, observability, robustness and optimal control," *Automatica*, vol. 42, no. 1, pp. 51 – 62, 2006.

[51] G. N. Nair, M. Huang, and R. J. Evans, "Optimal infinite horizon control under a low data rate 2," *IFAC Proceedings Volumes*, vol. 39, no. 1, pp. 1115–1120, 2006.

[52] M. Huang, G. N. Nair, and R. J. Evans, "Finite Horizon LQ Optimal Control and Computation with Data Rate Constraints," in *Proceedings of the 44th IEEE Conference on Decision and Control (CDC)*, Dec. 2005, pp. 179–184.

[53] M. D. Lemmon and R. Sun, "Performance-rate functions for dynamically quantized feedback systems," in *Proceedings of the 45th IEEE Conference on Decision and Control (CDC)*, Dec. 2006, pp. 5513–5518.

[54] M. Fu and L. Xie, "The sector bound approach to quantized feedback control," *IEEE Transactions on Automatic Control*, vol. 50, no. 11, pp. 1698–1711, Nov. 2005.

[55] K. Li and J. Baillieul, "Robust quantization for digital finite communication bandwidth (DFCB) control," *IEEE Transactions on Automatic Control*, vol. 49, no. 9, pp. 1573–1584, Sept. 2004.

[56] J. C. Delvenne, "An optimal quantized feedback strategy for scalar linear systems," *IEEE Transactions on Automatic Control*, vol. 51, no. 2, pp. 298–303, Feb. 2006.

[57] F. Fagnani and S. Zampieri, "Quantized stabilization of linear systems: complexity versus performance," *IEEE Transactions on Automatic Control*, vol. 49, no. 9, pp. 1534–1548, Sept. 2004.

[58] T. Fischer, "Optimal quantized control," *IEEE Transactions on Automatic Control*, vol. 27, no. 4, pp. 996–998, Aug. 1982.

[59] N. G. Dokuchaev and A. V. Savkin, "Recursive state estimation via limited capacity communication channels," in *Proceedings of the 38th IEEE Conference on Decision and Control (CDC)*, vol. 5, Dec. 1999, pp. 4929–4932.

[60] X. Li and W. S. Wong, "State estimation with communication constraints," *Systems & Control Letters*, vol. 28, no. 1, pp. 49–54, 1996.

[61] X. Liu and W. S. Wong, "Controllability of linear feedback control systems with communication constraints," in *Proceedings of the 36th IEEE Conference on Decision and Control (CDC)*, vol. 1, Dec. 1997, pp. 60–65.

[62] M. Rabi, C. Ramesh, and K. Johansson, "Separated design of encoder and controller for networked linear quadratic optimal control," *SIAM Journal on Control and Optimization*, vol. 54, no. 2, pp. 662–689, 2016.

[63] J. Zhou and W. Wang, "Adaptive control of quantized uncertain nonlinear systems," *IFAC-PapersOnLine*, vol. 50, no. 1, pp. 10 425 – 10 430, 2017, 20th IFAC World Congress.

[64] V. S. Borkar and S. K. Mitter, *LQG Control with Communication Constraints*. Boston, MA: Springer US, 1997, pp. 365–373.

[65] L. Bao, M. Skoglund, and K. H. Johansson, "Iterative encoder-controller design for feedback control over noisy channels," *IEEE Transactions on Automatic Control*, vol. 56, no. 2, pp. 265–278, Feb. 2011.

[66] A. Mahajan and D. Teneketzis, "Optimal performance of networked control systems with nonclassical information structures," *SIAM Journal on Control and Optimization*, vol. 48, no. 3, pp. 1377–1404, 2009.

[67] T. Berger, *Rate distortion theory: A mathematical basis for data compression*. Prentice-Hall, 1971.

[68] C. E. Shannon, "Coding theorems for a discrete source with a fidelity criterion," in *IRE Nat. Conv. Rec., Pt. 4*, 1959, pp. 142–163.

[69] A. Gorbunov and M. S. Pinsker, "Nonanticipatory and prognostic epsilon entropies and message generation rates," *Problemy Peredachi Informatsii*, vol. 9, no. 3, pp. 12–21, 1973.

[70] T. Linder and R. Zamir, "Causal coding of stationary sources and individual sequences with high resolution," *IEEE Transactions on Information Theory*, vol. 52, no. 2, pp. 662–680, Feb. 2006.

[71] S. Tatikonda, A. Sahai, and S. Mitter, "Stochastic linear control over a communication channel," *IEEE Transactions on Automatic Control*, vol. 49, no. 9, pp. 1549–1561, Sept. 2004.

[72] S. Yüksel and T. Başar, "Minimum Rate Coding for LTI Systems Over Noiseless Channels," *IEEE Transactions on Automatic Control*, vol. 51, no. 12, pp. 1878–1887, Dec. 2006.

[73] N. C. Martins and M. A. Dahleh, "Feedback Control in the Presence of Noisy Channels: "Bode-Like" Fundamental Limitations of Performance," *IEEE Transactions on Automatic Control*, vol. 53, no. 7, pp. 1604–1615, Aug. 2008.

[74] N. C. Martins, M. A. Dahleh, and J. C. Doyle, "Fundamental limitations of disturbance attenuation in the presence of side information," *IEEE Transactions on Automatic Control*, vol. 52, no. 1, pp. 56–66, Jan. 2007.

[75] E. I. Silva, M. S. Derpich, and J. Østergaard, "A framework for control system design subject to average data-rate constraints," *IEEE Transactions on Automatic Control*, vol. 56, no. 8, pp. 1886–1899, Aug. 2011.

[76] ——, "An achievable data-rate region subject to a stationary performance constraint for LTI plants," *IEEE Transactions on Automatic Control*, vol. 56, no. 8, pp. 1968–1973, Aug. 2011.

[77] E. I. Silva, M. S. Derpich, J. Østergaard, and M. A. Encina, "A characterization of the minimal average data rate that guarantees a given closed-loop performance level," *IEEE Transactions on Automatic Control*, vol. 61, no. 8, pp. 2171–2186, Aug. 2016.

[78] J. Massey, "Causality, feedback and directed information," in *Proceedings of the 1990 International Symposium on Information Theory and Its Applications (ISITA)*, 1990, pp. 303–305.

[79] M. S. Derpich, E. I. Silva, and J. Østergaard, "Fundamental inequalities and identities involving mutual and directed informations in closed-loop systems," *arXiv preprint arXiv:1301.6427*, 2013.

[80] E. I. Silva, M. S. Derpich, and J. Østergaard, "On the minimal average data-rate that guarantees a given closed loop performance level," *IFAC Proceedings Volumes*, vol. 43, no. 19, pp. 67 – 72, 2010, 2nd IFAC Workshop on Distributed Estimation and Control in Networked Systems (NecSys).

[81] R. Zamir and M. Feder, "On universal quantization by randomized uniform/lattice quantizers," *IEEE Transactions on Information Theory*, vol. 38, no. 2, pp. 428–436, Mar. 1992.

[82] T. Tanaka, P. M. Esfahani, and S. K. Mitter, "LQG control with minimum directed information: semidefinite programming approach," *IEEE Transactions on Automatic Control*, vol. 63, no. 1, pp. 37–52, Jan. 2018.

[83] V. Kostina and B. Hassibi, "Rate-cost tradeoffs in control," *arXiv preprint arXiv:1612.02126v2*, 2016.

[84] J. Zhang and C.-C. Wang, "On the rate-cost of Gaussian linear control systems with random communication delays," in *Proceedings of the 2018 IEEE International Symposium on Information Theory (ISIT)*, Jun. 2018, pp. 2441–2445.

[85] P. L. Tang and C. W. de Silva, "Compensation for transmission delays in an ethernet-based control network using variable-horizon predictive control," *IEEE Transactions on Control Systems Technology*, vol. 14, no. 4, pp. 707–718, Jul. 2006.

[86] G. P. Liu, Y. Xia, J. Chen, D. Rees, and W. Hu, "Networked predictive control of systems with random network delays in both forward and feedback channels," *IEEE Transactions on Industrial Electronics*, vol. 54, no. 3, pp. 1282–1297, Jun. 2007.

[87] D. E. Quevedo, E. I. Silva, and G. C. Goodwin, "Packetized predictive control over erasure channels," in *Proceedings of the 2007 American Control Conference (ACC)*, Jul. 2007, pp. 1003–1008.

[88] Z. Dong, S. Zhao, C. Han, and D. Sun, "Packetized predictive power control for CDMA systems with random delay," in *Proceedings of the 2nd International Conference on Intelligent Control and Information Processing*, vol. 2, Jul. 2011, pp. 797–801.

[89] M. Reble, D. E. Quevedo, and F. Allgöwer, "Stochastic stability and performance estimates of packetized unconstrained model predictive control for networked control systems," in *Proceedings of the 9th IEEE International Conference on Control and Automation (ICCA)*, Dec. 2011, pp. 171–176.

[90] D. E. Quevedo and D. Nešić, "On stochastic stability of packetized predictive control of non-linear systems over erasure channels*," *IFAC Proceedings Volumes*, vol. 43, no. 14, pp. 557 – 562, 2010, 8th IFAC Symposium on Nonlinear Control Systems.

[91] ——, "Input-to-state stability of packetized predictive control over unreliable networks affected by packet-dropouts," *IEEE Transactions on Automatic Control*, vol. 56, no. 2, pp. 370–375, Feb. 2011.

[92] ——, "Robust stability of packetized predictive control of nonlinear systems with disturbances and markovian packet losses," *Automatica*, vol. 48, no. 8, pp. 1803 – 1811, 2012.

[93] D. E. Quevedo, J. Østergaard, and D. Nešić, "Packetized predictive control of stochastic systems over bit-rate limited channels with packet loss," *IEEE Transactions on Automatic Control*, vol. 56, no. 12, pp. 2854–2868, Dec. 2011.

[94] J. Østergaard and D. E. Quevedo, "Multiple description coding for closed loop systems over erasure channels," in *Proceedings of the 2013 Data Compression Conference (DCC)*, Mar. 2013, pp. 311–320.

[95] ——, "Multiple descriptions for packetized predictive control over erasure channels," in *Proceedings of the 9th IEEE International Conference on Control and Automation (ICCA)*, Dec. 2011, pp. 165–170.

[96] E. G. W. Peters, D. E. Quevedo, and J. Østergaard, "Shaped Gaussian dictionaries for quantized networked control systems with correlated dropouts," *IEEE Transactions on Signal Processing*, vol. 64, no. 1, pp. 203–213, Jan. 2016.

[97] B. Dunham, "Automatic on/off switching gives 10-percent gas saving," *Popular Science*, vol. 205, no. 4, p. 170, 1974.

[98] C. C. Chan, "The state of the art of electric, hybrid, and fuel cell vehicles," *Proceedings of the IEEE*, vol. 95, no. 4, pp. 704–718, Apr. 2007.

[99] M. Athans, "Minimum-fuel feedback control systems: second-order case," *IEEE Transactions on Applications and Industry*, vol. 82, no. 65, pp. 8–17, Mar. 1963.

[100] R. R. Liu and I. M. Golovitcher, "Energy-efficient operation of rail vehicles," *Transportation Research Part A: Policy and Practice*, vol. 37, no. 10, pp. 917 – 932, 2003.

[101] B. D. Anderson and J. B. Moore, *Optimal control: linear quadratic methods*. Courier Corporation, 2007.

[102] M. Gallieri and J. M. Maciejowski, "ℓasso MPC: smart regulation of over-actuated systems," in *Proceedings of the 2012 American Control Conference (ACC)*, Jun. 2012, pp. 1217–1222.

[103] ——, "Model predictive control with prioritised actuators," in *Proceedings of the 2015 European Control Conference (ECC)*, Jul. 2015, pp. 533–538.

[104] R. P. Aguilera, R. Delgado, D. Dolz, and J. C. Agüero, "Quadratic MPC with ℓ_0-input constraint," in *Proceedings of the 19th IFAC World Congress*, vol. 19, no. 1, 2014, pp. 10 888–10 893.

[105] E. Henriksson, D. E. Quevedo, E. G. W. Peters, H. Sandberg, and K. H. Johansson, "Multiple-loop self-triggered model predictive control for network scheduling and control," *IEEE Transactions on Control Systems Technology*, vol. 23, no. 6, pp. 2167–2181, Nov. 2015.

[106] E. N. Hartley, M. Gallieri, and J. M. Maciejowski, "Terminal spacecraft rendezvous and capture with LASSO model predictive control," *International Journal of Control*, vol. 86, no. 11, pp. 2104–2113, 2013.

[107] S. K. Pakazad, H. Ohlsson, and L. Ljung, "Sparse control using sum-of-norms regularized model predictive control," in *Proceedings of the 52nd IEEE Conference on Decision and Control (CDC)*, Dec. 2013, pp. 5758–5763.

[108] M. Fardad, F. Lin, and M. R. Jovanović, "Sparsity-promoting optimal control for a class of distributed systems," in *Proceedings of the 2011 American Control Conference (ACC)*, Jun. 2011, pp. 2050–2055.

[109] O. I. Kostyukova, E. A. Kostina, and N. M. Fedortsova, "Parametric optimal control problems with weighted L_1-norm in the cost function," *Automatic Control and Computer Sciences*, vol. 44, no. 4, pp. 179–190, Aug. 2010.

[110] D. E. Quevedo, E. I. Silva, and D. Nešić, "Design of multiple actuator-link control systems with packet dropouts," *IFAC Proceedings Volumes*, vol. 41, no. 2, pp. 6642 – 6647, 2008, 17th IFAC World Congress.

[111] S. Bhattacharya and T. Başar, "Sparsity based feedback design: A new paradigm in opportunistic sensing," in *Proceedings of the 2011 American Control Conference (ACC)*, Jun. 2011, pp. 3704–3709.

[112] A. Charles, M. S. Asif, J. Romberg, and C. Rozell, "Sparsity penalties in dynamical system estimation," in *Proceedings of the 45th Annual Conference on Information Sciences and Systems*, Mar. 2011, pp. 1–6.

[113] M. B. Wakin, B. M. Sanandaji, and T. L. Vincent, "On the observability of linear systems from random, compressive measurements," in *Proceedings of the 49th IEEE Conference on Decision and Control (CDC)*, Dec. 2010, pp. 4447–4454.

[114] G. Joseph and C. R. Murthy, "On the observability of a linear system with a sparse initial state," *IEEE Signal Processing Letters*, vol. 25, no. 7, pp. 994–998, Jul. 2018.

[115] M. Nagahara and D. E. Quevedo, "Sparse representations for packetized predictive networked control," *IFAC Proceedings Volumes*, vol. 44, no. 1, pp. 84 – 89, 2011, 18th IFAC World Congress.

[116] M. Nagahara, D. E. Quevedo, T. Matsuda, and K. Hayashi, "Compressive sampling for networked feedback control," in *Proceedings of the 2012 IEEE International Conference on Acoustics, Speech and Signal Processing (ICASSP)*, Mar. 2012, pp. 2733–2736.

[117] M. Nagahara, T. Matsuda, and K. Hayashi, "Compressive sampling for remote control systems," *IEICE Transactions on Fundamentals of Electronics, Communications and Computer Sciences*, vol. 95, no. 4, pp. 713–722, 2012.

[118] M. Nagahara, D. E. Quevedo, and D. Nešić, "Maximum hands-off control: a paradigm of control effort minimization," *IEEE Transactions on Automatic Control*, vol. 61, no. 3, pp. 735–747, Mar. 2016.

[119] ——, "Maximum hands-off control and L^1 optimality," in *Proceedings of the 52nd IEEE Conference on Decision and Control (CDC)*, Dec. 2013, pp. 3825–3830.

[120] T. Ikeda and M. Nagahara, "Value function in maximum hands-off control for linear systems," *Automatica*, vol. 64, pp. 190 – 195, 2016.

[121] M. Nagahara, J. Østergaard, and D. E. Quevedo, "Discrete-time hands-off control by sparse optimization," *EURASIP Journal on Advances in Signal Processing*, vol. 2016, no. 1, p. 76, Jun. 2016.

[122] J. Huang and Y. Shi, "Guaranteed cost control for multi-sensor networked control systems using historical data," in *Proceedings of the 2012 American Control Conference (ACC)*, Jun. 2012, pp. 4927–4932.

[123] H. Kong, G. C. Goodwin, and M. M. Seron, "A cost-effective sparse communication strategy for networked linear control systems: an SVD-based approach," *International Journal of Robust and Nonlinear Control*, vol. 25, no. 14, pp. 2223–2240, 2015.

[124] M. Nagahara, D. E. Quevedo, and J. Østergaard, "Sparse packetized predictive control for networked control over erasure channels," *IEEE Transactions on Automatic Control*, vol. 59, no. 7, pp. 1899–1905, Jul. 2014.

[125] ——, "Packetized predictive control for rate-limited networks via sparse representation," in *Proceedings of the 51st IEEE Conference on Decision and Control (CDC)*, Dec. 2012, pp. 1362–1367.

[126] M. Nagahara, D. E. Quevedo, and J. Ostergaard, "Sparsely-packetized predictive control by orthogonal matching pursuit," *arXiv preprint arXiv:1308.0518*, 2013.

[127] J. K. Yook, D. M. Tilbury, and N. R. Soparkar, "A design methodology for distributed control systems to optimize performance in the presence of time delays," in *Proceedings of the 2000 American Control Conference (ACC)*, vol. 3, Jun. 2000, pp. 1959–1964.

[128] Y. Tipsuwan and M.-Y. Chow, "Network-based controller adaptation based on qos negotiation and deterioration," in *Proceedings of the 27th Annual Conference of the IEEE Industrial Electronics Society (IECON)*, vol. 3, Nov. 2001, pp. 1794–1799.

[129] D. Zhang, Q. Han, and X. Jia, "Network-based output tracking control for a class of T-S fuzzy systems that can not be stabilized by nondelayed output feedback controllers," *IEEE Transactions on Cybernetics*, vol. 45, no. 8, pp. 1511–1524, Aug. 2015.

[130] B. Zhang, Q. Han, X. Zhang, and X. Yu, "Sliding mode control with mixed current and delayed states for offshore steel jacket platforms," *IEEE Transactions on Control Systems Technology*, vol. 22, no. 5, pp. 1769–1783, Sept. 2014.

[131] B.-L. Zhang and Q.-L. Han, "Network-based modelling and active control for offshore steel jacket platform with TMD mechanisms," *Journal of Sound and Vibration*, vol. 333, no. 25, pp. 6796 – 6814, 2014.

[132] J. Nilsson *et al.*, "Real-time control systems with delays," Ph.D. dissertation, Lund Institute of Technology, 1998.

[133] G. C. Walsh and H. Ye, "Scheduling of networked control systems," *IEEE Control Systems Magazine*, vol. 21, no. 1, pp. 57–65, Feb. 2001.

[134] F.-L. Lian, J. R. Moyne, and D. M. Tilbury, "Performance evaluation of control networks: Ethernet, ControlNet, and DeviceNet," *IEEE Control Systems Magazine*, vol. 21, no. 1, pp. 66–83, Feb. 2001.

[135] W. Zhang, M. S. Branicky, and S. M. Phillips, "Stability of networked control systems," *IEEE Control Systems Magazine*, vol. 21, no. 1, pp. 84–99, Feb. 2001.

[136] Y. Halevi and A. Ray, "Integrated communication and control systems: part I—analysis," *Journal of Dynamic Systems, Measurement, and Control*, vol. 110, no. 4, pp. 367–373, 1988.

[137] R. Luck and A. Ray, "An observer-based compensator for distributed delays," *Automatica*, vol. 26, no. 5, pp. 903 – 908, 1990.

[138] ——, "Experimental verification of a delay compensation algorithm for integrated communication and control systems," *International Journal of Control*, vol. 59, no. 6, pp. 1357–1372, 1994.

[139] H. Chan and Ü. Özgüner, "Closed-loop control of systems over a communications network with queues," *International Journal of control*, vol. 62, no. 3, pp. 493–510, 1995.

[140] G. C. Walsh, O. Beldiman, and L. Bushnell, "Asymptotic behavior of networked control systems," in *Proceedings of the 1999 IEEE International Conference on Control Applications (ICCA)*, vol. 2, Aug. 1999, pp. 1448–1453.

[141] G. C. Walsh, H. Ye, and L. Bushnell, "Stability analysis of networked control systems," in *Proceedings of the 1999 American Control Conference (ACC)*, vol. 4, Jun. 1999, pp. 2876–2880.

[142] S. H. Hong, "Scheduling algorithm of data sampling times in the integrated communication and control systems," *IEEE Transactions on Control Systems Technology*, vol. 3, no. 2, pp. 225–230, Jun. 1995.

[143] N. Xi and T.-J. Tarn, "Planning and control of internet-based teleoperation," in *Telemanipulator and Telepresence Technologies V*, vol. 3524, 1998, pp. 189–196.

[144] Z. Du, D. Yue, and S. Hu, "H-infinity stabilization for singular networked cascade control systems with state delay and disturbance," *IEEE Transactions on Industrial Informatics*, vol. 10, no. 2, pp. 882–894, May 2014.

[145] Y. Zheng, H. Fang, and H. O. Wang, "Takagi-sugeno fuzzy-model-based fault detection for networked control systems with Markov delays," *IEEE Transactions on Systems, Man, and Cybernetics, Part B (Cybernetics)*, vol. 36, no. 4, pp. 924–929, Aug. 2006.

[146] M. A. Khanesar, O. Kaynak, S. Yin, and H. Gao, "Adaptive indirect fuzzy sliding mode controller for networked control systems subject to time-varying network-induced time delay," *IEEE Transactions on Fuzzy Systems*, vol. 23, no. 1, pp. 205–214, Feb. 2015.

[147] R. Lu, H. Cheng, and J. Bai, "Fuzzy-model-based quantized guaranteed cost control of nonlinear networked systems," *IEEE Transactions on Fuzzy Systems*, vol. 23, no. 3, pp. 567–575, Jun. 2015.

[148] J. Xiong, J. Lam, Z. Shu, and X. Mao, "Stability analysis of continuous-time switched systems with a random switching signal," *IEEE Transactions on Automatic Control*, vol. 59, no. 1, pp. 180–186, Jan. 2014.

[149] L. Qiu, Y. Shi, F. Yao, G. Xu, and B. Xu, "Network-based robust H_2/H_∞ control for linear systems with two-channel random packet dropouts and time delays," *IEEE Transactions on Cybernetics*, vol. 45, no. 8, pp. 1450–1462, Aug. 2015.

[150] Z. Pang, G. Liu, D. Zhou, and M. Chen, "Output tracking control for networked systems: A model-based prediction approach," *IEEE Transactions on Industrial Electronics*, vol. 61, no. 9, pp. 4867–4877, Sept. 2014.

[151] H. Li and Y. Shi, "Network-based predictive control for constrained nonlinear systems with two-channel packet dropouts," *IEEE Transactions on Industrial Electronics*, vol. 61, no. 3, pp. 1574–1582, Mar. 2014.

[152] W. Yao, L. Jiang, J. Wen, Q. Wu, and S. Cheng, "Wide-area damping controller for power system interarea oscillations: A networked predictive control approach," *IEEE Transactions on Control Systems Technology*, vol. 23, no. 1, pp. 27–36, Jan. 2015.

[153] T. M. Cover and J. A. Thomas, *Elements of information theory.* John Wiley & Sons, 2012.

[154] M. Nagahara, D. E. Quevedo, and D. Nesic, "Hands-off control as green control," *arXiv preprint arXiv:1407.2377*, 2014.

Part II

Papers

Paper A

Interplay Between Transmission Delay, Average Data Rate, and Performance in Output Feedback Control over Digital Communication Channels

Mohsen Barforooshan, Jan Østergaard, and Milan S. Derpich

The paper has been published in the proceedings of the
2017 American Control Conference (AAC), 2017.

The layout has been revised.

Abstract

The performance of a noisy linear time-invariant (LTI) plant, controlled over a noiseless digital channel with transmission delay, is investigated in this paper. The rate-limited channel connects the single measurement output of the plant to its single control input through a causal, but otherwise arbitrary, coder-controller pair. An information-theoretic approach is utilized to analyze the minimal average data rate required to attain the quadratic performance when the channel imposes a known constant delay on the transmitted data. This infimum average data rate is shown to be lower bounded by minimizing the directed information rate across a set of LTI filters and an additive white Gaussian noise (AWGN) channel. It is demonstrated that the presence of time delay in the channel increases the data rate needed to achieve a certain level of performance. The applicability of the results is verified through a numerical example.

1 Introduction

Rate-constrained NCSs are generally studied from two points of view; control theory and information theory. In the former case, classical nonlinear control methods are employed. In the latter case, the key idea is extending information-theoretic notions to the case of closed-loop control. In both frameworks, stability analysis of linear time-invariant (LTI) systems is well-studied (see, e.g., [1], [2] as early results and [3], [4] as recent contributions).

However, studies analyzing system performance from an information-theoretic viewpoint are less abundant in the literature. Fundamental results are presented in [5]. In this work, for a discrete-time LTI plant, the well-known Bode's integral is extended to the case of causal rate-limited arbitrary feedback. Along the lines of [5], research reported in [6, 7] has investigated bounds on the minimum data rate which is needed to attain a quadratic performance level in NCSs with delay-free channels. For the lower bound, [7] shows that the rate-constrained optimization to find desired infimal data rates over causal but otherwise arbitrary coder-controller pairs, is reduced to a convex SNR-constrained optimization problem over an auxiliary LTI feedback loop closed through an AWGN channel. In [6, 7], it is furthermore shown that the directed information from the plant output and to the control input provides a lower bound on the coding rate for any coding policy, and that it suffices to use linear coding policies, when the initial state and external disturbances are jointly Gaussian and the plant is linear. These findings were used by [8], to establish a general SDP framework for the problem of LQG control for fully observable multiple-input multiple-output (MIMO) LTI plants.

In this paper, we address output feedback control of an NCS comprised of a noisy LTI plant and a causal encoder-controller-decoder set connected through

a noiseless digital channel with a constant transmission delay. More specifically, the problem is obtaining the bounds on minimal average data rate required to guarantee that the steady-state variance of an error signal does not become larger than a certain value. Motivated by its merits such as simplicity and practical appeal, we use the approach pursued in [6, 7] to gain outer bounds and build upon [7]. However, the main departure of this work from [7] is considering a channel which is not delay-free. So, as the first contribution, we rederive fundamental information inequalities of the system under the delay assumption. Secondly, we characterize the trade-off among performance, delay, and minimal desired average data rate. It is shown through a numerical example that greater transmission delay necessitates greater minimal average data rate needed to guarantee achieving the considered quadratic level of performance. Simulation indicates that by employing a simple scalar uniform quantizer in the LTI architecture that gives the lower bound, the quadratic performance is attained by operational average data rates at most 0.3 bits away from the lower bound.

The outline of this work is as follows. Section 2 presents the notation and some preliminaries. Then the problem of interest is formalized in Section 3. Section 4 is dedicated to the lower bound characterization. An illustrative numerical simulation is provided in Section 5. Finally, Section 6 concludes the paper.

2 Notation And Preliminaries

The set of real numbers is denoted by $\mathbb{R}$ with subset $\mathbb{R}^+$ as the set of strictly positive real numbers. $\mathbb{N}$ represents the set of natural numbers, based upon which $\mathbb{N}_0 = \mathbb{N} \cup \{0\}$ is defined. Furthermore, k is the time index and for random processes considered in this paper, $k \in \mathbb{N}_0$ holds. Magnitude and H_2-norm of a signal are symbolized by $|.|$ and $\|.\|_2$, respectively. The set $\mathcal{U}_\infty$ is defined as the set of all proper and real rational stable transfer functions with inverses that are stable and proper as well. $\mathcal{E}$ denotes the expectation operator and log stands for the natural logarithm. The entry of matrix S on the i-th row and j-th column is denoted by $[S]_{i,j}$. Moreover, $\lambda_{\min}(S)$ and $\lambda_{\max}(S)$ represent eigenvalues of S with the smallest and largest magnitude, respectively.

All random variables and processes in this paper are assumed to be vector valued, unless otherwise stated. A random process ξ is said to be asymptotically wide-sense stationary (AWSS) if it satisfies $\lim_{k\to\infty} \mathcal{E}[\xi(k)] = \nu_\xi$ and $\lim_{k\to\infty} \mathcal{E}[(\xi(k+\tau) - \mathcal{E}[\xi(k+\tau)])(\xi(k) - \mathcal{E}[\xi(k)])^T] = R_\xi(\tau)$ hold, where ν_ξ is a constant. $C_\xi = R_\xi(0)$ denotes the corresponding steady-state covariance matrix upon which the steady-state variance of ξ is defined as $\sigma_\xi^2 \triangleq \text{trace}(C_\xi)$. The covariance matrix for a scalar random sequence $x_1^k \triangleq [x(1) \dots x(k)]^T$ is defined as $C_{x_1^k} = \mathcal{E}[(x_1^k - \mathcal{E}[x_1^k])(x_1^k - \mathcal{E}[x_1^k])^T]$. Considering $P_n, Q_n \in \mathbb{R}^{n\times n}$ as

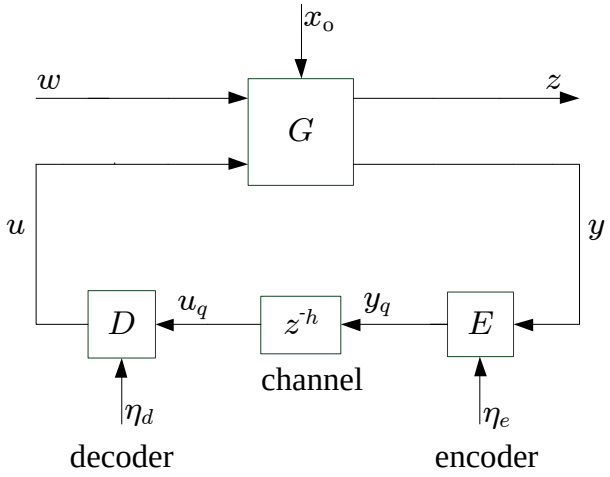

Fig. A.1: Considered NCS

two square matrices, the sequences $\{P_n\}_{n=1}^{\infty}$ and $\{Q_n\}_{n=1}^{\infty}$ are asymptotically equivalent if and only if the following holds for finite ϱ:

$$\lim_{n\to\infty} \frac{1}{n} \sum_{i=1}^{n} \sum_{j=1}^{n} |[P_n - Q_n]_{i,j}|^2 = 0$$
$$|\lambda_{\max}(P_n)|, |\lambda_{\max}(Q_n)| \leq \varrho, \quad \forall n \in \mathbb{N}$$

3 Problem Statement

The structure considered in this work can be found in Fig. A.1 where G is an LTI plant with $u \in \mathbb{R}$ as control input and $y \in \mathbb{R}$ as sensor output. Moreover, there is a disturbance represented by $w \in \mathbb{R}^{n_w}$ and the output signal $z \in \mathbb{R}^{n_z}$, with $n_w, n_z \in \mathbb{N}$, upon which the desired performance is characterized. The plant has the following transfer-function matrix description:

$$\begin{bmatrix} z \\ y \end{bmatrix} = \begin{bmatrix} G_{11} & G_{12} \\ G_{21} & G_{22} \end{bmatrix} \begin{bmatrix} w \\ u \end{bmatrix}, \tag{A.1}$$

in which every G_{ij} is proper and of suitable dimensions ($n_z \times n_w$, $n_z \times 1$, $1 \times n_w$ and 1×1 for G_{11}, G_{12}, G_{21} and G_{22}, respectively). The input alphabet of the channel is represented by $\mathcal{A}$ and is defined as a countable set of prefix-free binary words. Due to the delay, the output of the channel $u_q(k)$ follows $u_q(k) = y_q(k-h)$ for $k \geq h$ where $y_q(k)$ belongs to $\mathcal{A}$. The average data rate

across the channel is specified as follows:

$$\mathcal{R} \triangleq \lim_{k\to\infty} \frac{1}{k} \sum_{i=0}^{k-1} R(i), \tag{A.2}$$

where $R(i)$ denotes the expected length of the i-th binary word $y_q(i)$. The channel input is provided by the encoder E based on the following dynamics:

$$y_q(k) = E_k(y^k, \eta_e^k), \tag{A.3}$$

in which $\eta_e(k)$ is the side information at time k at the encoder with E_k representing an arbitrary (possibly nonlinear or time-varying) deterministic mapping. It should be noted that β^k is a shorthand for $[\beta(0), \cdots, \beta(k)]$. On the decoder side, we have

$$u(k) = \begin{cases} D_k(\eta_d^k), & 0 \le k < h, \\ D_k(y_q^{k-h}, \eta_d^k), & k \ge h. \end{cases}$$

D_k is assumed to be an arbitrary deterministic mapping, like E_k, and $\eta_d(k)$ signifies the side information available at the decoder at time k. It should be emphasized that E and D in Fig. A.1 are possibly time-varying or nonlinear causal systems.

Assumption 3.1
The plant G is LTI, proper and free of unstable hidden modes. Moreover, the open-loop transfer function from u to y is single-input single-output (SISO) and strictly proper. The disturbance signal, w, is a zero-mean white noise with identity covariance matrix $C_w = I$ and jointly Gaussian with $x_0 = [x(-h), \cdots, x(0)]^T$, the initial condition, having finite differential entropy.

Assumption 3.2
Each of processes η_e and η_d is jointly independent of (x_0, w). So regarding the dynamics of the system, $I(u(k); y^{k-h} \mid u^{k-1}) = 0$ holds for $0 \le k < h$. Moreover, upon knowledge of u^i and η_d^i, the decoder is invertible. It means that there exists a deterministic mapping Q_i such that $u_q^i = Q_i(u^i, \eta_d^i)$.

Now, suppose that Assumption 3.1 holds. Let $D_{\inf}(h)$ denote the infimum steady-state variance of the output z over all settings $u(k) = \mathcal{K}_k(\gamma^k)$ for $0 \le k < h$ and $u(k) = \mathcal{K}_k(y^{k-h})$ for $k \ge h$ with γ^k independent of x_0 and w. Then the problem of interest is finding

$$\mathcal{R}(D) = \inf_{\sigma_z^2 \le D} \mathcal{R} \tag{A.4}$$

for any $D \in (D_{\inf}(h), \infty)$, where the search is to be restricted to encoders with mapping E_k and decoders with mapping D_k which satisfy Assumption 3.2 and make the NCS of Fig. A.1 strongly asymptotically wide-sense stationary (SAWSS) (this notion of stability is defined in [7]). Moreover, σ_z^2 denotes the steady-state variance of z. The optimization problem in (A.4) is feasible if $D \in (D_{\inf}(h), \infty)$ (see Appendix A for the proof).

4 Main Results

Theorem 4.1
For the feedback loop depicted in Fig. A.1 and satisfying Assumptions 3.1 and 3.2, the following holds:

$$\mathcal{R} \geq I_{\infty}^{(h)}(y \to u) = \lim_{k\to\infty} \frac{1}{k} \sum_{i=0}^{k-1} I(u(i); y^{i-h} \mid u^{i-1}), \tag{A.5}$$

in which $I(.;. \mid .)$ indicates conditional mutual information (see [9] for the definition). Moreover, as defined in [10], $I_{\infty}^{(h)}(y \to u)$ denotes the directed information rate across the forward channel from y to u with delay h. The proof can be found in [11].

Now, a lower bound can be derived on the directed information across the coding scheme of Fig. A.1.

Lemma 4.1
For the NCS of Fig. A.1, assume that $(x(0), w, u, y)$ form a jointly second-order set of processes and that Assumptions 3.1 and 3.2 hold. Moreover, take y_G and u_G into account as the Gaussian counterparts of y and u where $(x(0), w, u_G, y_G)$ are jointly Gaussian with the same first-and second-order (cross-) moments as $(x(0), w, u, y)$. Then $I_{\infty}^{(h)}(y \to u) \geq I_{\infty}^{(h)}(y_G \to u_G)$.

Proof. The following inequalities and identities will justify the claim:

$$\begin{aligned}
&\sum_{i=0}^{k-1} I(u(i); y^{i-h} \mid u^{i-1}) \overset{\text{(a)}}{=} I(x(0), w^{k-1}; u^{k-1}) \\
&\overset{\text{(b)}}{\geq} I(x(0), w^{k-1}; u_G^{k-1}) \\
&\overset{\text{(c)}}{=} \sum_{i=0}^{k-1} I(x(0), w^{i}; u_G(i) \mid u_G^{i-1}) \\
&\overset{\text{(d)}}{\geq} \sum_{i=0}^{k-1} I(x(0), w^{i-1}, y_G^{i-h}; u_G(i) \mid u_G^{i-1}) \\
&\overset{\text{(e)}}{=} \sum_{i=0}^{k-1} I(y_G^{i-h}; u_G(i) \mid u_G^{i-1}),
\end{aligned} \tag{A.6}$$

where (a) follows from a slight modification in [7, Lemma B.4], (b) follows from [7, Lemma B.1], (c) holds form the Markov chain $u_G(i) - u_G^{i-1}, x(0), w^i - w_{i+1}^{k-1}$ based upon (51b) in [7, Theorem B.3], (d) is a consequence of Assumption 3.1 and y_G^i being a deterministic function of $u_G^{i-1}, x(0)$ and w^i, and (e) stems from (51a) in [7, Theorem B.3] and Assumption 3.1. This completes the proof. □

In what follows we will relate the directed information from y_G to u_G to their corresponding power spectral densities:

Lemma 4.2
Consider y and u as jointly Gaussian AWSS processes. Moreover, suppose that u is SAWSS with $|\lambda_{\min}(C_{u_1^n})| \geq \mu$, $\forall n \in \mathbb{N}$ where $\mu > 0$. Then the following can be obtained:

$$I_{\infty}^{(h)}(y \to u) = \frac{1}{4\pi} \int_{-\pi}^{\pi} \log\big(\frac{S_{\breve{u}}(e^{j\omega})}{\sigma_{\psi}^2}\big) d\omega, \tag{A.7}$$

in which ψ is a Gaussian AWSS process with independent samples defined as:

$$\psi(k) \triangleq u(k) - \tilde{u}(k), \tilde{u}(k) \triangleq E[u(k) \mid y^{k-h}, u^{k-1}]. \tag{A.8}$$

Moreover, $S_{\breve{u}}$ represents the steady-state power spectral density of u.

Proof. Having Gaussianity and joint AWSS-ness of (u, y) in mind and based on [12, Theorem 2.4] with a little modification, we can conclude that ψ is Gaussian and AWSS as well. We start by the following equalities:

$$\begin{aligned} I(u(i); y^{i-h} \mid u^{i-1}) &\overset{(f)}{=} h(u(i) \mid u^{i-1}) - h(u(i) \mid y^{i-h}, u^{i-1}) \\ &\overset{(g)}{=} h(u(i) \mid u^{i-1}) - h(\psi(i) + \tilde{u}(i) \mid y^{i-h}, u^{i-1}) \\ &\overset{(h)}{=} h(u(i) \mid u^{i-1}) - h(\psi(i) \mid y^{i-h}, u^{i-1}) \\ &\overset{(i)}{=} h(u(i) \mid u^{i-1}) - h(\psi(i)), \end{aligned} \tag{A.9}$$

where (f) follows from the definition of mutual information and (g) from the definition of ψ, (h) stems from [7, Property 2] and (A.8), and (i) holds from [7, Property 3]. So the directed information rate can therefore be rewritten as follows:

$$\begin{aligned} I_{\infty}^{(h)}(y \to u) &= \lim_{k\to\infty} \frac{1}{k} \sum_{i=0}^{k-1} \{h(u(i) \mid u^{i-1}) - h(\psi(i))\} \\ &\overset{(j)}{=} \lim_{k\to\infty} \frac{1}{k} h(u^{k-1}) - \lim_{k\to\infty} h(\psi(k)) \\ &\overset{(k)}{=} \frac{1}{4\pi} \int_{-\pi}^{\pi} \log(2\pi e S_{\breve{u}}(e^{j\omega})) d\omega - \frac{1}{2} \log(2\pi e \sigma_{\psi}^2), \end{aligned} \tag{A.10}$$

where (j) follows from the chain rule of the differential entropy and $\psi(k)$ being independent of ψ^{k-1}. Since the process u is SAWSS with $|\lambda_{\min}(C_{u_1^n})| \geq \mu$, $\forall n \in \mathbb{N}$ for some $\mu > 0$, [7, Lemma B.5] will approve the validity of the leftmost term in (k). The rightmost term is self-explanatory because ψ is Gaussian and AWSS. □

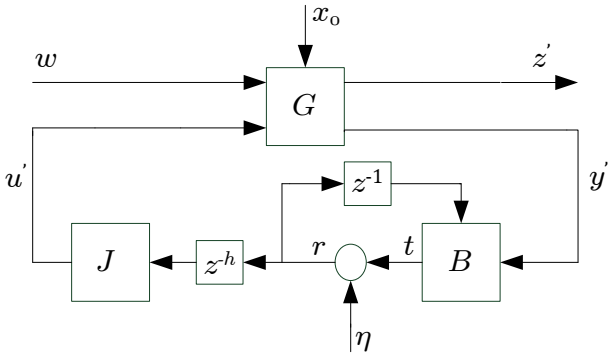

Fig. A.2: Auxiliary LTI NCS

It follows from Theorem 4.1, Lemma 4.1 and Lemma 4.2 that the rate-performance pair yielded by any encoder-decoder scheme which renders the NCS SAWSS, is attainable with a lower rate by a coding scheme comprised of LTI filters and an AWGN noise source. Such a scheme is depicted in Fig. A.2.

The NCS of Fig. A.2 is defined under the same conditions (Assumption 3.1) as the main system in Fig. A.1 except for one thing; the arbitrary mappings are replaced by proper LTI filters B and J. Moreover, the communication channel is a delayed AWGN channel with noiseless one-sample-delayed feedback. The dynamics of this auxiliary coding scheme can be summarized as follows:

$$u' = Jz^{-h}r, \quad r = t + \eta, \quad t = B\mathrm{diag}\{z^{-1}, 1\}\begin{bmatrix} r \\ y' \end{bmatrix}, \tag{A.11}$$

in which η is the AWGN with zero mean and variance σ_η^2. This noise is assumed to be independent of (x_0, w). Additionally, we suppose that the initial state of B, J, and the delay are deterministic.

Theorem 4.2
For the NCS depicted in Fig. A.1 and satisfying Assumptions 3.1 and 3.2, $\mathcal{R}(D)$ is lower bounded as follows if $D \in (D_{\inf}(h), \infty)$:

$$\mathcal{R}(D) \geq \vartheta'_u(D) \triangleq \inf_{\sigma^2_{z'} \leq D} \frac{1}{4\pi} \int_{-\pi}^{\pi} \log\left(\frac{S_{u'}(e^{j\omega})}{\sigma_\eta^2}\right), \tag{A.12}$$

where the feasible set for the optimization problem defining $\vartheta'_u(D)$ is all LTI filters B and the noise η with $\sigma_\eta^2 \in \mathbb{R}_+$ rendering the feedback loop of Fig. A.2 internally stable and well-posed when $J = 1$. In these expressions, $\sigma^2_{z'}$ and $S_{u'}$ denote the steady-state variance of z' and the steady-state power spectral density of u' in Fig. A.2, respectively.

Proof. Since $D > D_{\inf}(h)$, there is at least one pair, say $\hat{E}$ and $\hat{D}$, satisfying Assumption 3.2, rendering the NCS of Fig. A.1 SAWSS and producing $\hat{z}$, $\hat{y}$ and $\hat{u}$ where $\sigma_{\hat{z}}^2 \leq D$ holds and

$$\mathcal{R} \geq I_{\infty}^{(h)}(\hat{y} \to \hat{u}) \geq I_{\infty}^{(h)}(\hat{y}_G \to \hat{u}_G) = \frac{1}{4\pi}\int_{-\pi}^{\pi} \log\big(\frac{S_{\breve{u}}(e^{j\omega})}{\sigma_{\hat{\psi}_G}^2}\big)d\omega$$

can be concluded based on Theorem 4.1, if the conditions in Lemma 4.1 and Lemma 4.2 are met. It should be noted that $S_{\breve{u}}$ denotes the steady-state power spectral density of $\hat{u}_G$. A coding scheme comprised of linear filters with a unit-gain noisy channel and delay h can generate $\hat{y}_G$ and $\hat{u}_G$ which satisfy those conditions and keep $\sigma_{\hat{z}_G}^2$ within $(D_{\inf}(h), \infty)$. Such a scheme is described as follows:

$$\hat{u}_G(k) = L_k(\hat{y}_G^{k-h}, \hat{u}_G^{k-1}) + \hat{\psi}_G(k-h), \qquad k \in \mathbb{N}_0 \tag{A.13}$$

where $\hat{\psi}_G(k)$ represents a Gaussian noise with zero mean and independent of $(\hat{y}_G^k, \hat{u}_G^{k-1})$. Regarding the causality and linearity of L_k, $\hat{u}_G^k$ can be written as follows:

$$\hat{u}_G^k = Q_k\hat{\psi}_G^{k-h} + P_k\hat{y}_G^{k-h}, \qquad k \in \mathbb{N}_0. \tag{A.14}$$

According to the causality in (A.14), joint SAWSS-ness of $(\hat{y}_G, \hat{u}_G)$ and transitivity of asymptotic equivalence for products and sum of the matrices noted in [13], the sequences $\{Q_k\}$ and $\{P_k\}$ are asymptotically equivalent to sequences of lower triangular Toeplitz matrices. Moreover, L_k renders the NCS internally stable and well-posed. With all of this in mind, by setting $J = 1$ and B as a concatenation of linear filters with the steady-state behaviour of L_k in (A.13) and considering a variance for η equal to $\sigma_{\hat{\psi}_G}^2$, the system of Fig. A.2 will be rendered well-posed and internally stable where $S_{u'} = S_{\breve{u}}$ and $\sigma_{\hat{z}_G}^2 = \sigma_{z'}^2$ are resulted. Then according to Lemma 4.2, the following can be concluded:

$$I_{\infty}^{(h)}(y' \to u') = \frac{1}{4\pi}\int_{-\pi}^{\pi} \log\big(\frac{S_{u'}(e^{j\omega})}{\sigma_{\eta}^2}\big)d\omega = \frac{1}{4\pi}\int_{-\pi}^{\pi} \log\big(\frac{S_{\breve{u}}(e^{j\omega})}{\sigma_{\hat{\psi}_G}^2}\big)d\omega,$$

which completes the proof. □

Lemma 4.3
Consider the LTI loop of Fig. A.2 with fixed $\sigma_{\eta}^2 \in \mathbb{R}^+$. Define $\vartheta_r^{'}$ as follows:

$$\vartheta_r^{'}(B, J, \sigma_{\eta}^2) \triangleq \frac{1}{4\pi}\int_{-\pi}^{\pi} \log\big(\frac{S_r(e^{j\omega})}{\sigma_{\eta}^2}\big), \tag{A.15}$$

in which S_r represents the steady-state power spectral density of r. Then for any $\rho > 0$, upon the existence of the pair $(B, J) = (B_1, J_1)$ making the system of Fig. A.2 internally stable and well-posed, there exist another pair, comprised of the biproper filter J_2 and B_2, which renders the feedback loop of Fig. A.2

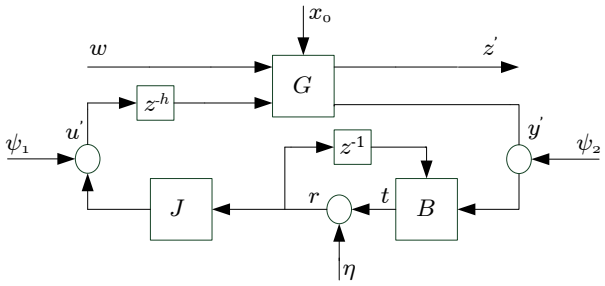

Fig. A.3: Equivalent archtiectural viewpoint of internal stability

internally stable and well-posed, preserves the the steady-state power spectral density of z' and satisfies the following:

$$\vartheta_r^{'}(B_1, J_1, \sigma_\eta^2) = \vartheta_r^{'}(B_2, J_2, \sigma_\eta^2) = \frac{1}{2}\log(1 + \frac{\sigma_t^2}{\sigma_\eta^2})|_{(B,J)=(B_2,J_2)} - \rho. \quad \text{(A.16)}$$

Proof. It is well-known that the system of Fig. A.2 is well-posed and internally stable if and only if the transfer function T from $[\eta, w, \psi_1, \psi_2]^T$ to $[z', y', r, u']^T$ in Fig. A.3 belongs to $\mathcal{RH}_\infty$. By T_i and r_i, we refer to the transfer-function matrix T and signal r when B and J are set such that $(B, J) = (B_i, J_i), i \in \{1, 2\}$. Moreover, B_{yi} and B_{ri} represent elements of B ($B = [B_r \quad B_y]$) in the situation where $B = B_i$. Now, consider the following set of filters:

$$J_2 = z^{d_1} J_1 V^{-1}, \quad B_{y2} = z^{-d_1} B_{y1}, \quad B_{r2} = z(1 - (1 - B_{r1} z^{-1})V^{-1}), \quad \text{(A.17)}$$

in which d_1 indicates the relative degree of J_1 and $V \in \mathcal{U}_\infty$ is chosen in such a way that $V(\infty) = 1$. Consequently, J_2 is biproper and T_2 can be written as follows:

$$T_2 = \text{diag}\{z^{d_1} I, z^{d_1} I, V, z^{d_1} I\} \times T_1 \times \text{diag}\{I, z^{-d_1} I, z^{-d_1} I, z^{-d_1} I\}.$$

So regarding the definition of d_1 and properties of V, $T_2 \in \mathcal{RH}_\infty$ if and only if $T_1 \in \mathcal{RH}_\infty$. Moreover, based on the same argument, using (B_2, J_2) would give the same power spectral density for z' as for the case where (B_1, J_1) is utilized. Let $\delta_1, \ldots, \delta_m$ represent the zeros of Γ_{r_1} lying on the unit circle. Now for $\zeta \in (0, 1)$ we define the following:

$$\hat{\Gamma}_{r_1} \triangleq \Gamma_{r_1} \prod_{i=1}^{m} z(z - \delta_i)^{-1}, \quad V_\zeta \triangleq (\hat{\Gamma}_{r_1})^{-1} \hat{\Gamma}_{r_1}(\infty) \prod_{i=1}^{m} z(z - \zeta\delta_i)^{-1}.$$

Hence, $V_\zeta \in \mathcal{U}_\infty$ and $V_\zeta(\infty) = 1$ can be deduced for every $\zeta \in (0, 1)$. By following the same procedure as for the proof of [6, Theorem 5.2], the existence of $\zeta \in (0, 1)$ will be shown in such a way that for any $\rho > 0$, setting $V = V_\zeta$ will give a pair (B_2, J_2) that satisfies (A.16). □

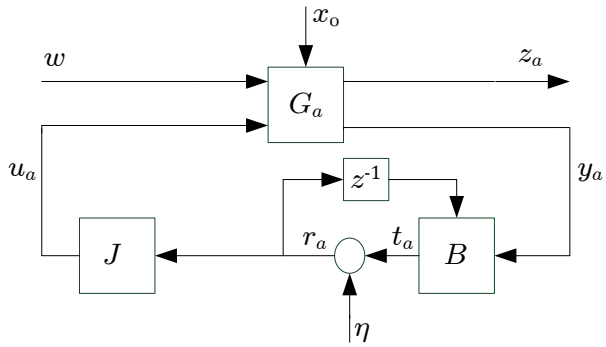

Fig. A.4: Auxiliary system for $\varphi'(D)$ minimization

Corollary 4.1
If Assumptions 3.1 and 3.2 hold for the NCS of Fig. A.1 and $D \in (D_{\inf}(h), \infty)$, then

$$\mathcal{R}(D) \geq \frac{1}{2}\log(1+\varphi'(D)), \varphi'(D) \triangleq \inf_{\sigma^2_{z'} \leq D} \frac{\sigma_t^2}{\sigma_\eta^2}, \tag{A.18}$$

where the optimization is done over all LTI filter pairs (B, J) and the noise variance $\sigma_\eta^2 \in \mathbb{R}^+$ making the system in Fig. A.2 internally stable and well-posed.

Proof. According to the feasibility of finding $\vartheta'_u(D)$ (see [11] for the proof), there exist the triplet $(B_\zeta, 1, \sigma^2_{\eta_\zeta})$, with B_ζ a proper LTI filter and $\sigma^2_{\eta_\zeta} \in \mathbb{R}^+$, that guarantees $\sigma^2_{z'} \leq D$ for the system of Fig. A.2. Furthermore, based upon the definition of ϑ'_u and ϑ'_r in (A.12) and (A.15), the following can be derived for any $\zeta > 0$:

$$\vartheta'_u(D) + \zeta \geq \vartheta'_r(B_\zeta, 1, \sigma^2_{\eta_\zeta}).$$

So regarding Lemma 4.3, since there exist a biproper filter $\tilde{J}_\zeta$ and a proper one $\tilde{B}_\zeta$ making the LTI feedback loop of Fig. A.2 internally stable and well-posed and keeping $\sigma^2_{z'}$ intact, the following can be concluded:

$$\vartheta'_u(D) + \zeta \geq \frac{1}{2}\log(1+\frac{\sigma_t^2}{\sigma_\eta^2})|_{(B,J,\sigma^2_\eta)=(\tilde{B}_\zeta,\tilde{J}_\zeta,\sigma^2_{\eta_\zeta})} - \rho \tag{A.19}$$

Now the proof is completed by noting that (A.19) holds for any $\zeta, \rho > 0$ □

To characterize $\varphi'(D)$, we will mostly use properties of linear systems and some results on H_2 optimization with input-delay. Consider the auxiliary structure of Fig. A.4, where except for shifting the delay block to the plant model, which leads to

$$G_a = \begin{bmatrix} G_{11} & z^{-h}G_{12} \\ G_{21} & z^{-h}G_{22} \end{bmatrix},$$

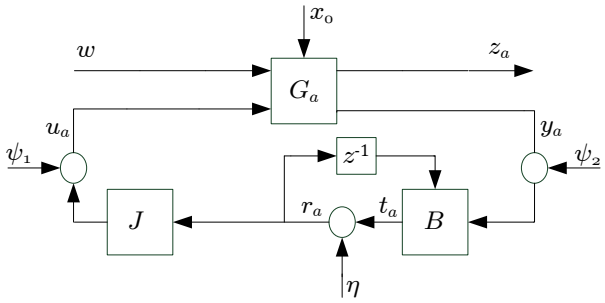

Fig. A.5: Stability analysis of the equivalent system

the same assumptions as Fig. A.2 hold. The NCS of Fig. A.4 is internally stable and well-posed if and only if the transfer function T_a from $[\eta, w, \psi_1, \psi_2]^T$ to $[z_a, y_a, r_a, u_a]^T$ in Fig. A.5 is a member of $\mathcal{RH}_\infty$. It can be easily shown that $T_a = T$. So the feedback loops of Fig. A.4 and Fig. A.2 are equivalent in the sense of internal stability and well-posed-ness. Moreover, the SNR and output variance of the NCS depicted in Fig. A.2 can be stated in terms of H_2-norms as follows:

$$\begin{aligned} \frac{\sigma_t^2}{\sigma_\eta^2} &= \|M-1\|_2^2 + \|B_y M G_{21}\|_2^2 \sigma_\eta^{-2}, \\ \sigma_{z'}^2 &= \left\| G_{11} + G_{12} N (1 - G_{22} N)^{-1} G_{21} \right\|_2^2 + \|G_{12} J M\|_2^2 \sigma_\eta^2, \end{aligned} \tag{A.20}$$

where $N \triangleq J B_y z^{-h} (1 - B_r z^{-1})^{-1}$ and $M \triangleq (1 - B_r z^{-1} - G_{22} J z^{-h} B_y)^{-1}$. Likewise, the following holds for the structure of Fig. A.4:

$$\begin{aligned} \frac{\sigma_{t_a}^2}{\sigma_\eta^2} &= \|M_a - 1\|_2^2 + \|B_y M_a G_{21}\|_2^2 \sigma_\eta^{-2}, \\ \sigma_{z_a}^2 &= \left\| G_{11} + G_{12} z^{-h} N_a (1 - G_{22} z^{-h} N_a)^{-1} G_{21} \right\|_2^2 + \|G_{12} J M_a\|_2^2 \sigma_\eta^2, \end{aligned} \tag{A.21}$$

in which $N_a = J B_y (1 - B_r z^{-1})^{-1}$ and $M_a = M$. As seen, comparing (A.20) and (A.21) signifies the equalities $(\sigma_t^2/\sigma_\eta^2) = (\sigma_{t_a}^2/\sigma_\eta^2)$ and $\sigma_{z'}^2 = \sigma_{z_a}^2$. So every triplet (B, J, σ_η^2) that can infimize the SNR while making the system output satisfy $\sigma_{z'}^2 \leq D$ for the NCS of Fig. A.4, can do the same for the the LTI system of interest, in Fig. A.2, and vice versa. In other words, the NCSs in Fig. A.2 and Fig. A.4 are equivalent regarding the SNR-performance optimization problem in (A.18) as well. This problem is studied for such feedback systems as auxiliary system of Fig. A.4 in [7]. Consequently, it can be concluded that the problem of finding $\varphi'(D)$ is equivalent to an SNR-constrained optimal control problem which was proved to be convex. As another result, $\varphi'(D)$ being a monotonically

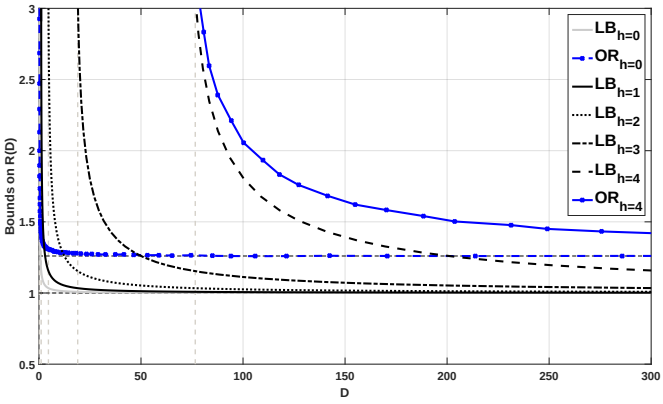

Fig. A.6: Bounds on $\mathcal{R}(D)$ in (A.4) for different values of time delay h

decreasing function of D can be deduced. All in all, the interplay between the desired performance, the average data rate and the time delay is characterized through (A.18), (A.20) and (A.21).

5 Simulation Example

Consider the the following transfer function representation for the plant G in NCS of Fig. A.1:

$$z = \frac{0.165}{(z-2)(z-0.5789)}(w+u), \quad y = z,$$

where (x_0, w) satisfies Assumption 3.1. Using the results of the previous section, we simulate the lower bound on $\mathcal{R}(D)$ obtained in (A.18) regarding five different values of delay ($h = \{0, 1, 2, 3, 4\}$) and for each h, over a range of $D > D_{\inf}(h)$. Fig. A.6 demonstrates the behaviour of the lower bound with respect to D and h. Additionally, it shows the operational rates when using scalar uniform quantizers for $h = 0$ and $h = 4$. First, as expected, $\varphi'(D)$ in (A.18) is a monotonically decreasing function of D. Secondly and more importantly, $D_{\inf}(h)$ increases when h grows (see [14]). So greater delay yields worse best performance. The most significant outcome is associated with the behaviour of $\mathcal{R}(D)$ in (A.4) with respect to delay. It can be observed from Fig. A.6 that for a fixed D, $\varphi'(D)$ is increasing in h. Therefore, a delay in the channel forces an increase in the required infimum data rate to achieve a quadratic level of performance. The greater delay, the higher rate to be spent in order to get a certain level of performance. Indeed, this finding extends the delay-free results of [7]. Another observation is the convergence of the obtained infimal data rates to the minimum rate required for stabilizability as

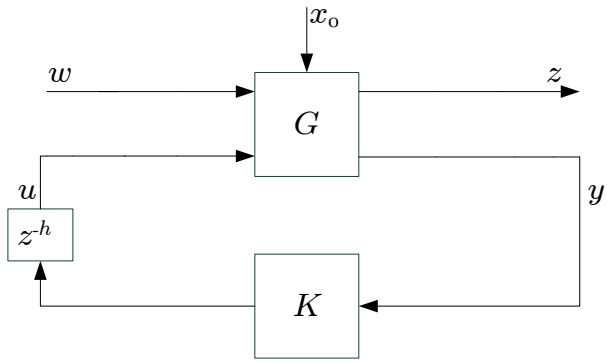

Fig. A.7: Standard feedback loop for proving feasibility of finding $\mathcal{R}(D)$

$D \to \infty$. As illustrated in Fig. A.6, high rates are required to attain the ideal non-networked performance $D_{\inf}(h)$. Along the lines of [6, 7], we now simply replace the AWGN η in the independent coding scheme depicted in Fig. A.2, by a uniform scalar quantizer in order to assess the operational performance caused by a simple coding scheme. It is interesting to note that the obtained operational average data rate in Fig. A.6 is at most around 0.3 bits away from the derived lower bound at all performance.

6 Conclusions

In this paper, rate-constrained networked control systems comprising noisy LTI plants, causal but otherwise arbitrary coding-control schemes and digital noiseless communication channels with time delay, have been studied. For such NCSs, a certain level of performance is attainable if and only if the average data rate does not fall below a minimal value. A lower bound on this infimum rate has been obtained. Through a numerical example, it has been illustrated that the channel's time delay increases the infimum average data rate needed to achieve a prescribed level of performance. Moreover, by using a simple scalar quantizer, operational average data rates fairly close (around 0.3 bits) to the lower bound have been obtained.

Appendices

A Feasibility Proof of $D_{\inf}(h)$

Suppose that in the standard architecture depicted in Fig. A.7, G, x_0 and w satisfy Assumption 3.1 and K follows $u(k) = \mathcal{K}_k(y^{k-h})$. Regarding the

Gaussianity of x_0 and w and the fact that G is LTI, it can be implied from some results in [15] that:

$$D_{\inf}(h) = \inf_{K \in \kappa} \sigma_z^2,$$

in which σ_z^2 denotes the variance of output z and κ is the set of all proper LTI filters which render the system of Fig. A.7 internally stable and well-posed. The assumptions considered for G guarantee that finding $D_{\inf}(h)$ is feasible. The feasibility of finding ${\vartheta'}_u(D)$ in (A.12) and ${\varphi'}_u(D)$ in (A.18) follows from the feasibility of $D_{\inf}(h)$ [11].

References

[1] W. S. Wong and R. W. Brockett, "Systems with finite communication bandwidth constraints. ii. stabilization with limited information feedback," *IEEE Transactions on Automatic Control*, vol. 44, no. 5, pp. 1049–1053, May 1999.

[2] G. N. Nair and R. J. Evans, "Stabilizability of stochastic linear systems with finite feedback data rates," *SIAM Journal on Control and Optimization*, vol. 43, no. 2, pp. 413–436, 2004.

[3] J. Østergaard and D. Quevedo, "Multiple descriptions for packetized predictive control," *EURASIP Journal on Advances in Signal Processing*, vol. 2016, no. 1, p. 45, Apr. 2016.

[4] M. F. Lupu, M. Sun, F. Wang, and Z. Mao, "Information-transmission rates in manual control of unstable systems with time delays," *IEEE Transactions on Biomedical Engineering*, vol. 62, no. 1, pp. 342–351, Jan. 2015.

[5] N. C. Martins and M. A. Dahleh, "Feedback control in the presence of noisy channels: "bode-like" fundamental limitations of performance," *IEEE Transactions on Automatic Control*, vol. 53, no. 7, pp. 1604–1615, Aug. 2008.

[6] E. I. Silva, M. S. Derpich, and J. Østergaard, "A framework for control system design subject to average data-rate constraints," *IEEE Transactions on Automatic Control*, vol. 56, no. 8, pp. 1886–1899, Aug. 2011.

[7] E. I. Silva, M. S. Derpich, J. Østergaard, and M. A. Encina, "A characterization of the minimal average data rate that guarantees a given closed-loop performance level," *IEEE Transactions on Automatic Control*, vol. 61, no. 8, pp. 2171–2186, Aug. 2016.

[8] T. Tanaka, K. H. Johansson, T. Oechtering, H. Sandberg, and M. Skoglund, "Rate of prefix-free codes in lqg control systems," in *Proceedings of the 2016 IEEE International Symposium on Information Theory (ISIT)*, Jul. 2016, pp. 2399–2403.

[9] T. M. Cover and J. A. Thomas, *Elements of information theory*. John Wiley & Sons, 2012.

[10] M. S. Derpich, E. I. Silva, and J. Østergaard, "Fundamental inequalities and identities involving mutual and directed informations in closed-loop systems," *arXiv preprint arXiv:1301.6427*, 2013.

[11] M. Barforooshan, J. Østergaard, and M. S. Derpich, "Interplay between transmission delay, average data rate, and performance in output feedback control over digital communication channels," *arXiv preprint arXiv:1702.06445*, 2017.

[12] B. Porat, *Digital processing of random signals: Theory and methods.* Prentice-Hall, Inc., 1994.

[13] R. M. Gray, *Toeplitz and circulant matrices: A review.* Now Publishers Inc., 2006.

[14] K. Hashikura, "H_2/H_∞ controller design for input-delay and preview systems based on state decomposition approach," Ph.D. dissertation, Tokyo Metropolitan University, 2014.

[15] K. J. Åström, *Introduction to stochastic control theory.* Courier Corporation, 2012.

Paper B

Achievable Performance of Zero-Delay Variable-Rate Coding in Rate-Constrained Networked Control Systems with Channel Delay

Mohsen Barforooshan, Jan Østergaard, and Photios A. Stavrou

The paper has been published in the proceedings of the
56th IEEE Annual Conference on Decision and Control, 2017.

The layout has been revised.

Abstract

This paper presents an upper bound on the minimum data rate required to achieve a prescribed closed-loop performance level in networked control systems (NCSs). The considered feedback loop includes a linear time-invariant (LTI) plant with single measurement output and single control input. Moreover, in this NCS, a causal but otherwise unconstrained feedback system carries out zero-delay variable-rate coding, and control. Between the encoder and decoder, data is exchanged over a rate-limited noiseless digital channel with a known constant time delay. Here we propose a linear source-coding scheme that with the use of entropy-coded dithered quantizers (ECDQs), attains each quadratic performance level with a rate that exceeds the lower bound in [1] by at most (approximately) 1.254 bits per sample. The upper bound obtained by ECDQ is demonstrated, via simulations, to be an increasing function of the channel time delay at any given performance. In other words, attaining a specific performance level necessitates achieving a higher data rate when the channel time delay grows. The theoretical framework is demonstrated via an illustrative example.

1 Introduction

There are two general approaches for analysis and design of rate-limited NCSs. One is based on classical nonlinear control arguments while the other applies information-theoretic tools to feedback systems. Stabilization of linear time-invariant (LTI) loops is covered well with both methodologies [2–5]. Performance results are reported, for instance, in [6, 7] where the control-based approach is used. It should be pointed out that despite the rich literature on NCSs subject to quantization, here the focus is on studies going beyond stability issues. Indeed, we focus on works analyzing operational rates that are necessary to achieve prescribed performance levels and that can be compared to existing bounds. In [6], the best mean squared error (MSE) performance is evaluated for different values of data rate. This work considers an NCS which is controlled according to a packetized predictive control (PPC) strategy together with fixed rate vector quantization. Feedback loop properties such as dual effect, certainty equivalence and separation between coding and control design are studied in [7] for a linear discrete-time plant, where a linear quadratic (LQ) cost is to be minimized. Employing information-theoretic approaches, [8–10] establish performance results. In [8, 9], the aim is obtaining the minimum data rate needed to attain a quadratic performance level in NCSs with delay-free channels. Inspired by a common approach in information theory, the authors of [8, 9] first derive a lower bound on the required minimum data rate. Then since the scheme giving such theoretical lower bound is not necessarily realiz-

able in practice, they propose a method to desgin practically implementable schemes that make the system meet the same performance requirement with rates that are higher than the lower bound but limited from above by a certain value. This upper bound determines how close the operational data rates can get to the corresponding lower bounds. Hence, in [8, 9], first it is shown that the desired minimum data rate is lower bounded by minimizing the directed information rate[1] over an LTI scheme including an additive white Gaussian noise (AWGN) channel. Then, they propose a method to design actual coding schemes by using ECDQs. The use of ECDQs is motivated by advantages such as analysis simplicity and easy implementation [13]. Following [8, 9], the concepts of directed information rate and ECDQ-based linear coding schemes are used in [10] for investigating the rate-performance trade-off in discrete-time LQG control problems.

Recent methods for dealing with delay in NCSs can be categorized into two frameworks: robustness and adaptation [14]. In the robustness framework, stability or performance conditions are obtained through constructing a Lyapunov-Krasovskii functional regardless of delay size information. For example, [15] derives a less conservative stability criterion by incorporating integral terms into the considered functional. In the adaptation approach, the differences between NCSs and conventional delay systems are taken into account. Most of the contributions utilizing this approach model NCSs as stochastic switched systems [16] or employ predictive control [17].

Although there are works in the literature studying the performance of NCSs with channels subject to both rate limitations and time-delays (see, e.g., [18] and [19]), only a few of them analyze system's performance by means of information theoretic tools. For instance, in [1], the authors consider a channel with time delay and derive a lower bound on minimal average data rate required to attain a certain level of performance. To do so, they use the idea of minimizing directed information as in [8]. Among others, in [1] the authors demonstrate via numerical simulations that when time-delay increases, this results in having larger lower bound. However, in [1], there are no results related to finding an upper bound on the desired data rate.

In [1], it was suggested (without any proof), that in order to achieve operational rates that are near the lower bound, one could use a simple ECDQ coding scheme. In this paper, we leverage upon this idea, and formally establish the technical results required to guarantee a desired closed-loop performance under an operational average data rate constraint and subject to a known channel delay. In particular, we first utilize the LTI pre-, post-, and feedback filters derived in [1], in order to stabilize the considered NCS so as to guarantee a desired performance, and to reduce the memory in the system by decorrelating the output of the quantizer. This makes it possible to employ zero-delay coding

[1] For details on directed information, see, e.g., [11, 12].

without introducing a significant rate loss. We propose a simple subtractively dithered uniform scalar quantizer, where the dither is uniformly distributed over the quantization cells, and then we apply memoryless entropy coding on the output of the scalar quantizer. We show how to design the coding scheme, in order to guarantee that the closed-loop system is stable, and furthermore that the desired performance is achieved. The cost in terms of an increase in the operational bitrate as compared to that described by the lower bound turns out to be small. We establish a loose upper bound, which is at most 1.254 bits greater than the lower bound, and demonstrate via simulations that the operational rates are in fact less than 0.64 bits above the lower bound. Our simulations also reveal that there is an increase in the operational bitrate caused by the delay. Hence, achieving a specific level of performance over a channel with greater time delay, requires higher average data rate. It is interesting to note that our results reveal that while any (stabilizable) LTI system can always be stabilized for any finite known channel delay, the support of the set of achievable performances decreases as the delay is increased. Thus, if the channel delay is too large, it is not possible to achieve certain performances even if one allows arbitrarily high bitrates and any coding scheme (which can even use memory).

The remainder of this paper is organized as follows. Section 2 provides the notation and preliminaries. Section 3 formulates the main problem. In Section 4, we give the main results. A numerical example is presented in Section 5. Finally, Section 6 draws conclusions.

2 Notation and Preliminaries

The set of natural numbers is represented by $\mathbb{N}$ and we define $\mathbb{N}_0 = \mathbb{N} \cup \{0\}$. k symbolizes the time index of one-sided random processes, $k \in \mathbb{N}_0$. Moreover, $\mathbb{R}$ and $\mathbb{R}^+$ denote the set of real numbers and strictly positive real numbers, respectively. In order to indicate the expectation operator, $\mathcal{E}$ is used and log is assumed to represent the natural logarithm. $[S]_{i,j}$ signifies the entry of matrix S on the i-th row and j-th column. For such a matrix, the eigenvalues with the smallest and largest magnitude are denoted by $\lambda_{\min}(S)$ and $\lambda_{\max}(S)$, respectively.

Unless otherwise stated, all random variables and processes are vector valued. If a random process ξ satisfies $\lim_{k\to\infty} \mathcal{E}[\xi(k)] = \nu_\xi$ and

$$\lim_{k\to\infty} \mathcal{E}[(\xi(k+\tau) - \mathcal{E}[\xi(k+\tau)])(\xi(k) - \mathcal{E}[\xi(k)])^T] = R_\xi(\tau),$$

then it is called asymptotically wide-sense stationary (AWSS). For such a process, the steady-state covariance matrix is specified by $C_\xi = R_\xi(0)$ which defines its steady-state variance as $\sigma_\xi^2 \triangleq \text{trace}(C_\xi)$. If x_1^k is a scalar random sequence, i.e. $x_1^k \triangleq [x(1) \dots x(k)]^T$, then its covariance matrix is defined

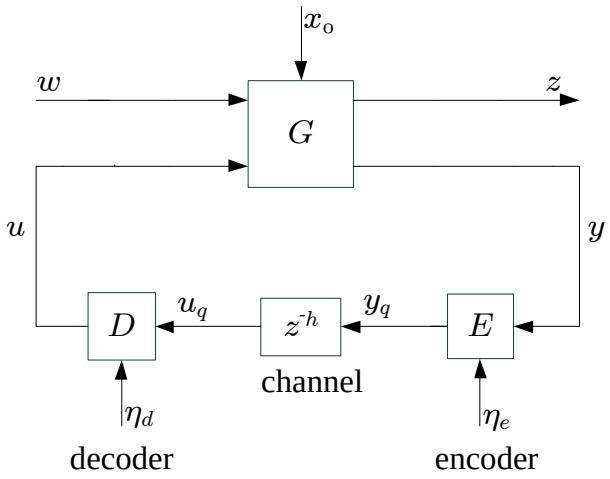

Fig. B.1: Considered NCS

as $C_{x_1^k} = \mathcal{E}[(x_1^k - \mathcal{E}[x_1^k])(x_1^k - \mathcal{E}[x_1^k])^T]$. Two sequences of square matrices $\{P_n\}_{n=1}^{\infty}$ and $\{Q_n\}_{n=1}^{\infty}$ ($P_n, Q_n \in \mathbb{R}^{n\times n}$) are asymptotically equivalent if and only if

$$\lim_{n\to\infty} \frac{1}{n} \sum_{i=1}^{n} \sum_{j=1}^{n} |[P_n - Q_n]_{i,j}|^2 = 0$$
$$|\lambda_{\max}(P_n)|, |\lambda_{\max}(Q_n)| \leq \varrho, \quad \forall n \in \mathbb{N}$$

for some $\varrho < \infty$.

3 Problem Formulation

The considered NCS is depicted in Fig. B.1 wherein G represents an LTI plant with a control input and a measurement output denoted by $u \in \mathbb{R}$ and $y \in \mathbb{R}$, respectively. The disturbance input is symbolized by $w \in \mathbb{R}^{n_w}$ while $z \in \mathbb{R}^{n_z}$ is the output that defines the performance measure. The relation between plant inputs and its outputs is characterized as follows:

$$\begin{bmatrix} z \\ y \end{bmatrix} = \begin{bmatrix} G_{11} & G_{12} \\ G_{21} & G_{22} \end{bmatrix} \begin{bmatrix} w \\ u \end{bmatrix}, \tag{B.1}$$

where every G_{ij} is a proper transfer matrix with suitable dimensions ($n_z \times n_w$, $n_z \times 1$, $1 \times n_w$ and 1×1 for G_{11}, G_{12}, G_{21} and G_{22}, respectively). Let us define the input alphabet of the channel as a countable set of prefix-free binary words and denote it by $\mathcal{A}$. According to Fig. B.1, the noiseless communication

link is described by $u_q(k) = y_q(k-h)$ for $k \geq h$, where $h \in \mathbb{N}_0$ stands for the constant delay induced by the channel and $y_q(k)$ belongs to $\mathcal{A}$. The expected length of the i-th binary word $y_q(i)$ is denoted by$R(i)$. Accordingly, we adopt the following definition for the average data rate over the channel[2]:

$$\mathcal{R} \triangleq \lim_{k\to\infty} \frac{1}{k} \sum_{i=0}^{k-1} R(i). \tag{B.2}$$

Moreover, the dynamics of the encoder is specified by an arbitrary (possibly nonlinear or time-varying) deterministic mapping E_k as follows:

$$y_q(k) = E_k(y^k, \eta_e^k), \tag{B.3}$$

where $\eta_e(k)$ denotes the side information at time k at the encoder. It is worth pointing out that β^k stands for $[\beta(0), \cdots, \beta(k)]$. Likewise, the arbitrary deterministic mapping D_k determines the following input-output relationship for the decoder:

$$u(k) = \begin{cases} D_k(\eta_d^k), & 0 \leq k < h, \\ D_k(y_q^{k-h}, \eta_d^k), & k \geq h. \end{cases} \tag{B.4}$$

The side information available at the decoder at time k is represented by $\eta_d(k)$. Note that E and D in Fig. B.1 are possibly time-varying or nonlinear causal systems.

Assumption 3.1
The transfer matrix in (B.1) represents a proper LTI plant without any unstable hidden modes. Furthermore, G_{22} is an strictly proper transfer function describing the single-input single-output (SISO) open-loop system from u to y. The initial condition, $x_0 = [x(-h), \cdots, x(0)]^T$, has finite differential entropy and is jointly Gaussian with the disturbance signal w. This signal is a zero-mean white noise with identity covariance matrix $C_w = I$.

Assumption 3.2
There is a joint statistical independence held between side information processes η_e and η_d, and the sequence (x_0, w). This independence together with the dynamics of the system yields the conclusion that $I(u(k); y^{k-h} \mid u^{k-1}) = 0$ holds for $0 \leq k < h$. Furthermore, the decoder input can be reconstructed from the past and present of control input and side information. So the decoder is invertible given u^i and η_d^i; there exists a deterministic mapping Q_i such that $u_q^i = Q_i(u^i, \eta_d^i)$.

To state the main problem, we first define $D_{\inf}(h)$ as the infimum steady-state variance of the output z over all mappings $u(k) = \mathcal{K}_k(\gamma^k)$ for $0 \leq k < h$ and $u(k) = \mathcal{K}_k(y^{k-h})$ for $k \geq h$. For such a setting, it is assumed that γ^k is independent of x_0 and w. Let us further suppose that Assumption 3.1 holds

[2] All rates are measured in bits/sample.

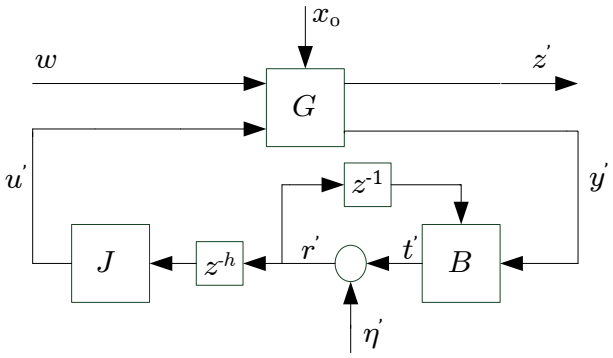

Fig. B.2: Auxiliary LTI NCS

for the NCS of Fig. B.1. Now, the problem of interest can be cast as follows:

$$\mathcal{R}(D) = \inf_{\sigma_z^2 \leq D} \mathcal{R}, \tag{B.5}$$

where σ_z^2 denotes the steady-state variance of z, and $D \in (D_{\text{inf}}(h), \infty)$. The optimization in (B.5) is performed over all encoders E_k and decoders D_k satisfying Assumption 3.2 and rendering the NCS of Fig. B.1 SAWSS (this notion of stability is defined in [8, Definition 2.2]). Moreover, D belonging to the interval $(D_{\text{inf}}(h), \infty)$ is a necessary assumption for the feasibility of the optimization problem in (B.5).

4 Upper Bound Problem

In this section, we show that $\mathcal{R}(D)$ can be bounded from above by an average data rate that is about 1.254 bits per sample larger than the corresponding theoretical lower bound. Therefore, achieving any stationary performance level $D \in (D_{\text{inf}}(h), \infty)$ is possible with rates within a gap of 1.254 bits per sample above the lower bound. We show that such average data rates are given by constructing coding schemes that make use of filters which, when placed around an AWGN channel, yield a directed information feedback rate equal to the lower bound on $\mathcal{R}(D)$. We start by restating some key results from [1]. Since the lower bound is given based on an SNR-constrained optimization over the LTI scheme in Fig. B.2, first we need to describe this system. The auxiliary NCS of Fig. B.2 results from setting a set of LTI filters and an AWGN channel as coding scheme for the system of Fig. B.1. This scheme is specified by the following dynamics:

$$u' = Jz^{-h}r', \quad r' = t' + \eta', \quad t' = B\text{diag}\{z^{-1}, 1\} \begin{bmatrix} r' \\ y' \end{bmatrix}, \tag{B.6}$$

where B and J are proper LTI filters, and η' indicates AWGN with zero mean and variance $\sigma^2_{\eta'}$. We assume that η' is independent of (x_0, w).

Lemma 4.1 ([1, Lemma 4.3])
Consider the LTI loop of Fig. B.2 with fixed $\sigma^2_{\eta'} \in \mathbb{R}^+$. Define $\vartheta'_{r'}$ as follows:

$$\vartheta'_{r'}(B, J, \sigma^2_{\eta'}) \triangleq \frac{1}{4\pi} \int_{-\pi}^{\pi} \log\big(\frac{S_{r'}(e^{j\omega})}{\sigma^2_{\eta'}}\big), \tag{B.7}$$

in which $S_{r'}$ represents the steady-state power spectral density of r'. Then for any $\rho > 0$, upon the existence of the pair $(B, J) = (B_1, J_1)$ making the system of Fig. B.2 internally stable and well-posed, there exist another pair, comprised of the biproper filter J_2, and B_2, which renders the feedback loop of Fig. B.2 internally stable and well-posed, preserves the steady-state power spectral density of z' and satisfies the following:

$$\vartheta'_{r'}(B_1, J_1, \sigma^2_{\eta'}) = \vartheta'_{r'}(B_2, J_2, \sigma^2_{\eta'}) = \frac{1}{2}\log(1 + \frac{\sigma^2_{t'}}{\sigma^2_{\eta'}})|_{(B,J)=(B_2,J_2)} - \rho. \tag{B.8}$$

Corollary 4.1 ([1, Corollary 4.1])
If Assumptions 3.1 and 3.2 hold for the NCS of Fig. B.1 and $D \in (D_{\inf}(h), \infty)$, then

$$\mathcal{R}(D) \geq \frac{1}{2}\log(1 + \varphi'(D)), \varphi'(D) \triangleq \inf_{\sigma^2_{z'} \leq D} \frac{\sigma^2_{t'}}{\sigma^2_{\eta'}}, \tag{B.9}$$

where the optimization is done over all LTI filter pairs (B, J) and the noise variance $\sigma^2_{\eta'} \in \mathbb{R}^+$ making the system in Fig. B.2 internally stable and well-posed. Moreover, $\sigma^2_{t'}$ and $\sigma^2_{z'}$ represent the steady-state variances of t' and z', respectively.

Definition 4.1
According to the time delay in the channel, the coding scheme formulated in (B.3) and (B.4) is called linear if and only if there exist proper LTI filters B and J, and zero-mean i.i.d random sequence η in such a way that the dynamics of the coding scheme can be rewritten as follows:

$$u = Jz^{-h}r, \quad r = t + \eta, \quad t = B\mathrm{diag}\{z^{-1}, 1\}\begin{bmatrix} r \\ y \end{bmatrix}, \tag{B.10}$$

where η is assumed to be independent of (x_0, w). Moreover, the initial condition of B, J and feedback channel delay z^{-1} are deterministic. The coding scheme defined in (B.10) extends the class of linear coding schemes defined in [8] to the case where the channel imposes a constant delay of h.

A linear source-coding scheme can be realized by entropy-coded dithered quantization accompanied with LTI filters, as depicted in figures B.3 and B.4.

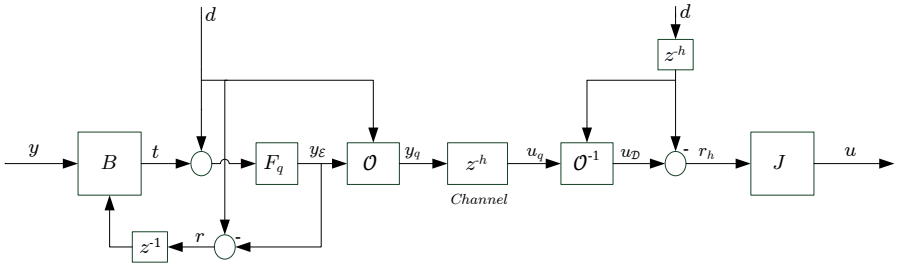

Fig. B.3: The proposed ECDQ-based linear coding scheme

In other words, by implementing an ECDQ and making use of LTI filters, the linear dynamics described by (B.10) are related to the main general scheme in (B.3) and (B.4) as follows:

$$\begin{aligned} y_\mathcal{E}(k) &= \mathcal{F}_q(t(k) + d(k)) \\ y_q(k) &= \mathcal{O}_k(y_\mathcal{E}(k), d(k)) \\ u_\mathcal{D}(k) &= \mathcal{O}_{k-h}^{-1}(u_q(k), d(k-h)) \\ r_h(k) &= u_\mathcal{D}(k) - d(k-h), \end{aligned} \tag{B.11}$$

where $\mathcal{F}_q$ represents a uniform quantizer with resolution $\Delta \in \mathbb{R}^+$, $\mathcal{F}_q : \mathbb{R} \to \{i\Delta ; i \in \mathbb{Z}\}$. Furthermore, $d(k)$ is a dither signal to be accessed at both encoder and decoder. Entropy coding for the lossless parts are denoted by the mapping $\mathcal{O}_k$ and its complementary $\mathcal{O}_k^{-1}$ for the encoder and decoder, respectively. So the symbol $y_q(k)$ sent through the channel is a function of $y_\mathcal{E}(k)$ conditioned

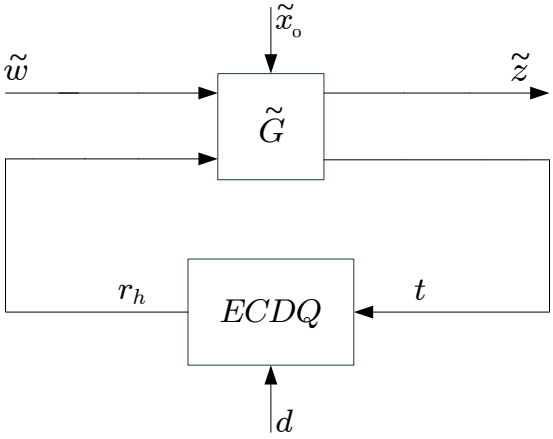

Fig. B.4: ECDQ setup in the feedback path

upon $d(k)$.

Lemma 4.2
For the architecture depicted in Fig. B.4, consider $\tilde{G}$ as a proper real rational transfer matrix where the scalar transfer function from r_h to t is strictly proper. Assume that the ECDQ in the feedback path follows the dynamics of (B.11) and has finite and positive step size Δ. Furthermore, suppose that the disturbance $\tilde{w}$ is a white noise process second-order with $\tilde{x}_0$, the initial state of $\tilde{G}$. Then given the dither d as an i.i.d process with a uniform distribution over $(-\Delta/2, \Delta/2)$ and independent of $(\tilde{w}, \tilde{x}_0)$, the error $r - t$ is i.i.d, uniformly distributed over $(-\Delta/2, \Delta/2)$ and independent of $(\tilde{w}, \tilde{x}_0)$.

Proof. Considering the schemes described through (B.10) and (B.11), let us call the transfer matrix from $[\tilde{w} \quad r]^T$ to $[\tilde{z} \quad t]^T$ in Fig. B.4 $\tilde{G}_h$. It can be deduced from the relation between r an r_h ($r_h = rz^{-h}$) that $\tilde{G}_h$ has the same characteristics as $\tilde{G}$, in that $\tilde{G}_h$ is proper and real rational and the SISO open-loop transfer function from r to t is strictly proper. The remainder of the proof follows immediately from [8, Lemma 5.1]. □

According to Lemma 4.2, when used in the setting of Fig. B.1, the coding scheme stated through (B.11) together with the filters in (B.10) form a linear coding scheme if $d(k)$ has the same properties as the dither considered in Lemma 4.2. This class of linear coding schemes is called ECDQ-based linear coding schemes [8, 9]. The ECDQ-based linear coding scheme built based on (B.11) and (B.10) is depicted in Fig. B.3. An upper bound on the operational average data rate in the NCS of Fig. B.1 is characterized in next lemma when utilizing an ECDQ-based linear coding scheme in the feedback path.

Lemma 4.3
Provided that the Assumption 3.1 holds, for any ECDQ-based linear source-coding scheme rendering the NCS of Fig. B.1 SAWSS, the average data rate is upper bounded as follows:

$$\mathcal{R} < \frac{1}{2}\log\left(1 + \frac{\sigma_t^2}{\sigma_\eta^2}\right) + \frac{1}{2}\log\left(\frac{2\pi e}{12}\right) + \log 2. \tag{B.12}$$

As for (B.10), σ_t^2 denotes the steady-state variance of the signal t, and $\sigma_\eta^2 = \frac{\Delta^2}{12}$ is the variance of the quantization error (noise) in the ECDQ-based linear source-coding scheme.

Proof. Based on Assumption 3.1, [1, Appendix A] shows that the problem of finding $\varphi'(D)$ in (B.9) is feasible. So there exist proper LTI filters B and J, and an AWGN, say η, that brings SAWSS-ness to the NCS of Fig. B.1. Regarding the definition of internal stability, keeping such a pair of filters and setting $\eta = 0$ will not alter the stability status of the system. Therefore, the open-loop system between r and t is internally stable and well-posed when using

unity feedback ($t = r$). Now according to the properties of the dither stated in Lemma 4.2, (B.12) is immediately concluded from [9, Corollary 5.3]. □

Now, according to Lemma 4.3, the desired minimal average data rate $\mathcal{R}(D)$ can be bounded from above through an ECDQ-based linear coding scheme based on the following result:

Theorem 4.1
Let the feedback loop of Fig. B.1 satisfy Assumption 3.1. For any $D > D_{\inf}(h)$, there exists an ECDQ-based linear source-coding scheme that meets Assumption 3.2, renders the NCS of Fig. B.1 SAWSS, and outputs $\sigma_z^2 \leq D$ in such a way that

$$\mathcal{R} < \frac{1}{2}\log\left(1 + \varphi'(D)\right) + \frac{1}{2}\log\left(\frac{2\pi e}{12}\right) + \log 2, \tag{B.13}$$

where $\varphi'(D)$ is as defined in (B.9).

Proof. Here the feasibility of finding $\varphi'(D)$ in (B.9) is used again. So since $D \in (D_{\inf}(h), \infty)$, for any $\zeta > 0$, the triplet $(B_\zeta, J_\zeta, \sigma_{\eta_\zeta}^2)$ exists in such a way that setting proper LTI filters $B = B_\zeta$, $J = J_\zeta$ and the AWGN $\sigma_{\eta'}^2 = \sigma_{\eta_\zeta}^2 \in \mathbb{R}^+$, will render the NCS of Fig. B.2 internally stable and well-posed, results in $\sigma_{z'}^2 \leq D$ and

$$\frac{\sigma_{t'}^2}{\sigma_{\eta'}^2} \leq \varphi'(D) + \zeta. \tag{B.14}$$

Without loss of generality and according to Jensen's inequality and Lemma. 4.1, J_ζ can be considered as a biproper filter. Now, let us set an ECDQ-based linear coding scheme comprising $(B, J, \Delta) = (B_\zeta, J_\zeta, \sqrt{12\sigma_{\eta_\zeta}^2})$, as coding scheme in the NCS of Fig. B.1, with zero initial state for filters and delays. Considering the dynamics of the system and the variance of uniform processes, such a setting is guaranteed to be SAWSS by construction and based on lemma 4.2 and definition of B_ζ, J_ζ and $\sigma_{\eta_\zeta}^2$. Moreover, in this case, the following holds for the steady-state variance of the signal t in (B.10) and system output z:

$$\sigma_z^2 \leq D, \qquad \frac{\sigma_t^2}{\sigma_\eta^2} \leq \varphi'(D) + \zeta. \tag{B.15}$$

The aforementioned setup meets the conditions in Lemma 4.3 as well. So for a suitable choice of $\rho > 0$, the following bound can be derived on the average length of y_q:

$$\mathcal{R} < \frac{1}{2}\log\left(1 + \frac{\sigma_t^2}{\sigma_\eta^2}\right) + \frac{1}{2}\log\left(\frac{2\pi e}{12}\right) + \log 2 - \rho.$$

Then, the rightmost inequality in (B.15) will give

$$\mathcal{R} < \frac{1}{2}\log\left(1 + \varphi'(D) + \zeta\right) + \frac{1}{2}\log\left(\frac{2\pi e}{12}\right) + \log 2 - \rho. \tag{B.16}$$

The upper bound in (B.13) can be obtained by setting ζ small enough. We go on with the proof by proving that the ECDQ-based linear coding scheme noted above satisfies Assumption 3.2. Based on Lemma 4.2, every condition in Assumption 3.2 can be guaranteed for the proposed scheme except invertibility of the decoder. According to the definition of ECDQ-based linear coding schemes, by taking the same steps as in [9, Corollary 5.1], it can be shown that knowing r^k and d^k is equivalent to knowing u_q^k. Moreover, since J is biproper with deterministic initial state, knowledge of r^k is equal to knowledge of u^{k+h}. As a result, u_q^{k-h} can be reconstructed from u^k conditioned upon knowing $\eta_d^k = d^k$. So the decoder is invertible and the proof is complete. □

Technically speaking, a design approach is proposed in the proof of Theorem 4.1. This approach indicates the way of building a linear coding scheme that can render the NCS of Fig. B.1 SAWSS and guarantee $\sigma_z^2 \leq D$ with a rate less than the upper bound derived in (B.13).

5 Simulation Results

Suppose that the generalized plant G, to be controlled in the architecture of Fig. B.1, is described as follows:

$$z = \frac{0.165}{(z-2)(z-0.5789)}(w+u), \quad y = z.$$

Moreover, assume that (x_0, w) is set in such a way that Assumption 3.1 holds. We calculate the lower bound stated in (B.9) for three different values of time delay, $h = \{0, 1, 2\}$, over an interval from $D > D_{\inf}(h)$ to 50. To do so, we utilize the technique proposed in [1]. As a departure form the results in [1] and as the most important part of this simulation example, we design actual coding and control schemes by employing the results of Section 4, and apply those to the system of interest. The results are illustrated in Fig. B.5. For each $D > D_{\inf}(h)$, we use the corresponding controllers (B, J) obtained from the optimization problem in (B.9). Furthermore, for the sake of quantization and coding, we utilize ECDQs with properties stated in Lemma 4.2. Those properties include the quantization resolution and the support for the uniform dither, which are determined based on the optimal noise variance from (B.9). As shown in Fig. B.5, the behaviour of the lower bound on $\mathcal{R}(D)$ (all the curves referred to as LB) with respect to the channel time delay, is in agreement with stated results form our previous work [1]. Moreover, Fig. B.5 demonstrates that the upper bound (the curves referred to as UB) varies as a function of delay, in the same manner as the lower bound. So for a specific $D > D_{\inf}(h)$, increasing delay makes the upper bound larger. This result follows from (B.13) where the derived upper bound differs from the lower bound by only a constant.

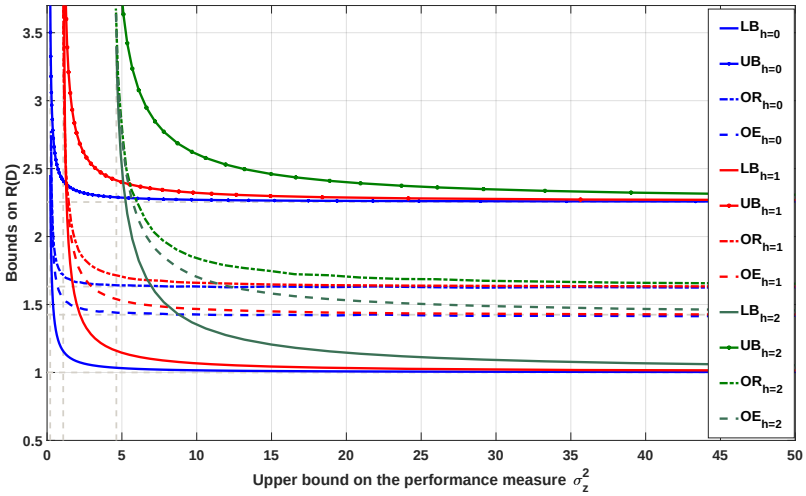

Fig. B.5: Bounds on $\mathcal{R}(D)$ in (B.5) for different values of time delay h

The operational rates and entropies, the main outcomes of this simulation study, are illustrated in Fig. B.5 as well. We have used 10^6-sample-long realizations, where the dither is fully known at both sides of the channel. The operational data rates, referred to as OR, are achieved by employing memoryless Huffman entropy coding that does not incorporate dither values into the prior information for coding. However, the rates are at most about 0.6 less than the upper bound. So even when using an entropy-coder encoding unconditioned upon dither knowledge, the upper bound is rather loose. The operational entropy of output of the quantizer, referred to as OE, is measured under the same conditions. Another interesting result is related to the behaviour of the operational average data rates with respect to the delay. It can be observed from the curves that for a fixed $D > D_{\text{inf}}(h)$, the desired average data rate grows by increasing h. In other words, larger delay in the channel necessitates spending higher average data rates to achieve a certain level of quadratic performance. The same goes for the estimated entropy. Compared to the delay-free case, an NCS closed over a channel with time delay incurs greater entropy to meet a specific performance requirement.

6 Conclusions

This paper has investigated the performance of a rate-limited NCS. In the considered system, a noisy LTI plant is controlled over a noiseless channel with rate constraints and known constant time delay. For this system, we have derived an upper bound on this minimal data rate. More precisely, we have suggested

a simple coding and control scheme using a zero-delay ECDQ that can attain the prescribed performances with rates at most 1.254 bits/sample away from the corresponding lower bounds. We have illustrated via a numerical example that systems with larger time delays in the channel need higher operational average data rates to attain a quadratic cloosed-loop performance level.

References

[1] M. Barforooshan, J. Østergaard, and M. S. Derpich, "Interplay between transmission delay, average data rate, and performance in output feedback control over digital communication channels," in *2017 American Control Conference (ACC)*, May 2017, pp. 1691–1696, there is an arXiv version as well.

[2] D. F. Delchamps, "Stabilizing a linear system with quantized state feedback," *IEEE Transactions on Automatic Control*, vol. 35, no. 8, pp. 916–924, Aug. 1990.

[3] Z. Qiu, L. Xie, and Y. Hong, "Quantized leaderless and leader-following consensus of high-order multi-agent systems with limited data rate," *IEEE Transactions on Automatic Control*, vol. 61, no. 9, pp. 2432–2447, Sept. 2016.

[4] G. N. Nair and R. J. Evans, "Stabilizability of stochastic linear systems with finite feedback data rates," *SIAM Journal on Control and Optimization*, vol. 43, no. 2, pp. 413–436, 2004.

[5] A. A. Zaidi, T. J. Oechtering, S. Yüksel, and M. Skoglund, "Stabilization of linear systems over Gaussian networks," *IEEE Transactions on Automatic Control*, vol. 59, no. 9, pp. 2369–2384, Sept. 2014.

[6] E. G. W. Peters, D. E. Quevedo, and J. Østergaard, "Shaped Gaussian dictionaries for quantized networked control systems with correlated dropouts," *IEEE Transactions on Signal Processing*, vol. 64, no. 1, pp. 203–213, Jan. 2016.

[7] M. Rabi, C. Ramesh, and K. H. Johansson, "Separated design of encoder and controller for networked linear quadratic optimal control," *SIAM Journal on Control and Optimization*, vol. 54, no. 2, pp. 662–689, 2016.

[8] E. I. Silva, M. S. Derpich, J. Østergaard, and M. A. Encina, "A characterization of the minimal average data rate that guarantees a given closed-loop performance level," *IEEE Transactions on Automatic Control*, vol. 61, no. 8, pp. 2171–2186, Aug. 2016.

[9] E. I. Silva, M. S. Derpich, and J. Østergaard, "A framework for control system design subject to average data-rate constraints," *IEEE Transactions on Automatic Control*, vol. 56, no. 8, pp. 1886–1899, Aug. 2011.

[10] T. Tanaka, K. H. Johansson, and M. Skoglund, "Optimal block length for data-rate minimization in networked LQG control," *IFAC-PapersOnLine*, vol. 49, no. 22, pp. 133 – 138, 2016, 6th IFAC Workshop on Distributed Estimation and Control in Networked Systems (NECSYS).

[11] J. Massey, "Causality, feedback and directed information," in *Proceedings of the 1990 International Symposium on Information Theory and Its Applications (ISITA)*, 1990, pp. 303–305.

[12] C. D. Charalambous and P. A. Stavrou, "Directed information on abstract spaces: Properties and variational equalities," *IEEE Transactions on Information Theory*, vol. 62, no. 11, pp. 6019–6052, Nov. 2016.

[13] R. Zamir and M. Feder, "On universal quantization by randomized uniform/lattice quantizers," *IEEE Transactions on Information Theory*, vol. 38, no. 2, pp. 428–436, Mar. 1992.

[14] L. Zhang, H. Gao, and O. Kaynak, "Network-induced constraints in networked control systems—A survey," *IEEE Transactions on Industrial Informatics*, vol. 9, no. 1, pp. 403–416, Feb. 2013.

[15] A. Farnam and R. M. Esfanjani, "Improved linear matrix inequality approach to stability analysis of linear systems with interval time-varying delays," *Journal of Computational and Applied Mathematics*, vol. 294, pp. 49–56, 2016.

[16] L. Qiu, F. Yao, G. Xu, S. Li, and B. Xu, "Output feedback guaranteed cost control for networked control systems with random packet dropouts and time delays in forward and feedback communication links," *IEEE Transactions on Automation Science and Engineering*, vol. 13, no. 1, pp. 284–295, Jan. 2016.

[17] D. Wu, X. Sun, C. Wen, and W. Wang, "Redesigned predictive event-triggered controller for networked control system with delays," *IEEE Transactions on Cybernetics*, vol. 46, no. 10, pp. 2195–2206, Oct. 2016.

[18] M. S. Mahmoud and N. B. Almutairi, "Feedback fuzzy control for quantized networked systems with random delays," *Applied Mathematics and Computation*, vol. 290, pp. 80–97, 2016.

[19] Y. Nakahira, "LQ vs. ℓ_∞ in controller design for systems with delay and quantization," in *Proceedings of the 55th IEEE Conference on Decision and Control (CDC)*, Dec. 2016, pp. 2382–2389.

Paper C

The Effect of Time Delay on the Average Data Rate and Performance in Networked Control Systems

Mohsen Barforooshan, Milan S. Derpich, Photios A. Satvrou, and Jan Østergaard,

The paper has been submitted to the
IEEE Transaction on Automatic Control, 2018.

The layout has been revised.

Abstract

This paper studies the performance of a feedback control loop closed via an error-free digital communication channel with transmission delay. The system comprises a discrete-time noisy linear time-invariant (LTI) plant whose single measurement output is mapped into its single control input by a causal, but otherwise arbitrary, coding and control scheme. We consider a single-input multiple-output (SIMO) channel between the encoder-controller and the decoder-controller which is lossless and imposes random time delay. We derive a lower bound on the minimum average feedback data rate that guarantees achieving a certain level of average quadratic performance over all possible realizations of the random delay. For the special case of a constant channel delay, we obtain an upper bound by proposing linear source-coding schemes that attain desired performance levels with rates that are at most 1.254 bits per sample greater than the lower bound. We give a numerical example demonstrating that bounds and operational rates are increasing functions of the constant delay. In other words, to achieve a specific performance level, greater channel delay necessitates spending higher data rate.

Keywords

Networked control systems, data rate constraints, time delay, information theory, optimal control.

1 Introduction

Taking communication imperfections into account for analysis and design has proved to be an interesting topic within the area of control theory during recent years. This interest is motivated by advantages of communication networks over point-to-point wiring and, on the other side, by the complexity that communication constraints impose on classical control problems [1]. Time delay, packet dropout and data rate constraints (quantization) are among prominent challenges [2–5].

Using an information-theoretic approach, [6, 7] report primary derivations related to system performance. In these works, it is shown that the presence of a finite-capacity communication channel in a strictly causal feedback loop introduces a new performance limitation which differs from conventional Bode's formula by a constant quantifying channel information rate. Moreover, the authors derive inequalities among entropy rate of internal signals (inside the loop) and external signals (outside the loop), resulting in a general performance bound which is affected by finite feedback capacity. Inspired by [6, 7], lower and upper bounds are derived on the minimum data rate that guarantees

achieving a prescribed level of quadratic performance in [8–10]. These works consider noisy linear time-invariant (LTI) plants with Gaussian disturbances, controlled over an error-free digital channel without delay. In particular, [10] shows that over all causal mappings which represent coding and control, the average data rate is bounded from below by the directed information rate generated by the mappings that render the sensor input and control output jointly Gaussian. Moreover, it is proved in [10] that in an auxiliary LTI structure, the minimum signal-to-noise ratio (SNR) which guarantees stability and meeting a quadratic performance requirement gives the lower bound on the desired minimal data rate. For the upper bound analysis, [10] suggests employing entropy-coded dithered quantizers (ECDQs). Such a simple coding scheme is designed based on the aforementioned SNR-constrained optimization giving the lower bound. Inspired by [8] and [10], the authors of [11] present a method based upon semidefinite programming (SDP) to characterize the trade-off between directed information rate and linear quadratic Gaussian (LQG) performance in rate-constrained networked control systems (NCSs) with fully-observable multiple-input multiple-output (MIMO) plants. In [12], the authors derive a lower bound on the zero-delay rate distortion function associated with vector-valued Gauss-Markov processes and mean-square error distortion constraint. Based on the separation principle, this bound is in fact the lower bound on the minimum data rate required for attaining LQG performance in control of fully observable plants. Then [12] utilizes the optimal realization that corresponds to the foreshadowed class of vector-valued Gaussian sources to derive an upper bound on zero-delay rate distortion function using variable-length entropy coding with lattice quantization. Similar ideas are employed in [13] for establishing bounds on minimum mutual informations, across a delay-free channel, that guarantee achieving specific linear quadratic regulator (LQR) performance levels. Specifically, [13] derives the lower bound based on Shannon's lower bound and power entropy inequalities whereas the upper bound is established via variable-length coding and lattice-based quantization methods.

NCSs subject to network-induced delays are generally analyzed according to two methodologies: robustness and adaptation [3]. The aim in the robustness framework is deriving conditions for certain stability or performance requirements by constructing Lyapunov-Krasovskii functionals that do not incorporate time-stamp information as a variable. For instance, in [14], stabilization and H_∞ performance conditions for a singular cascade NCS are obtained. Fuzzy-model-based control is another approach in the robustness framework, where the rules are based on the size of delays, and the controller is required to be robust over the delay range [15, 16]. In the adaptation framework, one method is modelling NCSs as stochastic switched systems. The recent results on stability and H_2/H_∞ performance of Markov jump linear systems (MJLSs) are reported in [17] and [18], respectively. The second approach in this framework is predictive control; a method which is currently quite popular in NCSs. According

to this technique, the actuator selects among a sequence of control commands based on the transmission delays experienced by them [19–21].

In all the aforementioned results on system performance, either the effect of channel delay is neglected, or the rate limitation is not taken into account. However, looking into the literature, one can find works investigating performance issues in NCSs with both rate constraints and network-induced delays (see, e.g., [22–25]). Even so, a few has utilized the information-theoretic approach to treat systems with such limitations. For example, [26] derives bounds on the minimum individual (non-asymptotic) rate needed to guarantee meeting an individual performance requirement (boundedness of the maximum ℓ_2-norm of states).

In this paper, we study the performance of a discrete-time LTI plant with Gaussian initial state in a loop with Gaussian exogenous inputs and random or constant channel delay on the feedback path. For the setup with random delay in the channel, we seek the infimum average data rate required to achieve a prescribed quadratic performance level. We show that the average data rate over all possible realizations of the delay is lower bounded by the average directed information rate. We prove for the random channel delay case that under certain stationarity assumptions, the average directed information rate can be stated in terms of average power spectral densities of the involved signals. We obtain a lower bound on the desired minimal average data rate which is stated as the average of a function of the power spectral densities of feedback path signals over all possile realizations of the delay. To establish all these results, we utilize the tools adopted in [8] and [10]. However, compared to [10] and [8], the channel is not delay-free in our setup. In other words, we extend the information inequalities in [10] to the case where there exists a random time delay between the sensor output and the control input.

For the setup with known constant delay in the channel, we show that the above lower bound on the infimum average data rate required for attaining quadratic performance is equal to a function of infimum SNR of the channel over schemes comprised of LTI filters and AWGN channels with feedback and delay that meet the quadratic performance constraint. Our contribution in this case is showing how the presence of the channel delay affects the scheme yielding the lower bound. This gives an insight to the interplay between time delay, average data rate and performance in the considered NCS. We also prove that even over a channel with a constant delay, any admissible performance level can be achieved by an EDCQ-based linear coding scheme which generates an average data rate at most (approximately) 1.254 bits per sample away from the corresponding lower bound. We illustrate via a numerical example that lower and upper bounds as well as empirical rates and entropies are all increasing functions of channel delay. This in turn implies that channels with larger delays demand higher average data rates to allow for attaining a certain system performance.

Compared to our previous works in [27] and [28], first, we here study the case of random channel delay and second, we employ a simpler proof than information inequalities and identities in [27] and [28]. In this work, we also show the effect of having a delay at different places in the loop on system signals. The last departure from our previous results is that we incorporate some eliminated proofs of [27] into this paper.

The remainder of the paper is organized as follows. Section 2 introduces the notation. Section 3 formulates the main problem. Section 4 analyzes the lower bound problem for the setup with random channel delay. Section 5 derives a lower bound on the desired minimal data rate in the case of constant channel delay. The analysis of upper bound problem in the constant delay case is presented in Section 6 where the equivalence between systems with different delay locations is investigated. A numerical example is given in Section 7. Finally, Section 8 concludes the paper.

2 Notation

By $\mathbb{R}$, we denote the set of real numbers whose subset $\mathbb{R}^+$ represents the set of strictly positive real numbers. The set $\mathbb{N}_0$ is defined as $\mathbb{N}_0 \triangleq \mathbb{N} \cup \{0\}$ where $\mathbb{N}$ symbolizes the set of natural numbers. The time index of every considered signal, denoted by k in most cases, belongs to $\mathbb{N}_0$. Symbols $\mathbf{E}$, log, $|.|$, and $\|.\|_2$ represent operators for expectation, natural logarithm, magnitude and H_2-norm, respectively. Moreover, $\lambda_{\min}(S)$ and $\lambda_{\max}(S)$ are respectively the largest and smallest eigenvalues of the square matrix S for which the element on the i-th row and j-th column is denoted by $[S]_{i,j}$. In addition, β^k is shorthand for $\beta(0), \ldots, \beta(k)$ where $\beta(k)$ denotes the k-th sample of a discrete-time signal. Furthermore, for the time-dependent set $\alpha(i), i \in \mathbb{N}_0$, α^k is defined as $\alpha^k \triangleq \alpha(0) \times \cdots \times \alpha(k)$. However, if α is a fixed set, then $\alpha^k \triangleq \alpha \times \cdots \times \alpha$ (k times).

Random variables and processes are vector valued, unless otherwise stated. Take v and q into account as two random variables with known marginal and joint probability distribution functions (PDFs). Their joint PDF is represented by $f(v, q)$ while the marginal PDFs of v and q are symbolized by $f(v)$ and $f(q)$, respectively. The conditional PDf of v given q is denoted by $f(v|q)$ and $\mathbf{E}_v(.)$ is the operator for the expectation with respect to the distribution of v. We define the differential entropy of v and the conditional differential entropy of v given q as $h(v) \triangleq -\mathbf{E}_v(\log f(v))$ and $h(v|q) \triangleq -\mathbf{E}_{v,q}(\log f(v|q))$, respectively. The mutual information between v and q is symbolized by by $I(v; q)$ and

defined as $I(v; q) \triangleq -\mathbf{E}_{v,q}(\log(f(v)f(q)/f(v, q)))$. Moreover, the definition of the conditional mutual information between random variables v and q given the random variable r is given by $I(v; q|z) \triangleq I(v, r; q) - I(r; q)$. All the information-theoretic definitions presented in this paragraph are standard and

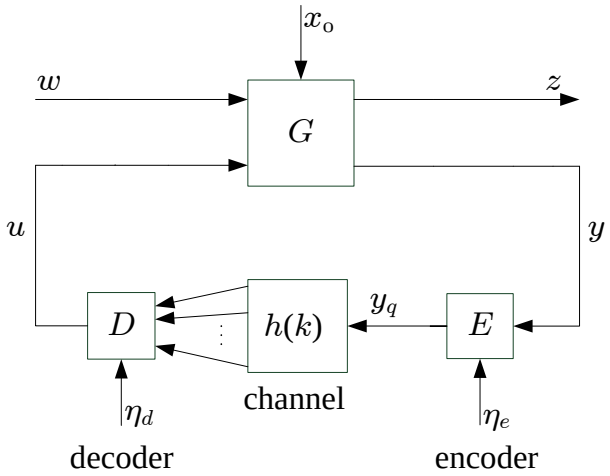

Fig. C.1: Considered NCS with a channel imposing random delay

follow [29].

We call the random process ξ asymptotically wide-sense stationary (AWSS) if $\lim_{k\to\infty} \mathbf{E}[\xi(k)] = \nu_\xi$ and $C_\xi \triangleq R_\xi(0)$ and

$$\lim_{k\to\infty} \mathbf{E}[(\xi(k+\tau) - \mathbf{E}[\xi(k+\tau)])(\xi(k) - \mathbf{E}[\xi(k)])^T] = R_\xi(\tau)$$

hold, where ν_ξ is a finite constant. Accordingly, the steady-state covariance matrix and the steady-state variance of ξ are defined as $\sigma_\xi^2 \triangleq \text{trace}(C_\xi)$, respectively. For the scalar random sequence $x_1^k \triangleq [x(1)\dots x(k)]^T$, we define the covariance matrix as $C_{x_1^k} = \mathbf{E}[(x_1^k - \mathbf{E}[x_1^k])(x_1^k - \mathbf{E}[x_1^k])^T]$. Assume that $P_n, Q_n \in \mathbb{R}^{n\times n}$ are square matrices. Then the sequences $\{P_n\}_{n=1}^\infty$ and $\{Q_n\}_{n=1}^\infty$ are called asymptotically equivalent if and only if they satisfy the following expression for finite ϱ:

$$\lim_{n\to\infty} \frac{1}{n} \sum_{i=1}^{n} \sum_{j=1}^{n} |[P_n - Q_n]_{i,j}|^2 = 0$$
$$|\lambda_{\max}(P_n)|, |\lambda_{\max}(Q_n)| \leq \varrho, \quad \forall n \in \mathbb{N}.$$

3 Problem Formulation

We consider the feedback loop of Fig. C.1 where the plant is LTI with one control input and one sensor output denoted by $u \in \mathbb{R}$ and $y \in \mathbb{R}$, respectively. The plant G is disturbed by a vector-valued zero-mean white noise which is represented by $w \in \mathbb{R}^{n_w}$ and has identity covariance matrix, i.e. $C_w = I$. Moreover, as depicted in Fig. C.1, the plant outputs the vector-valued signal $z \in \mathbb{R}^{n_z}$ upon

which the performance measure is characterized. The relationship between the mentioned set of inputs and outputs is described by a transfer-function matrix as follows:

$$\begin{bmatrix} z \\ y \end{bmatrix} = \begin{bmatrix} G_{11} & G_{12} \\ G_{21} & G_{22} \end{bmatrix} \begin{bmatrix} w \\ u \end{bmatrix}, \tag{C.1}$$

where the dimensionality of each G_{ij} is determined by the dimensions of corresponding pair of inputs and outputs. So $n_z \times n_w$, $n_z \times 1$, $1 \times n_w$ and 1×1 are the dimensions for G_{11}, G_{12}, G_{21} and G_{22}, respectively.

Assumption 3.1
Every entry of the transfer-function matrix in (C.1) is proper with no unstable hidden modes. Moreover, G_{22}, which describes the single-input single-output (SISO) open-loop system from u to y, is strictly proper. The initial states of the plant denoted by $x_0 = \{x(-h_{\max}), \ldots, x(0)\}$ are jointly Gaussian with and independent of the disturbance signal w and has a finite differential entropy.

As depicted in Fig. C.1, the output of the plant, y, is processed into a binary word by the encoder E and transmitted over the error-free channel. Such transmission is accompanied with a random delay. Let $h(k)$ denote the delay experienced by the binary word $y_q(k)$ constructed at time k at the encoder. We assume that $h(k)$ is an independent and identically distributed (i.i.d.) process which has a bounded support at each time step, i.e., $h(k) \in \{h_1, \ldots, h_m\}$, $\forall k \in \mathbb{N}_0$ where $h_i < h_{i+1}$ $(i = 1, 2, \ldots, m-1)$. In order to avoid unnecessary notational complexity and without loss of generality, we set h_1 as $h_1 = 0$ and h_m as $h_m = h_{\max}$. The marginal distribution of the delay is assumed to be known and described by $Pr\{h(k) = h_j\} = \alpha_j$ where $\sum_{j=1}^{m} \alpha_j = 1$. Such characteristics introduce a channel with the following input-output relationship:

$$u_q(k) = [y_q(i)]_{i \in S(k)}, \qquad k \in \mathbb{N}_0 \tag{C.2}$$

where $S(k)$ is defined as

$$S(k) \triangleq \{i : i + h(i) = k\} \tag{C.3}$$

for every $k, i \in \mathbb{N}_0$. Denoting the cardinality of $S(k)$ by $s(k)$, we can imply form (C.2) that $u_q(k)$ is a vector comprised of $s(k) \leq h_{\max} + 1$ binary words which specifies the output of the channel at time k. Note that $s(k)$ is a random variable depending on the channel delay. We assume that $y_q(i)$ is discarded at the decoder-controller side if $i < 0$. Moreover, under aforementioned circumstances, binary words transmitted over the considered channel are not necessarily received in the same order they were emitted. It should be also emphasized that the channel does not allow for any data loss. The average data rate across the channel is defined as

$$\mathcal{R} \triangleq \lim_{k \to \infty} \frac{1}{k} \sum_{i=0}^{k-1} R(i), \tag{C.4}$$

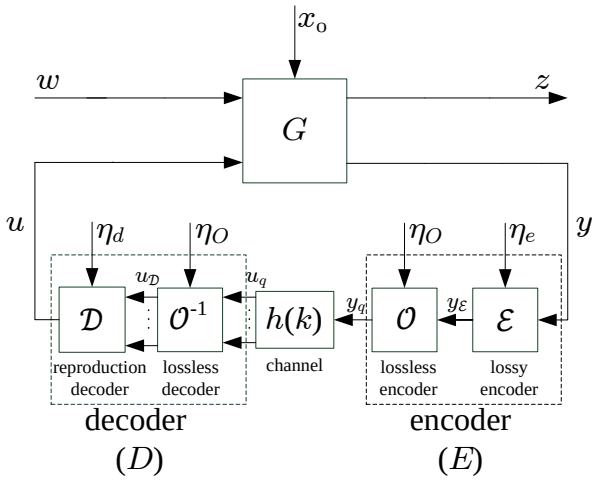

Fig. C.2: Considered NCS with a detailed model of coding and control scheme

where $R(i)$ indicates the expected length of the binary word $y_q(i)$.

A more detailed presentation of the feedback path in the NCS of Fig. C.1 is provided by Fig. C.2. As depicted, the encoder-controller is comprised of a lossy and a lossless component. The lossy part $\mathcal{E}$ outputs the symbol $y_\mathcal{E}$ according to the following dynamics:

$$y_\mathcal{E}(k) = \mathcal{E}_k(y^k, \eta_e^k), \tag{C.5}$$

where $\eta_e(k) \in \Lambda_e(k)$ symbolizes the side information at time k at the lossy encoder. $\mathcal{E}_k : \mathbb{R}^{k+1} \times \Lambda_e^k \mapsto \mathcal{A}_s$ is a deterministic map and $\mathcal{A}_s$ represents a fixed countable set. At each time instant, the encoder is assumed to know the time delays experienced by previous binary words and the time delay of the current binary word to be sent over the channel. Therefore, h^k is known at the encoder $\forall k \in \mathbb{N}_0$. This implies that $y_\mathcal{E}(k)$ can be reconstructed perfectly $h(k)$ steps later at the decoder if $y_q(k)$ is constructed by using $y_\mathcal{E}(k)$ and only those samples of $y_\mathcal{E}^{k-1}$ which will be already available at the decoder at time $k + h(k)$. Note that having access to y_q^k at the decoder at the time $k + h(k)$ is not assured. So the lossless encoder $\mathcal{O}$ outputs the binary symbol y_q based on

$$y_q(k) = \mathcal{H}_{\mathcal{E}k}(y_\mathcal{E}(k), y_{\mathcal{E}f}(k), \eta_o^k), \tag{C.6}$$

in which $y_{\mathcal{E}f}(k)$ is a sequence comprising the elements of $y_\mathcal{E}^{k-1}$ for which the associated binary words will have reached the decoder by the time $k + h(k)$, i.e., $\{y_\mathcal{E}(i) : i \in \mathbb{N}_0, i \leq k-1, i + h(i) \leq k + h(k)\}$. Moreover, $\eta_o(k) \in \Lambda_o(k)$, and $\mathcal{H}_{\mathcal{E}k} : \mathcal{A}_s^{f(k)} \times \Lambda_o^k \mapsto \mathcal{A}(k)$ is an arbitrary deterministic mapping where $k - h_{\max} + h(k) + 1 \leq f(k) \leq k + 1$. So $f(k) - 1$ specifies the cardinality of

the sequence $y_{\mathcal{E}f}(k)$. Note that since no dropout occurs during data transmission, $y_q^{k-h_{\max}+h(k)}$ will certainly have been received at the decoder by the time $k+h(k)$. In addition, $\mathcal{A}(k)$ is a countable set of prefix-free binary code words, which specifies the input alphabet of the channel at each time instant.

On the receiver side, $u_q(k)$ is available as the input to the lossless decoder. This decoder, shown by $\mathcal{O}^{-1}$, generates $u_{\mathcal{D}}$ as

$$u_{\mathcal{D}}(k) = \mathcal{H}_{\mathcal{D}k}(u_{qf}(k), \eta_o^k, S(k)), \tag{C.7}$$

where $u_{qf}(k)$ is a sequence comprised of elements of u_q^k that have time indices less than or equal to the largest time index of y_q in $u_q(k)$, i.e., $u_{qf}(k) \triangleq \{y_q(i) : i \in \mathbb{N}_0, y_q(i) \in u_q^k, i \leq m(k)\}$ where $m(k) = \max S(k)$, $\forall k \in \mathbb{N}_0$. Such selection of data for lossless decoding is in accordance with the information utilized in (C.6) for encoding. Furthermore, $\mathcal{H}_{\mathcal{D}k} : \mathcal{A}^{g(k)} \times \Lambda_o^k \times {\mathbb{N}_0}^{s(k)} \mapsto \mathcal{A}_s^{s(k)}$, where $k - h_{\max} + 1 \leq g(k) \leq k+1$, represents an arbitrary deterministic mapping. It should be noted that according to the channel model, $g(k)$ is a random variable denoting the cardinality of $u_{qf}(k)$ and $\sum_{i=0}^{k} s(i) \leq k$ holds for all $k \in \mathbb{N}_0$. Moreover, based on the definition of u_{qf} and (C.6), the information provided by $(u_{qf}(k), \eta_o^k, S(k))$ is enough for the lossless decoder to reconstruct every element of $\{y_{\mathcal{E}}(i)\}_{i\in S(k)}$ perfectly. Therefore

$$u_{\mathcal{D}}(k) = [y_{\mathcal{E}}(i)]_{i\in S(k)}, \qquad k \in \mathbb{N}_0$$

where $S(k)$ is defined as in (C.3). Indeed for such reconstruction, the knowledge of the delay is required at the decoder. Hence, we further assume that the decoder is provided by $S(k)$ through for example timestamping. Finally, the decoder-controller gives the control input via

$$u(k) = \mathcal{D}_k(u_{\mathcal{D}}^k, \eta_d^k). \tag{C.8}$$

where $\eta_d(k)$ signifies the side information available at the decoder at time k and is contained in the well-defined set $\Lambda_d(k)$. So $\eta_d(k)$ satisfies $\eta_d(k) \in \Lambda_d(k)$. Moreover, $\mathcal{D}_k : \mathcal{A}_s^{t_u(k)} \times \Lambda_d^k \mapsto \mathbb{R}$, $k - h_{\max} + 1 \leq t_u(k) \leq k+1$, is an arbitrary deterministic mapping where $t_u(k)$ is the cardinality of S^k. It should be noted that $\Lambda_o(k)$ in $\eta_o(k) \in \Lambda_o(k)$ is defined as $\Lambda_o(k) \triangleq \Lambda_e(k) \cap \Lambda_d(k)$. We state some additional properties of the setting described above in the following remarks.

Remark 3.1
It can be implied from (C.5)-(C.8) that $u(k)$ and u^k are functions of $(y^{l_k}, {\eta_e}^{l_k}, \eta_d^k)$ where $l_k = \max S^k$ for every $k \in \mathbb{N}_0$. It thus follows from the definition of $S(k)$ and assuming no dropout in the considered channel that $k - h_{\max} \leq l_k \leq k$. This implies that the controller has access to the largest and smallest amount of sensor information when the channel delay is zero and $h_{\max}$, respectively.

Remark 3.2
It can be implied from the definition of $S(k)$ in (C.3) that $u_q(k)$ can have at most $h_{\max}+1$ entries at each time step. So the number of the words that can be received at the decoder at each time instant belongs to the set $\{0, \ldots, h_{\max}+1\}$. Therefore, since the channel input y_q is a scalar process, (C.2) describes a single-input multiple-output (SIMO) channel. Moreover, $S(k)$, as a stochastic process, cannot be i.i.d because in the considered channel, no transmitted binary word is received at the decoder more than once.

For further analysis, we consider the following assumption.

Assumption 3.2
At each time instant $k \in \mathbb{N}_0$, the side information pair $(\eta_e(k), \eta_d(k))$ together with $h(k)$, and consequently $S(k)$, are statistically independent of $(x_0, w(k))$. Therefore, it can be implied from the dynamics of the system that

$$I(u(k); y(k-h_i) \mid u^{k-1}) = 0$$

for any $h_i \in \{1, ..., h_{\max}\}$ with $k - h_i < 0$. Moreover, upon knowledge of u^i, η_d^i and S^i, the decoder is invertible. It means that for each $i \in \mathbb{N}_0$, there exists a deterministic mapping Q_i such that $u_q^i = Q_i(u^i, \eta_d^i, S^i)$.

Remark 3.3
In Appendix A, we will prove that for the architecture of Fig. C.2, any encoder and non-invertible decoder with mappings $\mathcal{E}$, $\mathcal{O}$, $\mathcal{O}^{-1}$ and $\mathcal{D}$, can be replaced by another set of mappings with the same input-output relationship and lower average data rate where the decoder is invertible .

For the purpose of expressing the information rate in terms of spectral densities of the signals of the system, we use the following notion of stability:

Definition 3.1
A scalar AWSS process x is called strongly asymptotically wide-sense stationary (SAWSS) if its covariance matrix is asymptotically equivalent to the covariance matrix of the wide sense stationary (WSS) process, say $\bar{x}$, to which it converges, i.e., $\{C_{x_1^n}\}_{n=1}^{\infty}$ and $\{C_{\bar{x}_1^n}\}_{n=1}^{\infty}$ are asymptotically equivalent. Furthermore, in an SAWSS NCS, all internal signals are SAWSS and their cross-covariance matrices are asymptotically equivalent to the cross-covariance matrices of corresponding WSS processes to be converged to.

Clearly, SAWSS-ness implies AWSS-ness but not vice versa; for both signals and systems. For each coding scheme satisfying (C.5)-(C.8) and rendering the NCS of Fig. C.1 SAWSS, the steady-state variance of the output z is a random variable which depends on the realization of $h(k)$. The same goes for the average data rate. We make explicit such dependence by writing $\sigma_z^2(h^k)$ and $\mathcal{R}(h^k)$, and consider the means of these variables (over all realizations of

h^k) as our performance measure and data rate of interest, respectively. Such notions of performance and rate, represented by σ_{za}^2 and $\mathcal{R}_a$ respectively, are formulated as follows:

$$\begin{aligned}\sigma_{za}^2 &= \sum_{\substack{h^k \in \mathfrak{H} \\ k\to\infty}} Pr(h^k)\sigma_z^2(h^k) \\ \mathcal{R}_a &= \sum_{\substack{h^k \in \mathfrak{H} \\ k\to\infty}} Pr(h^k)\mathcal{R}(h^k)\end{aligned} \tag{C.9}$$

where $\mathfrak{H}$ denotes the support set for possible realizations of the delay $h(k)$. Moreover, $\mathcal{R}(h^k)$ and $\sigma_z^2(h^k)$ indicate that the average data rate and steady-state variance are functions of delay. Generally speaking, we are interested in finding the minimal $\mathcal{R}_a$ for which having a bounded σ_{za}^2 is feasible. Let $D_{\inf}(h_r)$ denote the smallest average steady-state variance of z that can be achieved, when the random delay $h(k)$, with the aforementioned properties, is present in the channel. Hence, $D_{\inf}(h_r)$ is obtained by minimizing the average steady-state variance of z over all (possibly nonlinear and time-varying) settings $u(k) = \mathcal{K}_k(y^{l_k})$ that render the NCS of Fig. C.1 SAWSS. Note that l_k is defined as in Remark 3.1. Under the condition that Assumption 3.1 holds, the problem of our interest is to find

$$\mathcal{R}_a(D) = \inf_{\sigma_{za}^2 \le D} zz\mathcal{R}_a, \tag{C.10}$$

where $D \in (D_{\inf}(h_r), \infty)$, and σ_{za}^2 represents the average steady-state variance of the output z over all realizations of the delay. The feasible set of the optimization problem in (C.10) is comprised of all encoder-controller and decoder-controller pairs described by (C.5)-(C.8), satisfying Assumption 3.2 and rendering the NCS of Fig. C.1 SAWSS.

Remark 3.4
It is straightforward to see from (C.5)-(C.8) that the concatenation of the decoder-controller pair and the channel in the NCS of Fig. C.1 is equivalent to a decoder-controller pair with the same mapping and side information that applies a time delay with same properties as characterized in (C.2), on its received data, and that is followed by a delay-free channel. So the system depicted in Fig. C.1 is equivalent to the feedback loop of Fig. C.3 in which the encoder and the plant are the same and the inputs have the same properties as in Fig. C.1.

The equivalence pointed out in Remark 3.4 between systems of Fig. C.1 and the NCS of Fig. C.3 will assist us deriving a lower bound on the average data rate $\mathcal{R}_a$ in the next Section.

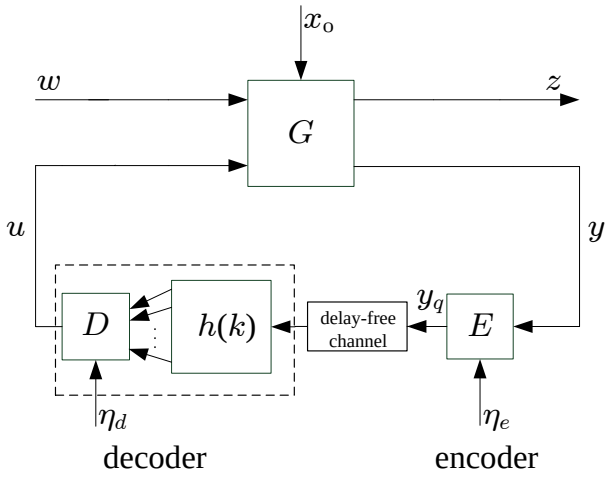

Fig. C.3: Auxiliary system equivalent to the main NCS in the random delay case

4 Lower Bound Problem in the Presence of Random Delay

In this section, we establish a lower bound on $\mathcal{R}_a(D)$. To do so, we derive inequalities and identities that describe the relationship between the flow of information and system performance in the NCS of Fig. C.1. Therefore, we will update fundamental derivations in [10, 28] for the case where the channel delay is randomly distributed. As the first result, we show how the average data rate $\mathcal{R}_a$ is bounded from below in the following theorem.

Theorem 4.1
Consider the feedback loop depicted in Fig. C.1 for which Assumptions 3.1 and 3.2 hold. Then

$$\mathcal{R}_a \geq I_\infty^{h_a}(y \to u) = \lim_{k\to\infty} \frac{1}{k} \sum_{h^{k-1}\in\mathfrak{H}} [Pr(h^{k-1}) \sum_{i=0}^{k-1} I(u(i); y^{l_i} \mid u^{i-1})]$$

where $I(.;. \mid .)$ represents conditional mutual information. According to [30], $I_\infty^{h_a}(y \to u)$ specifies the average directed information rate across the forward channel from y to u in the NCS of Fig. C.1 over all possible realizations of the channel delay.

Proof. It can be implied from [10, Theorem 3.1] that, for each realization h^∞ of the delays, the average data rate (C.4) in the feedback loop of Fig. C.3 is

bounded from below as

$$\mathcal{R}(h^{\infty}) \geq I_{\infty}(y \to u) = \lim_{k\to\infty} \frac{1}{k} \sum_{i=0}^{k-1} I(u(i); y^i \mid u^{i-1}). \tag{C.11}$$

Based upon the chain rule of mutual information, the bound in (C.11) can be restated as

$$\mathcal{R}(h^{\infty}) \geq \lim_{k\to\infty} \frac{1}{k} \sum_{i=0}^{k-1} [I(u(i); y^{l_i} \mid u^{i-1}) + I(u(i); y_{l_i+1}^{i} \mid u^{i-1}, y^{l_i})], \tag{C.12}$$

where the definition of l_i is given in Remark 3.1. From the dynamics of the plant, we can easily conclude that the sequence $y_{l_i+1}^{i}$ is only a function of $x(0)$ and w, once u^{i-1} is given. Furthermore, it stems from (C.2)-(C.8) that upon the knowledge of y^{l_i}, side informations η_d^i and $\eta_e^{l_i}$ will be the only variables describing $u(i)$, $\forall i \in \mathbb{N}_0$. Latter observations together with the fact that Assumption 3.2 holds for the system of Fig. C.1 yield the conclusion that the rightmost term of (C.12) amounts to zero, $\forall i \in \mathbb{N}_0$. So we have

$$\mathcal{R}(h^{\infty}) \geq \lim_{k\to\infty} \frac{1}{k} \sum_{i=0}^{k-1} I(u(i); y^{l_i} \mid u^{i-1}) \tag{C.13}$$

for the NCS of Fig. C.3. Now by averaging both sides of (C.13) with respect to the delay realizations, as in (C.9), and noting that the feedback loop of Fig. C.3 is equivalent to the system of Fig. C.1, based on Remark 3.4, our claim follows immediately. □

The next lemma shows that joint Gaussianity of two signals lowers the directed information rate between them when these are connected through a channel with random delay.

Lemma 4.1
Suppose that the NCS of Fig. C.1 satisfies Assumption 3.1 and Assumption 3.2. For this system, if $(x(0), w, u, y)$ represents a jointly second-order set of processes, then the following holds:

$$I_{\infty}^{h_a}(y \to u) \geq I_{\infty}^{h_a}(y_G \to u_G),$$

where y_G and u_G symbolize the Gaussian counterparts of y and u, respectively, in a way that $(x(0), w, u_G, y_G)$ are jointly Gaussian with the same first-and second-order (cross-) moments as $(x(0), w, u, y)$.

Proof. According to [10, Lemma 3.1], the directed information rate from sensor output to the control input in the auxiliary NCS of Fig. C.3 is bounded as follows:

$$I_{\infty}(y \to u) \geq I_{\infty}(y_G \to u_G),$$

where $I_\infty(y \to u)$ and $I_\infty(y_G \to u_G)$ are defined as in (C.11). We conclude based on (C.2)-(C.8), the dynamics of the plant and the system of Fig. C.3 satisfying Assumption 3.2 that $I(u(i); y_{l_i+1}^i \mid u^{i-1}, y^{l_i}) = 0, \forall i \in \mathbb{N}_0$. This together with the chain rule of mutual information lead to

$$\lim_{k\to\infty} \frac{1}{k} \sum_{i=0}^{k-1} I(u(i); y^{l_i} \mid u^{i-1}) \geq \lim_{k\to\infty} \frac{1}{k} \sum_{i=0}^{k-1} I(u_G(i); {y_G}^{l_i} \mid {u_G}^{i-1}). \tag{C.14}$$

Now the proof is complete by taking average over all possible realizations of the delay from both sides of (C.14) and considering that based on Remark 3.4, the system of Fig. C.1 is equivalent to the feedback loop in Fig. C.3. □

If the above Gaussian signals are stationary as well, then the average directed information rate can be stated in terms of the average power spectral density of the involved signals. The next lemma will state such result formally.

Lemma 4.2
Suppose that the control input u in the NCS of Fig. C.1 is SAWSS for every realization of the channel delay. For each realization, assume that there exists a $\mu > 0$ in such a way that $|\lambda_{\min}(C_{u_1^n})| \geq \mu$, $\forall n \in \mathbb{N}$. Let further consider the sensor output y jointly AWSS with u. Then the average directed information rate is equal to an integral term as follows:

$$I_\infty^{h_a}(y \to u) = \sum_{\substack{h^k \in \mathfrak{H} \\ k\to\infty}} Pr(h^k)[\frac{1}{4\pi} \int_{-\pi}^{\pi} \log\big(\frac{S_{\tilde{u}}(e^{j\omega}, h^k)}{\sigma_\psi^2(h^k)}\big) d\omega],$$

where ψ is a Gaussian AWSS process that has independent samples. Such a random process is described as

$$\psi(k) \triangleq u(k) - \tilde{u}(k), \tilde{u}(k) \triangleq \mathbf{E}[u(k) \mid y^{l_k}, u^{k-1}] \tag{C.15}$$

for each realization of the random delay. Moreover, $S_{\tilde{u}}$ represents the steady-state power spectral density of u.

Proof. It can be deduced from [10, Lemma 3.2] that in the NCS of Fig. C.3, the following holds for the directed information rate :

$$I_\infty(y \to u) = \frac{1}{4\pi} \int_{-\pi}^{\pi} \log\big(\frac{S_{\bar{u}}(e^{j\omega})}{\sigma_n^2}\big) d\omega,$$

in which n is a Gaussian AWSS process with independent samples and $I_\infty(y \to u)$ is defined as in (C.11). The noise n is calculated as follows:

$$n(k) \triangleq u(k) - \hat{u}(k), \hat{u}(k) \triangleq \mathbf{E}[u(k) \mid y^k, u^{k-1}].$$

As already mentioned before, based on the plant dynamics, the knowledge of u^{i-1} will render $y_{l_i+1}^i$ dependent only on $x(0)$ and w^i for any $i \in \mathbb{N}_0$. Moreover, according to (C.2)-(C.8), knowing y^{l_i}, one can determine $u(i)$ by only figuring out ${\eta_d}^i$ and ${\eta_e}^{l_i}$, $\forall i \in \mathbb{N}_0$. Since, based on Assumption 3.2, (x_0, w) and (η_d, η_e) are independent, the following is yielded:

$$\lim_{k\to\infty} \frac{1}{k} \sum_{i=0}^{k-1} I(u(i); y^{l_i} \mid u^{i-1}) = \frac{1}{4\pi} \int_{-\pi}^{\pi} \log\big(\frac{S_{\breve{u}}(e^{j\omega})}{\sigma_n^2}\big) d\omega, \qquad \text{(C.16)}$$
$$\mathbf{E}[u(k) \mid y^k, u^{k-1}] = \mathbf{E}[u(k) \mid y^{l_k}, u^{k-1}].$$

From (C.16), it can be concluded that $n(k)$ is actually equal to $\psi(k)$ as in (C.15) for the NCS of Fig. C.3. Now, our claim is given by taking average from both sides of upper (C.16) and noting that based on Remark 3.4, the systems in Fig. C.3 and Fig. C.1 are equivalent. □

We are now ready to present a lower bound on $\mathcal{R}_a(D)$. A corollary follows:

Corollary 4.1
Suppose that the NCS of Fig. C.1 satisfies Assumption 3.1. Then $\mathcal{R}_a(D)$ is lower bounded as follows:

$$\mathcal{R}_a(D) \geq \inf_{\sigma_{z_a}^2 \leq D} \sum_{\substack{h^k \in \mathfrak{H} \\ k\to\infty}} Pr(h^k) \frac{1}{4\pi} \int_{-\pi}^{\pi} \log\big(\frac{S_{\breve{u}}(e^{j\omega}, h^k)}{\sigma_{\psi}^2(h^k)}\big) d\omega,$$

where ψ and $\breve{u}$ are defined as in (C.15) and the infimum is restricted to all mappings satisfying (C.5)-(C.8) and Assumption 3.2, and producing signals y and u with properties as stated in Lemma 4.2.

Proof. The claim follows immediately from Theorem 4.1 and Lemma 4.2. □

5 Lower Bound Problem in the Case of the Constant Delay

In this section, we consider the same NCS as described in Section 3 but with a channel that imposes a known constant delay, say h steps, on the transmitted data. The corresponding feedback loop is depicted by Fig. C.4. The problem we investigate here is a special case of the problem formalized in (C.10) where the channel delay is constant and therefore, there is only one realization for the channel delay. In this case, we consider the notation $\mathcal{R}_a(D) = \mathcal{R}(D)$ and $D_{\inf}(h_r) = D_{\inf}(h)$. In Appendix B.1, we prove that finding $\mathcal{R}(D)$ is feasible if $D \in (D_{\inf}(h), \infty)$. We show that in order to obtain a lower bound on $\mathcal{R}(D)$, one can minimize the directed information rate over an auxiliary coding scheme formed of LTI filters and an AWGN channel with feedback and delay.

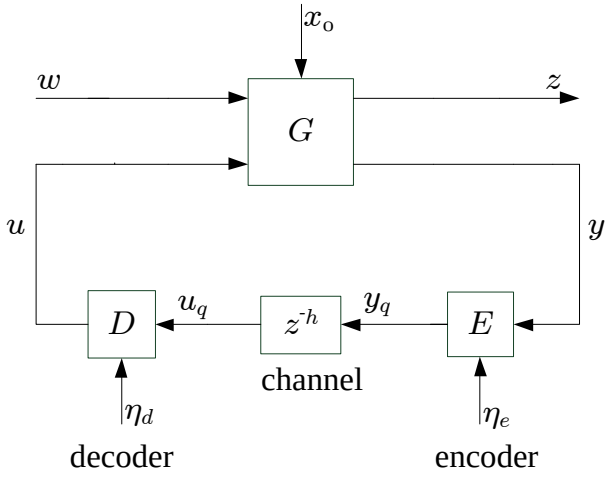

Fig. C.4: Considered NCS in the constant delay case

Inequalities and identities related to the delay-free version of this optimization derived in [10] will be extended to the case with a constant channel delay. We start by deriving a lower bound on the average data rate $\mathcal{R}$ in the following theorem.

Theorem 5.1
Suppose that the feedback system of Fig. C.4 satisfies Assumptions 3.1 and 3.2. Then the average data rate $\mathcal{R}$ is lower bounded as follows:

$$\mathcal{R} \geq I_{\infty}^{(h)}(y \to u) = \lim_{k\to\infty} \frac{1}{k} \sum_{i=0}^{k-1} I(u(i); y^{i-h} \mid u^{i-1}), \tag{C.17}$$

where $I_{\infty}^{(h)}(y \to u)$ is the directed information rate across the forward channel from y to u with constant delay h (see [30, Definition 1] for the formal definition).

Proof. Considering that $l_k = h$ holds at any $k \in \mathbb{N}_0$ for the NCS of Fig. C.4, we can conclude the claim immediately from Theorem 4.1. □

The directed information rate in (C.17) will be reduced if the involved signals are jointly Gaussian. This result is formalized by the following lemma.

Lemma 5.1
Suppose that Assumptions 3.1 and 3.2 hold for the NCS of Fig. C.4. Furthermore, consider $(x(0), w, u, y)$ as a jointly second-order set of random processes. Denote the Gaussian counterparts of y and u by y_G and u_G, respectively, where $(x(0), w, u_G, y_G)$ are jointly Gaussian with the same first-and second-order (cross-) moments as $(x(0), w, u, y)$. Then $I_{\infty}^{(h)}(y \to u) \geq I_{\infty}^{(h)}\ (y_G \to u_G)$.

Proof. Recall that $l_k = h$, $\forall k \in \mathbb{N}_0$, for the considered case with constant channel delay. The claim follows immediately from Lemma 4.1. □

It can be implied from Lemma 5.1 that by minimizing directed information rate over a scheme that renders y and u jointly Gaussian, one can obtain a lower bound on $\mathcal{R}(D)$. Now, we will show that the directed information rate can be stated in terms of power spectral densities of the involved processes if such signals meet certain stationarity conditions.

Lemma 5.2
Suppose that u is an SAWSS process with $|\lambda_{\min}(C_{u_1^n})| \geq \mu$, $\forall n \in \mathbb{N}$ where $\mu > 0$. Moreover, assume that u is jointly Gaussian and AWSS with the sensor output y. Then the directed information rate between u and y is expressed as

$$I_{\infty}^{(h)}(y \to u) = \frac{1}{4\pi} \int_{-\pi}^{\pi} \log \big(\frac{S_{\breve{u}}(e^{j\omega})}{\sigma_{\psi}^2}\big) d\omega,$$

where ψ represents a Gaussian AWSS process with independent samples defined by

$$\psi(k) \triangleq u(k) - \tilde{u}(k), \tilde{u}(k) \triangleq \mathbf{E}[u(k) \mid y^{k-h}, u^{k-1}].$$

Furthermore, $S_{\breve{u}}$ denotes the steady-state power spectral density of u.

Proof. Immediate from Lemma 4.2 by noting that $l_k = h$ holds for the NCS of Fig. C.4 at every time instant $k \in \mathbb{N}_0$. □

It can be implied from Theorem 5.1 and Lemma 5.2 that the rate-performance pair yielded by any coding and control scheme satisfying Assumption 3.2 which renders the NCS of Fig. C.4 SAWSS is attainable with a lower or equal rate if there exists a scheme that generates (y, u) jointly Gaussian with (x_0, w) while rendering the system SAWSS. Due to the Gaussianity of (x_0, w) and the fact that the plant is LTI, a jointly Gaussian pair (y, u) can be produced by a coding-control scheme comprised of LTI filters and an AWGN noise source. Such a scheme is depicted in Fig. C.5. The NCS of Fig. C.5 satisfies all of the assumptions and conditions that hold for the system of Fig. C.4. However, the arbitrary mappings are replaced by proper LTI filters B and J in the auxiliary feedback loop of Fig. C.5.

In addition, for such an NCS, a delayed AWGN channel with noiseless one-sample-delayed feedback serves as communication channel. The coding-control scheme in the NCS of Fig. C.5 is described via the following dynamics:

$$u' = Jz^{-h}r, \quad r = t + \eta, \quad t = B\mathrm{diag}\{z^{-1}, 1\} \begin{bmatrix} r \\ y' \end{bmatrix},$$

where η is a zero-mean white Gaussian noise with variance σ_{η}^2 and independent of (x_0, w), and $B = [B_r \quad B_y]$. It should be emphasized that Assumption 3.1

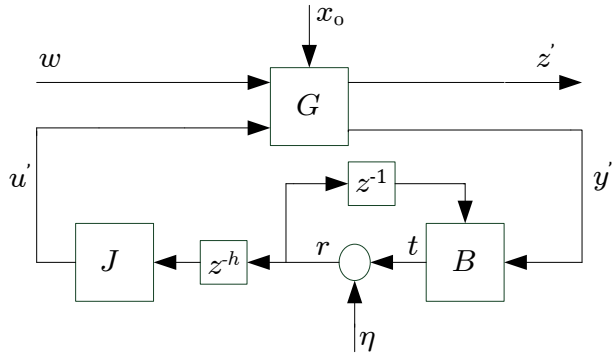

Fig. C.5: The LTI structure giving the lower bound in the constant delay case

holds for the initial states x_0, the plant G and the disturbance input w in the NCS of Fig. C.5. Furthermore, the initial states of the filters B and J, and the delay blocks are deterministic. As the system depicted in Fig. C.5 is a special case of the structure of Fig. C.4, we use apostrophes for presenting signals in Fig. C.5 that have counterparts in the NCS of Fig. C.4.

Theorem 5.2
If the NCS of Fig. C.4 satisfies Assumption 3.1 and Assumption 3.2 and $D \in (D_{\inf}(h), \infty)$ holds, then

$$\mathcal{R}(D) \geq \vartheta'_u(D) \triangleq \inf_{\sigma^2_{z'} \leq D} \frac{1}{4\pi} \int_{-\pi}^{\pi} \log\big(\frac{S_{u'}(e^{j\omega})}{\sigma^2_\eta}\big), \tag{C.18}$$

where $\sigma^2_{z'}$ and $S_{u'}$ represent the steady-state variance of z' and the steady-state power spectral density of u' in Fig. C.5, respectively. Moreover, the feasible set for the optimization in (C.18) is the set comprised of all LTI filters B and the noise η with $\sigma^2_\eta \in \mathbb{R}_+$ that render the system of Fig. C.5 internally stable and well-posed with $J = 1$.

Proof. See Appendix B.2. □

Theorem 5.2 implies that doing the optimization in (C.18) over the auxiliary LTI system of Fig. C.5, with the AWGN channel and delay, will give a lower bound on the minimal data rate required to achieve a certain performance level in the arbitrary (possibly nonlinear and time-varying) structure of Fig. C.4. The following results show how the lower bound derived in (C.18) can be simplified to a bound which is easier to compute.

Lemma 5.3
For the NCS of Fig. C.5, let describe ϑ'_r by

$$\vartheta'_r(B, J, \sigma^2_\eta) \triangleq \frac{1}{4\pi} \int_{-\pi}^{\pi} \log\big(\frac{S_r(e^{j\omega})}{\sigma^2_\eta}\big), \tag{C.19}$$

where $\sigma_\eta^2 \in \mathbb{R}^+$ is fixed and S_r denotes the steady-state power spectral density of r. Moreover, suppose that the pair $(B, J) = (B_1, J_1)$ renders the feedback loop of Fig. C.5 internally stable and well-posed. Then for any $\rho > 0$, there exists another pair with a biproper filter, say J_2, and a proper one, say B_2, that renders the system of Fig. C.5 internally stable and well-posed, and preserves the steady-state power spectral density of z' in a way that the following holds:

$$\vartheta_r^{'}(B_1, J_1, \sigma_\eta^2) = \vartheta_r^{'}(B_2, J_2, \sigma_\eta^2) = \frac{1}{2}\log(1 + \frac{\sigma_t^2}{\sigma_\eta^2})|_{(B,J)=(B_2,J_2)} - \rho. \quad \text{(C.20)}$$

Proof. See Appendix B.3. □

Intuitively speaking, the results of Theorem 5.2 and Lemma 5.3 imply that $\mathcal{R}(D)$ can be bounded from below by a logarithmic term as in (C.20) which is a function of channel SNR in the NCS of Fig. C.5. Such an intuition will assist us with deriving a lower bound which is computationally appealing in the following corollary.

Corollary 5.1
Take the feedback loop of Fig. C.4 into account as an NCS that satisfies Assumptions 3.1 and 3.2. Then for every $D \in (D_{\inf}(h), \infty)$, the following holds:

$$\mathcal{R}(D) \geq \frac{1}{2}\log(1 + \varphi'(D)), \quad \varphi'(D) \triangleq \inf_{\sigma_{z'}^2 \leq D} \frac{\sigma_t^2}{\sigma_\eta^2}, \quad \text{(C.21)}$$

in which σ_t^2 and $\sigma_{z'}^2$ symbolize the steady-state variances of t and z' in the auxiliary system of *Fig. C.5*, respectively. For the optimization problem in (C.21), a candidate solution is an LTI filter pair (B, J) together with noise variance $\sigma_\eta^2 \in \mathbb{R}^+$ that cause the system in Fig. C.5 to become internally stable and well-posed.

Proof. See Appendix B.4. □

6 Upper Bound Problem in the Presence of Constant Delay

In this section, we show that for any $D \in (D_{\inf}(h), \infty)$, one can always find a scheme that guarantees attaining $\sigma_z^2 \leq D$ with an average data rate which has a distance of about 1.254 bits per sample from the theoretical lower bound. For such a scheme, we propose a design approach which utilizes the filters that together with an AWGN with feedback and delay, render the directed information rate over the channel equal to the lower bound on $\mathcal{R}(D)$.

Definition 6.1
We call a coding scheme with input-output relationship as in (C.5)-(C.8) in the constant channel delay case linear if and only if its dynamics can be restated as follows:

$$u = Jz^{-h}r, \quad r = t + \eta, \quad t = B\mathrm{diag}\{z^{-1}, 1\} \begin{bmatrix} r \\ y \end{bmatrix}, \tag{C.22}$$

where $B = [B_r \quad B_y]$ and J are proper LTI filters with deterministic initial condition. Moreover, η represents a zero-mean i.i.d random sequence independent of (x_0, w). The initial state of the one-step-delay feedback channel is assumed to be deterministic.

The realization of linear source coding schemes can be carried out by using entropy-coded dithered quantizers (ECDQs) together with LTI filters. First, implementing an ECDQ causes the following relationship between (u_q, y_q) in (C.2) and (C.6), and (r, t) in (C.22):

$$\begin{aligned} y_{\mathcal{E}}(k) &= \mathcal{F}_q(t(k) + d(k)) \\ y_q(k) &= \mathcal{O}_k(y_{\mathcal{E}}(k), d(k)) \\ u_{\mathcal{D}}(k) &= \mathcal{O}_{k-h}^{-1}(u_q(k), d(k-h)) \\ r_h(k) &= u_{\mathcal{D}}(k) - d(k-h), \end{aligned} \tag{C.23}$$

in which by $\mathcal{F}_q$, we denote a uniform quantizer with resolution $\Delta \in \mathbb{R}^+$, $\mathcal{F}_q : \mathbb{R} \to \{i\Delta; i \in \mathbb{Z}\}$. Additionally, $d(k)$ represents a dither signal whose access are provided to both encoder and decoder. The mapping $\mathcal{O}_k$ and its complementary $\mathcal{O}_k^{-1}$ formalize entropy coding for the lossless parts at the encoder and decoder, respectively. The following lemma presents an interesting property of ECDQs when being set up in an LTI feedback loop.

Lemma 6.1
Consider the feedback loop depicted in Fig. C.6 and suppose that the plant $\tilde{G}$ is described by a proper real rational transfer-function matrix in which the transfer function from r_h to t is scalar and strictly proper. For such a system, assume that the input-output relationship of the ECDQ in the feedback path is given by (C.23) with finite and positive quantization step size Δ. Moreover, take the disturbance $\tilde{w}$ into account as a white noise process jointly second-order with $\tilde{x}_0$, the initial state of $\tilde{G}$. Then if the dither d is an i.i.d process with a uniform distribution over $(-\Delta/2, \Delta/2)$ and independent of $(\tilde{w}, \tilde{x}_0)$, the error $r - t$ is i.i.d, uniformly distributed over $(-\Delta/2, \Delta/2)$ and independent of $(\tilde{w}, \tilde{x}_0)$.

Proof. See Appendix B.5. □

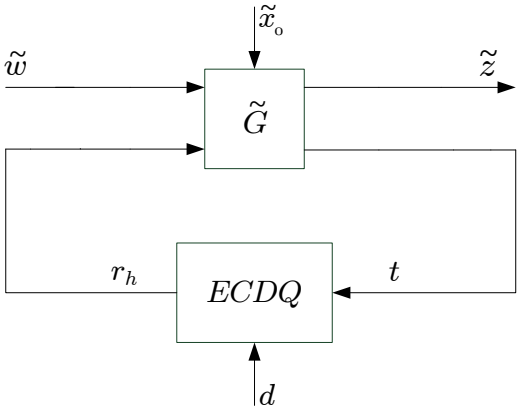

Fig. C.6: ECDQ setup in the feedback path

It can be implied from above that combining the LTI filters in (C.22) with the ECDQ in (C.23) in a setting as depicted in Fig. C.7 will lead to a linear coding scheme for the NCS of Fig. C.4 as long as $d(k)$ meets the same criteria as for the dither in Lemma 6.1. If so, the obtained coding scheme is called a linear ECDQ-based coding scheme. If such a scheme is implemented on the feedback path of the main NCS of Fig. C.4, the average data rate is bounded from above by a certain value which is shown in the following lemma.

Lemma 6.2
Suppose that Assumption 3.1 holds for the NCS of Fig. C.4. Then the existence of an ECDQ-based linear source-coding scheme rendering the NCS of Fig. C.4 SAWSS is certified in such a way that the average data rate satisfies

$$\mathcal{R} < \frac{1}{2}\log\left(1+\frac{\sigma_t^2}{\sigma_\eta^2}\right)+\frac{1}{2}\log\left(\frac{2\pi e}{12}\right)+\log 2. \tag{C.24}$$

In (C.24), the variance of the quantization error (noise) of the ECDQ-based

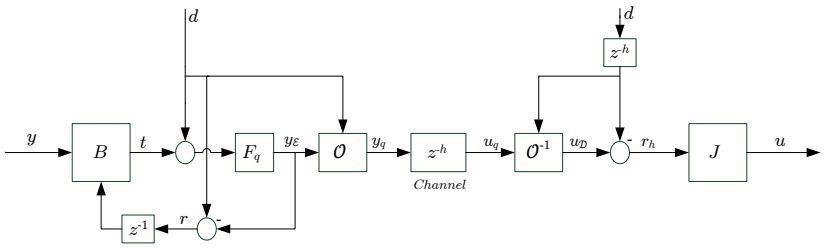

Fig. C.7: The proposed ECDQ-based linear coding scheme

linear source-coding scheme is set as $\sigma_\eta^2 = \Delta^2/12$. Moreover, σ_t^2 represents the steady-state variance of the signal t in (C.22).

Proof. See Appendix B.6. □

Now, through the following theorem, we use the result of Lemma 6.2 to show that utilizing ECDQ-based linear coding schemes can lead to an upper bound on the desired minimal average data rate $\mathcal{R}(D)$.

Theorem 6.1
Let Assumption 3.1 hold for the closed-loop system of Fig. C.4. Then for each $D \in (D_{\inf}(h), \infty)$, one can always find an ECDQ-based linear source-coding scheme satisfying Assumption 3.2 and rendering the feedback loop of Fig. C.4 SAWSS in such a way that $\sigma_z^2 \leq D$ is resulted and the average data rate is bounded as

$$\mathcal{R} < \frac{1}{2}\log\left(1 + \varphi'(D)\right) + \frac{1}{2}\log\left(\frac{2\pi e}{12}\right) + \log 2, \tag{C.25}$$

where the definition of $\varphi'(D)$ is given in (C.21).

Proof. See Appendix B.7. □

In the following remark, we state how the upper bound derived in Theorem 6.1 can be considered as an upper bound on $\mathcal{R}_a(D)$ in the case of random channel delay.

Remark 6.1
The upper bound in (C.25) will be an upper bound on $\mathcal{R}_a(D)$ in the random channel delay case if coding and control schemes are linear ECDQ-based schemes designed as in the proof of Theorem 6.1 for the delay $h_{\max}$ where the decoder-controllers have buffers installed at their inputs sending only $y_q(k-h_{\max})$ for processing at each time instant $k \in \mathbb{N}_0$. Clearly, this is due to the fact that at every time step $k \in \mathbb{N}_0$, $y_q(k - h_{\max})$ is available at the decoder. Such an upper bound does not seem to be tight since imposing a delay of $h_{\max}$ steps on transmitted data is actually a worst-case scenario.

The bounds derived in this section and the previous section limit the desired average data rate $\mathcal{R}(D)$ in the NCS of Fig. C.4. In this system, the constant delay is induced by the digital communication channel between the encoder-controller and the decoder-controller. One concern is the effect of delay location on the derived bounds. The following lemma takes a step in addressing this issue by showing how the system signals change when the time delay block is moved to a different location in the feedback loop of Fig. C.4.

Lemma 6.3
Consider the NCS of Fig. C.4 and two other systems each of which yielded by moving the delay component in the NCS of Fig. C.4 to either the measurement

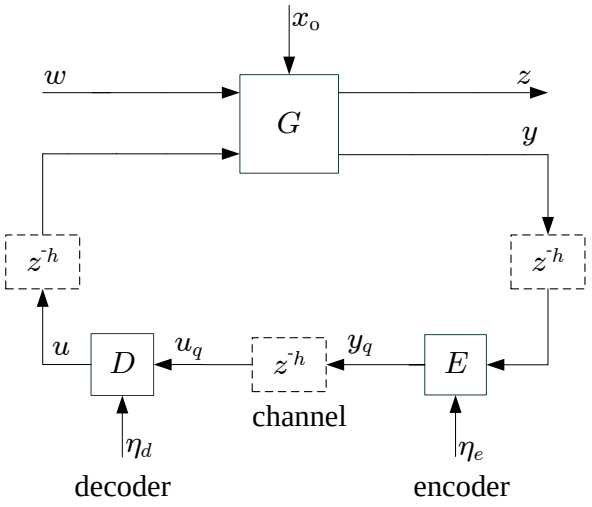

Fig. C.8: Three possible locations for the delay component in the case with constant channel delay

path (between the sensor and the encoder-controller) or the actuation path (between the decoder-controller and the plant). Fig. C.8 depicts the locations where the time delay occurs in these cases. Then systems are not necessarily equivalent across the cases if the only difference between them is the delay location. However, the equivalence can be assured by allowing the side information to change across the cases.

Proof. See Appendix B.8. □

7 Numerical Simulation

Take the following transfer function into account as the model describing the generalized plant G in the NCS of Fig. C.4:

$$z = \frac{0.165}{(z-2)(z-0.5789)}(w+u), \quad y = z,$$

Let us set the disturbance signal w and initial states x_0 in such a way that Assumption 3.1 is satisfied. We calculated lower and upper bounds on $\mathcal{R}(D)$ as derived in (C.21) and (C.25). For computing these bounds, we made use of the equivalence between the NCSs of Fig. C.5 and Fig. C.12, shown in the proof of Lemma 5.3, in that we adopted the method in [10] which solves SNR-performance optimization problems similar to the one defining $\varphi'(D)$ for such systems as the NCS of Fig. C.12. The bounds are computed for three

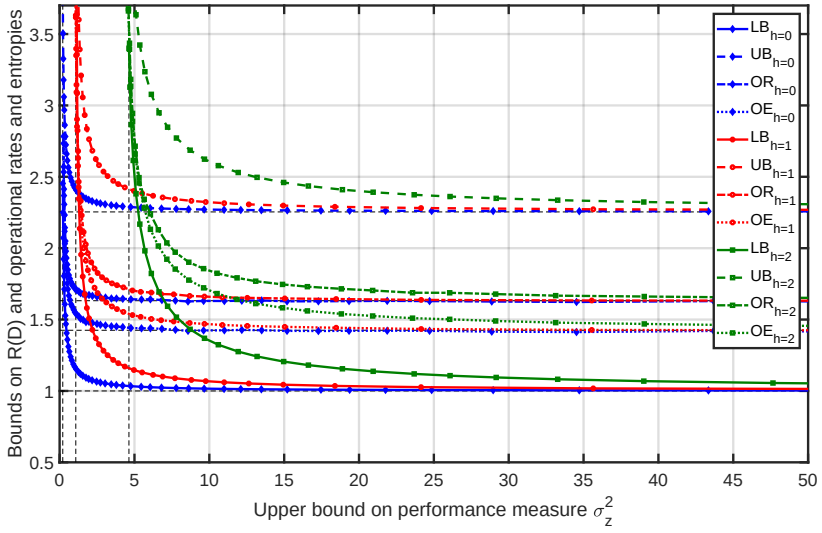

Fig. C.9: Bounds on $\mathcal{R}(D)$ in (C.21) and actual data rates and entropies for different values of time delay h

different values of channel delay, $h = \{0, 1, 2\}$, with respect to D varying over a range from $D_{\text{inf}}(h)$ to 50 for each h. Moreover, we designed actual linear ECDQ-based coding schemes, and for each selected D in the latter interval, we simulated the NCS of Fig. C.4. To do so, we utilized the filters giving the lower bound on $\mathcal{R}(D)$ according to the procedure suggested in [10, Theorem 5.1]. The results are demonstrated in Fig. C.9. In this figure, the curves referred to as LB and UB present the lower and upper bounds on $\mathcal{R}(D)$, respectively. We can compare $D_{\text{inf}}(h)$ among cases with different values of channel delay as well. As shown, greater $D_{\text{inf}}(h)$ is associated with larger channel delay, as expected according to [31]. Evaluating how the bounds change in response to changes in the delay is one of the main purposes of this simulation study. We can observe from the bounds plotted in Fig. C.9 that when D is fixed, increasing the delay will enlarge the bounds on $\mathcal{R}(D)$. In other words, the greater the delay is, the higher average data rate is to be used in order to achieve a fixed quadratic performance level. Moreover, Fig. C.9 shows that the lower (upper) bound curves converge to the minimum data rate required for mean square stability as D grows larger. From [32], we know that the minimal data rate guaranteeing stabilizability of the NCS of Fig. C.5 is only a function of unstable poles of the plant G. On the other hand, we use the equivalent system of Fig. C.12 for the purpose of calculating bounds. So the observation with convergence of bounds to the minimal data rate needed for stability comes from the fact that incorporating time delay into the model of the plant G_a will

not affect its unstable poles.

Simulation results are illustrated in Fig. C.9 as well. The curves referred to as OR and OE present the average data rates and entropies achieved by using actual linear coding schemes. Furthermore, 10^6-sample-long realizations have been considered for the dither. The coding task in all utilized schemes is done by memory-less Huffman coders which do not take the past information of the dither into account as prior knowledge for coding. In addition to the average data rate, the entropy of the output of the quantizer has been estimated for the aforementioned setup. The gap of around 0.4 bits per sample between the measured entropy and the lower bound indicates that for each $h \in \{0, 1, 2\}$, 0.4 bits per sample of the gap between the actual rates and lower bound is caused by replacing the AWGN with uniform dither and the remainder 0.25 bits per sample corresponds to sample-by-sample coding. It can be observed that the actual rates and entropies have the same properties as the properties of bounds mentioned in the previous paragraph. The most prominent property is related to the behaviour of the achieved rates and entropies as a function of channel delay, i.e., for a system with greater time delay in the channel, higher rates are required to guarantee quadratic performance requirements.

8 Conclusions

In this paper, the trade-off between average data rate and performance in networked control systems has been studied. Two setups have been investigated, each of which incorporates an LTI plant with Gaussian disturbance and initial states, and scalar control input and sensor output. Moreover, both of them have causal, but otherwise arbitrary, mappings on their feedback paths which are responsible for coding and control. The only difference between the two considered systems is the model of the channel that carries out data transmission between the encoder-controller and the decoder-controller. In one case, the digital communication channel is SIMO and information to be exchanged are exposed to random delay. In the other system, the channel is error-free as well but it is SISO and imposes constant delay on transmitted data. For the case with random channel delay, we considered notions for rate and performance which show the average behaviour of the system over all realizations of the delay. We have shown that for such a setup, data rate is lower bounded by average directed information rate from the sensor output to control input, and if y and u are jointly Gaussian, the average directed information rate would be lowest. Moreover, we have shown that when y and u satisfy certain stationarity assumptions, the average directed information rate between them is a function of the average power spectral densities of these signals over all realizations of the channel delay. We have shown that infimum value of this function over all arbitrary coders and controllers that cause system signals have those Gaus-

sianity and staionarity properties lower bounds the infimum average data rate required to attain a prescribed quadratic performance.

For the constant delay case, which is a special case of the system with random channel delay, we approximated (by deriving bounds) the minimal average data rate that certifies attaining a certain performance level. Employing the fundamental information inequalities and identities derived for the random delay case, we showed that this desired minimal average data rate is bounded from below when coder-controllers and the channel behave as a concatenation of proper LTI filters and an AWGN channel with feedback and delay. Then we showed that by approximating such schemes with simply implementable linear ECDQ-based coding schemes, one can achieve any (legitimate) performance level by actual rates which are at most 1.254 bits per sample higher than the lower bound. The results illustrated through the simulation show that bounds and empirical rates are increasing functions of channel delay for a fixed performance level. It means larger delay in the channel necessitates higher minimal average data rate that is needed for achieving a certain level of quadratic performance.

Future research will concern with finding closed-form solution for the lower and upper bound problems in the case of random channel delay, finding analytic expression for the desired infimum data rate, deriving lower and upper bounds with shorter gap between them, plants with model uncertainties and vector quantization.

Appendices

A Invertibility of the Decoder

Lemma A.1
Consider a coding scheme described through (C.5)-(C.8) that has a non-invertible decoder, and let $\check{R}(k)$ be defined as $\check{R}(k) \triangleq H(y_{\mathcal{E}}(k) \mid y_{\mathcal{E}f}(k), \eta_o^k)$. For such scheme, assume that $u(k) = u_0(k)$ and $\check{R}_f(k) = \check{R}_{f0}(k)$, $\forall k \in \mathbb{N}_0$, where $\check{R}_f(k) \triangleq [\check{R}(i))]_{i\in S(k)}^T$. Then there exists another coding scheme constructing the control input $u(k) = u_0(k)$ with an invertible decoder in such a way that $\check{R}_f(k) \leq \check{R}_{f0}(k)$, $\forall k \in \mathbb{N}_0$.

Proof. Suppose that mappings in (C.7)-(C.8) represent a non-invertible decoder at time k in a way that upon knowledge of η_d^i and S^i, perfect reconstruction of u_q^i from u^i has been possible for all $i \leq k-1$. Then there exist $u_{\mathcal{D}1}, u_{\mathcal{D}2} \in \mathcal{A}_s$ such that $u(k) = \mathcal{D}_k(u_{\mathcal{D}1}, u_{\mathcal{D}}^{k-1}, \eta_d^k) = \mathcal{D}_k(u_{\mathcal{D}2}, u_{\mathcal{D}}^{k-1}, \eta_d^k)$. Let S_1 and S_2 be associated with $u_{\mathcal{D}1}$ and $u_{\mathcal{D}2}$ respectively. Two possible cases can occur. In the first case, S_1 and S_2 are unequal, i.e., $S_1 \neq S_2$. Since S is known at the decoder at each time step, this case does not contradict the invertibility. That is due

to the fact that the knowledge of S would determine whether $u(k)$ is caused by $u_{\mathcal{D}1}$ or $u_{\mathcal{D}2}$. However, the situation is not the same in the case where $S_1 = S_2$. Since both $u_{\mathcal{D}1}$ and $u_{\mathcal{D}2}$ are vector-valued variables, $u_{\mathcal{D}1} \neq u_{\mathcal{D}2}$ means that at least one entry of $u_{\mathcal{D}1}$ is not equal to the entry with the same dimension in $u_{\mathcal{D}2}$. The corresponding elements of $u_{\mathcal{D}1}$ and $u_{\mathcal{D}2}$ that are not equal to each other are denoted by pairs $(u_{\mathcal{D}1j}, u_{\mathcal{D}2j})$, $1 \leq j \leq m$, $1 \leq m \leq h_{\max}+1$. Since $S_1 = S_2$, for each j, both $u_{\mathcal{D}1j}$ and $u_{\mathcal{D}2j}$ have been exposed to the same delay, say h_j, $0 \leq h_j \leq h_{\max}$. So if we denote the output of the lossy encoder that corresponds to $u_{\mathcal{D}nj}$ by $y_{\mathcal{E}nj}$, then $u_{\mathcal{D}nj}(k) = y_{\mathcal{E}nj}(k-h_j)$. It should be noted that n is a positive integer which is at most equal to the size of the set $\mathcal{A}_s$. Let p_{nj} represent the conditional probability of having $y_{\mathcal{E}nj}$ at the encoder given $(y_{\mathcal{E}f}(k-h_j), \eta_o^{k-h_j})$ at time $k-h_j$. The encoder-decoder set $(\bar{\mathcal{E}}, \bar{\mathcal{D}})$ can be defined with exactly the same properties as $(\mathcal{E}, \mathcal{D})$ but different from it in the sense that $\bar{\mathcal{E}}$ outputs only $y_{\mathcal{E}1j}$ at time $k-h_j$ with probability $p_{1j}+p_{2j}$. This means having only $u_{\mathcal{D}1j}$ at time k as decoder input instead of receiving either $u_{\mathcal{D}1j}$ or $u_{\mathcal{D}2j}$. Let us define $t_j \triangleq k-h_j; k \geq h_j$. Then

$$\begin{aligned}
\check{R}(t_j)\mid_{(\mathcal{E},\mathcal{D})} &= \check{R}_0(t_j) \\
&\overset{(aa)}{=} -\sum_{n\notin\{1,2\}} p_{nj}\ln p_{nj} - p_{1j}\ln p_{1j} - p_{2j}\ln p_{2j} \\
&\overset{(ab)}{\geq} -\sum_{n\notin\{1,2\}} p_{nj}\ln p_{nj} - (p_{1j}+p_{2j})\ln(p_{1j}+p_{2j}) \\
&\overset{(ac)}{=} \check{R}(t_j)\mid_{(\bar{\mathcal{E}},\bar{\mathcal{D}})}
\end{aligned}$$

in which (aa) results from the definition of entropy and $\check{R}(k)$, (ab) can be concluded based on the fact that the function $-\ln(p_{nj})$ is monotonically decreasing, and (ac) follows from the definition of $\check{R}(k)$ for the scheme $(\bar{\mathcal{E}}, \bar{\mathcal{D}})$. So $\check{R}(t_j)\mid_{(\bar{\mathcal{E}},\bar{\mathcal{D}})} \leq \check{R}(t_j)\mid_{(\mathcal{E},\mathcal{D})}$ for $t_j \geq 0$, and consequently $\check{R}_f(k) \leq \check{R}_{f0}(k)$.

The above procedure can be iterated for every pair with the same characteristics as $(u_{\mathcal{D}1}, u_{\mathcal{D}2})$ to make sure that there are no two inputs of the reproduction decoder mapped into one identical $u(k)$ at time instant k. Such iteration will then yield an invertible decoder. In other words, when the pair $(\bar{\mathcal{E}}, \bar{\mathcal{D}})$ is used, knowing (u^i, η_d^i, S^i) is equivalent to knowing $(u_{\mathcal{D}}^i, \eta_d^i, S^i)$ with $u(i) = u_0(i)$ and $\check{R}_f(i) \leq \check{R}_{f0}(i)$, $\forall i \leq k$. Our main claim now follows by repeating the above for every $k \geq 0$. □

B Proofs

B.1 Feasibility Proof for $D_{\inf}(h)$, $\vartheta_u'(D)$ and $\varphi'(D)$

Suppose that in the standard architecture depicted in Fig. C.10, G, x_0 and w satisfy Assumption 3.1 and K follows $u(k) = \mathcal{K}_k(y^{k-h})$. Considering the

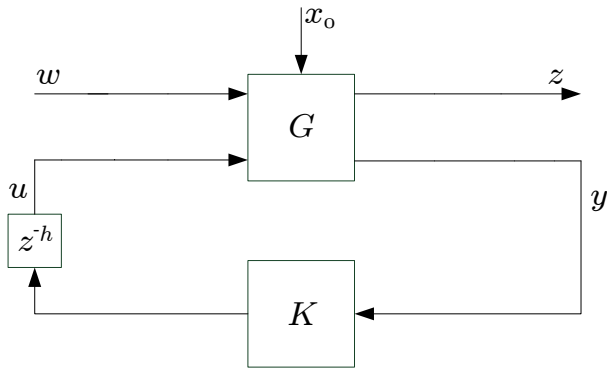

Fig. C.10: Standard feedback loop over which $D_{\inf}(h)$ is defined

Gaussianity of x_0 and w and the fact that G is LTI, we can imply from some results in [33] that:

$$D_{\inf}(h) = \inf_{K \in \kappa} \sigma_z^2,$$

in which σ_z^2 denotes the steady-state variance of output z and κ is the set of all proper LTI filters which render the system of Fig. C.10 internally stable and well-posed. The assumptions considered for G guarantee that finding $D_{\inf}(h)$ is feasible. Since $D_{\inf}(h)$ can be obtained, for every $\zeta \in (0, D - D_{\inf}(h))$, there exists $K_1 \in \kappa$ which gives $\sigma_{z_1}^2 \triangleq \sigma_z^2 \mid_{K=K_1} \leq D_{\inf}(h) + \zeta < D$ for the system of Fig. C.10. Applying K_1 to this system results in a stable setting which is a special case of the NCS depicted in Fig. C.5 with $J = 1$ and $r = t = K_1 y'$ where the steady-state variance of t, $\sigma_t^2 = \sigma_{t_1}^2$, is finite. Therefore, since $K_1 \in \kappa$, it can bring internal stability and well-posed-ness to the feedback loop of Fig. C.5 in the presence of any additive noise η with steady-sate variance $\sigma_\eta^2 \in \mathbb{R}^+$. So $\sigma_{z'}^2 = \sigma_{z_1}^2 + \chi_z \sigma_\eta^2$ and $\sigma_t^2 = \sigma_{t_1}^2 + \chi_t \sigma_\eta^2$ can be concluded, when taking η into account as an AWGN with finite variance σ_η^2 for the system of Fig. C.5. It should be noted that $\chi_t, \chi_z \geq 0$ depend only on K_1. Now by choosing $\zeta = (D - D_{\inf}(h))/3$ and the variance $\sigma_\eta^2 = (D - D_{\inf}(h))/(3\chi_z)$ for the AWGN, there exists $K_1 \in \kappa$ rendering the NCS of Fig. C.5 internally stable and well-posed in a way that $\sigma_{z'}^2|_{(B,J,\sigma_\eta^2)=(K_1,1,\sigma_\eta^2)} \leq D_{\inf}(h) + \frac{2}{3}(D - D_{\inf}(h)) < D$. Then the following can be obtained for the structure of Fig. C.5:

$$\frac{\sigma_t^2}{\sigma_\eta^2}|_{(B,J,\sigma_\eta^2)=(K_1,1,\sigma_\eta^2)} = \frac{3\sigma_{t_1}^2 \chi_z}{D - D_{\inf}(h)} + \chi_t < \infty. \tag{C.26}$$

So considering Jensen's inequality and concavity of logarithm, we can deduce that the problem of finding $\vartheta_u'(D)$ in (C.18) is feasible for every $D > D_{\inf}(h)$. The feasibility of the problem of finding $\varphi'(D)$ in (C.21) is inferred immediately

from (C.26) for any $D > D_{\inf}(h)$.

B.2 Proof of Theorem 5.2

Due to the validity of $D > D_{\inf}(h)$, one can always find at least one coding-control pair, say $\hat{E}$ and $\hat{D}$, that while satisfying Assumption 3.2, renders the NCS of Fig. C.4 SAWSS in such a way that $\sigma_{\hat{z}}^2 \leq D$ and

$$\mathcal{R} \geq I_{\infty}^{(h)}(\hat{y} \to \hat{u}) \geq I_{\infty}^{(h)}(\hat{y}_G \to \hat{u}_G) = \frac{1}{4\pi} \int_{-\pi}^{\pi} \log\big(\frac{S_{\check{u}}(e^{j\omega})}{\sigma_{\hat{\psi}_G}^2}\big) d\omega. \quad \text{(C.27)}$$

In (C.27), processes $\hat{z}$, $\hat{y}$ and $\hat{u}$ are the counterparts of z, y and u in Fig. C.4, respectively. Moreover, the inequalities and identities in (C.27) stem from Theorem 5.1 if conditions in Lemma 5.1 and Lemma 5.2 are satisfied. Therefore, $(\hat{y}_G, \hat{u}_G)$ are jointly Gaussian counterparts of $(\hat{y}, \hat{u})$ as in Lemma 5.1 and $S_{\check{u}}$ represents the steady-state power spectral density of $\hat{u}_G$ as in Lemma 5.2. The pair $(\hat{y}_G, \hat{u}_G)$ with conditions stated in Lemma 5.1 can be generated by a scheme which certifies $\sigma_{\hat{z}_G}^2 \in (D_{\inf}(h), \infty)$ and is comprised of linear filters with a unit-gain noisy channel and delay h as follows:

$$\hat{u}_G(k) = L_k(\hat{y}_G^{k-h}, \hat{u}_G^{k-1}) + \hat{\psi}_G(k-h), \qquad k \in \mathbb{N}_0, \quad \text{(C.28)}$$

in which $\hat{\psi}_G(k)$ denotes a Gaussian noise with zero mean and independent of $(\hat{y}_G^k, \hat{u}_G^{k-1})$. Since L_k is a linear and causal mapping, we can redescribe $\hat{u}_G^k$ as

$$\hat{u}_G^k = Q_k \hat{\psi}_G^{k-h} + P_k \hat{y}_G^{k-h}, \qquad k \in \mathbb{N}_0. \quad \text{(C.29)}$$

It follows from causality in (C.29) that $\forall k \in \mathbb{N}$, B_k and G_k are lower triangular matrices with B_{k-1} and G_{k-1} on the top left corners. This together with the fact that $(\hat{y}_G, \hat{u}_G)$ are jointly SAWSS allow us to conclude that based on transitivity of asymptotic equivalence for products and sum of the matrices in [34], the sequences $\{Q_k\}$ and $\{P_k\}$ are asymptotically equivalent to sequences of lower triangular Toeplitz matrices. Furthermore, using L_k as in (C.28) will bring internal stability and well-posed-ness to the corresponding NCS. Now let us set $J = 1$ and B as a concatenation of linear filters with the same behaviour as steady-state behaviour of L_k in (C.28) for the auxiliary system of Fig. C.5. Moreover, suppose that η has a variance equal to $\sigma_{\hat{\psi}_G}^2$. So based on the asymptotic equivalence between the matrix representations of L and $\{L_k\}$, choosing J, B and η as above will render the system of Fig. C.5 well-posed and internally stable. More specifically, the latter set of filters and the noise will give WSS processes to which $\hat{u}_G$ and $\hat{z}_G$ converge. Therefore, for the control input u' and error signal z' in the feedback loop of Fig. C.5, $S_{u'} = S_{\check{u}}$ and $\sigma_{\hat{z}_G}^2 = \sigma_{z'}^2$ hold. Then based on Lemma 5.2, the directed information rate in

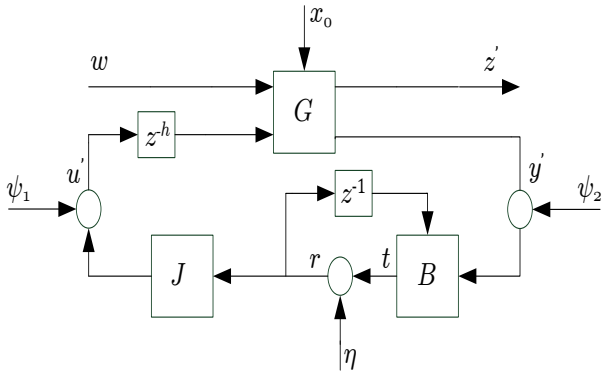

Fig. C.11: The LTI system whose internal stability guarantees the internal stability of the auxiliary system in Fig. C.5

the NCS of Fig. C.5 can be expressed as

$$I_{\infty}^{(h)}(y' \to u') = \frac{1}{4\pi}\int_{-\pi}^{\pi} \log\big(\frac{S_{u'}(e^{j\omega})}{\sigma_{\eta}^2}\big)d\omega = \frac{1}{4\pi}\int_{-\pi}^{\pi} \log\big(\frac{S_{\breve{u}}(e^{j\omega})}{\sigma_{\hat{\psi}_G}^2}\big)d\omega, \quad \text{(C.30)}$$

First, we can deduce that any pair $(\hat{E}, \hat{D})$ with properties stated above has a counterpart comprised of LTI filter B, $J = 1$ and the white Gaussian noise η in architecture of Fig. C.5 in such a way that $I_{\infty}(y' \to u') \leq I_{\infty}(\hat{y} \to \hat{u})$ and $\sigma_{\hat{z}}^2 = \sigma_{z'}^2$. Secondly, the main problem is finding the infimum of $\mathcal{R}$ over all mappings $(\hat{E}, \hat{D})$. With all of this in mind, it can be implied from (C.30) and (C.27) that the lower bound for $\mathcal{R}(D)$ would be equal to the rightmost term of (C.18) which completes the proof.

B.3 Proof of Lemma 5.3

The necessary and sufficient condition for the feedback loop of Fig. C.5 to be internally stable and well-posed is that every entry of the transfer function matrix from input $[\eta, w, \psi_1, \psi_2]^T$ to outputs $[z', y', r, u']^T$ in the system of Fig. C.11 belongs to $\mathcal{RH}_{\infty}$ [35]. Such a transfer function matrix, which we denote by T, is described as follows:

$$T = \begin{bmatrix} G_{12}Jz^{-h}M & G_{11} + G_{12}Jz^{-h}B_yMG_{21} & G_{12}z^{-h}(1 - B_rz^{-1})M & G_{12}Jz^{-h}B_yM \\ G_{22}Jz^{-h}M & G_{21}(1 - B_rz^{-1})M & G_{22}z^{-h}(1 - B_rz^{-1})M & G_{22}Jz^{-h}B_yM \\ M & G_{21}B_yM & G_{22}z^{-h}B_yM & B_yM \\ JM & G_{21}JB_yM & (1 - B_rz^{-1})M & JB_yM \end{bmatrix},$$

where

$$M \triangleq (1 - B_rz^{-1} - G_{22}Jz^{-h}B_y)^{-1}.$$

Now, let us shift the delay block in the system of Fig. C.5 to the plant model

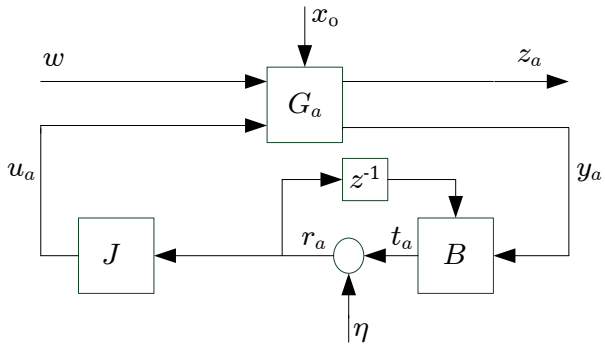

Fig. C.12: The equivalent system with the same $\varphi'(D)$ as the NCS of Fig. C.5

in a way that for the newly obtained system, the plant is described by

$$G_a = \begin{bmatrix} G_{11} & z^{-h}G_{12} \\ G_{21} & z^{-h}G_{22} \end{bmatrix}. \tag{C.31}$$

Such an auxiliary NCS is depicted by Fig. C.12. Except for the plant model (C.31), everything in the feedback loop of Fig. C.12 is assumed to be the same as in the system of Fig. C.5. The internal stability and well-posed-ness of the feedback loop of Fig. C.12 is guaranteed if and only if every entry of the transfer-function matrix, say T_a, from $[\eta, w, \psi_1, \psi_2]^T$ to $[z_a, y_a, r_a, u_a]^T$ in Fig. C.13 belongs to $\mathcal{RH}_\infty$. It is straightforward to see that $T_a = T$. So an equivalence holds between internal stability and well-posed-ness of the system of Fig. C.12 and the NCS of Fig. C.5. In other words, every triplet (B, J, σ_η^2) rendering the feedback loop of Fig. C.12 internally stable and well-posed, will bring internal stability and well-posed-ness to the NCS of Fig. C.5 as well. One

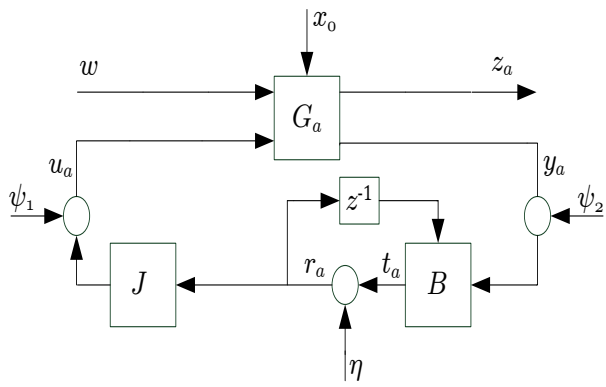

Fig. C.13: The auxiliary feedback loop characterizing the internal stability of the NCS of Fig. C.12

other implication of $T_a = T$ is that using an stabilizing (B, J, σ_η^2) commonly for NCSs of Fig. C.5 and Fig. C.12 will lead to an identical $\vartheta_r^{'}(B, J, \sigma_\eta^2)$. This is due to the properties of LTI systems exposed to Gaussian and stationary inputs. Furthermore, those properties lead to deriving the following H_2-norm expressions for SNR and variance of the output z' in the NCS of Fig. C.5:

$$\begin{aligned} \frac{\sigma_t^2}{\sigma_\eta^2} &= \|M-1\|_2^2 + \|B_y M G_{21}\|_2^2 \sigma_\eta^{-2}, \\ \sigma_{z'}^2 &= \left\| G_{11} + G_{12} N (1 - G_{22} N)^{-1} G_{21} \right\|_2^2 + \|G_{12} J M\|_2^2 \sigma_\eta^2, \end{aligned} \tag{C.32}$$

in which $N \triangleq J B_y z^{-h} (1 - B_r z^{-1})^{-1}$. Likewise, the SNR and variance of the output z in the NCS of Fig. C.12 is formalized in terms of H_2-norms as follows:

$$\begin{aligned} \frac{\sigma_{t_a}^2}{\sigma_\eta^2} &= \|M_a - 1\|_2^2 + \|B_y M_a G_{21}\|_2^2 \sigma_\eta^{-2}, \\ \sigma_{z_a}^2 &= \left\| G_{11} + G_{12} z^{-h} N_a (1 - G_{22} z^{-h} N_a)^{-1} G_{21} \right\|_2^2 + \|G_{12} J M_a\|_2^2 \sigma_\eta^2, \end{aligned} \tag{C.33}$$

where $M_a = M$ and $N_a \triangleq J B_y (1 - B_r z^{-1})^{-1}$. It follows from (C.32) and (C.33) that $(\sigma_t^2/\sigma_\eta^2) = (\sigma_{t_a}^2/\sigma_\eta^2)$ and $\sigma_{z'}^2 = \sigma_{z_a}^2$. Therefore, upon using the same stabilizing triplet (B, J, σ_η^2), the channel SNR and the variance of the output characterizing performance will be the same for the NCSs of Fig. C.5 and Fig. C.12.

According to [10, Lemma 4.1], for any pair $(B, J) = (B_1, J_1)$ that renders the feedback loop of Fig. C.12 internally stable and well-posed, there exists another pair with the same properties as for (B_2, J_2) in this lemma. Then our claims follow immediately from the above equivalences between the NCS of Fig. C.12 and the NCS of Fig. C.5.

B.4 Proof of Corollary 5.1

The feasibility of obtaining $\vartheta'_u(D)$, caused by D belonging to $(D_{\inf}(h), \infty)$, certifies the existence of a triplet, say $(B_\zeta, 1, \sigma_{\eta_\zeta}^2)$, that leads to $\sigma_{z'}^2 \leq D$ for the system of Fig. C.5. In the latter triplet, B_ζ is assumed to be a proper LTI filter and $\sigma_{\eta_\zeta}^2 \in \mathbb{R}^+$. This together with the definition of ϑ'_u and ϑ'_r in (C.18) and (C.19), respectively, yields the following:

$$\vartheta'_u(D) + \zeta \geq \vartheta_r^{'}(B_\zeta, 1, \sigma_{\eta_\zeta}^2), \forall \zeta \in \mathbb{R}^+.$$

Moreover, the triplet $(B_\zeta, 1, \sigma_{\eta_\zeta}^2)$ with aforementioned properties meets the conditions in Lemma 5.3. Therefore, another triplet, say $(\tilde{B}_\zeta, \tilde{J}_\zeta, \sigma_{\eta_\zeta}^2)$, exists in

such a way that implementing it brings internal stability and well-posed-ness, keeps $\sigma_{z'}^2$ intact, and yields

$$\vartheta'_u(D) + \zeta \geq \frac{1}{2}\log(1 + \frac{\sigma_t^2}{\sigma_\eta^2})|_{(B,J,\sigma_\eta^2)=(\tilde{B}_\zeta,\tilde{J}_\zeta,\sigma_{\eta_\zeta}^2)} - \rho \tag{C.34}$$

for the LTI feedback loop of Fig. C.5. Note that $\tilde{J}_\zeta$ is a biproper filter while $\tilde{B}_\zeta$ only needs to be proper. Now the fact that (C.34) holds for any $\zeta, \rho > 0$, the definition of $\varphi'(D)$ in (C.21), and the claim of Theorem 5.2 complete the proof.

B.5 Proof of Lemma 6.1

Let $\tilde{G}_h$ denote the transfer-function matrix from $[\tilde{w} \quad r]^T$ to $[\tilde{z} \quad t]^T$ in Fig. C.6. Since r_h is related to r by $r_h = rz^{-h}$, we can conclude that $\tilde{G}_h$ meets the conditions of being proper and real rational, and containing a strictly proper SISO open-loop transfer function from r to t. Now having the schemes described via (C.22) and (C.23) in mind, we can deduce our claim immediately from [10, Lemma 5.1].

B.6 Proof of Lemma 6.2

Let us assume that a linear source coding scheme is implemented in the feedback path of the main system in Fig. C.4. Due to the feasibility of finding $\varphi'(D)$, which necessitates satisfaction of Assumption 3.1, we can conclude the existence of proper LTI filters B and J that together with an AWGN, say η, render the NCS of Fig. C.4 SAWSS. It stems from some properties of internal stability that the system will still be stable if one keeps the latter filters B and J and only sets η as $\eta = 0$. This signifies that in the case of unity feedback ($t = r$), internal stability and well-posed-ness are guaranteed for the open-loop system between r and t. We come immediately to the conclusion that (C.24) holds based on [8, Corollary 5.3] and statistical characteristics of the dither mentioned in Lemma 6.1.

B.7 Proof of Theorem 6.1

Considering the feasibility of finding $\varphi'(D)$, results of Lemma 5.3, lemma 6.1, and Lemma 6.2, and invertibility of the decoder, we conclude the claim by following the same steps as in [10, Theorem 5.1].

B.8 Proof of Lemma 6.3

One of the common feedback loop components across the considered cases in Fig. C.8 is the LTI plant G which is described by state-space difference

equations as follows:

$$G : \begin{cases} x(k+1) = Ax(k) + B_1 w(k) + B_2 u(k) \\ z(k) = C_1 x(k) + D_{11} w(k) + D_{12} u(k) \\ y(k) = C_2 x(k) + D_{21} w(k), \end{cases} \tag{C.35}$$

where $x \in \mathbb{R}^{n_x}$ represents plant states and u, w, y and z are inputs and outputs defined as in (C.1). Moreover, A, B_1, B_2, C_1, C_2, D_{11}, D_{12}, and D_{21} are time-invariant matrices of appropriate dimensions. According to the recursion in (C.35), the states and outputs of the plant at each time instant $i \in \mathbb{N}_0$ can be expressed in terms of initial conditions, disturbance and control inputs as follows:

$$\begin{cases} x(i) = A^i x(0) + \mathcal{B}_1(i) w^{i-1} + \mathcal{B}_2(i) u^{i-1} \\ z(i) = C_1 A^i x(0) + \mathcal{D}_{11}(i) w^i + \mathcal{D}_{12}(i) u^i \\ y(i) = C_2 A^i x(0) + \mathcal{D}_{21}(i) w^i + \mathcal{D}_{22}(i) u^{i-1}, \end{cases} \tag{C.36}$$

where the involved matrices are defined as

$$\begin{aligned} \mathcal{B}_1(i) &= [A^{i-1}B_1 \; A^{i-2}B_1 \dots B_1] \\ \mathcal{B}_2(i) &= [A^{i-1}B_2 \; A^{i-2}B_2 \dots B_2] \\ \mathcal{D}_{11}(i) &= [C_1A^{i-1}B_1 \; C_1A^{i-2}B_1 \dots C_1B_1 \; D_{11}] \\ \mathcal{D}_{12}(i) &= [C_1A^{i-1}B_2 \; C_1A^{i-2}B_2 \dots C_1B_2 \; D_{12}] \\ \mathcal{D}_{21}(i) &= [C_2A^{i-1}B_1 \; C_2A^{i-2}B_1 \dots C_2B_1 \; D_{21}] \\ \mathcal{D}_{22}(i) &= [C_2A^{i-1}B_2 \; C_2A^{i-2}B_2 \dots C_2B_2]. \end{aligned}$$

For the case where the time delay is imposed by the error-free digital channel between the encoder-controller and the decoder-controller, the relationship between the control input and the sensor output is characterized based on (C.5)-(C.8). The dynamics described by (C.5)-(C.8) can be summarizd in the constant channel delay case as follows:

$$\begin{aligned} y_q(k) &= E_k(y^k, \eta_e^k) \\ u_q(k) &= y_q(k-h) \\ u(k) &= D_k(u_q^k, \eta_d^k), \end{aligned} \tag{C.37}$$

where E_k and D_k represent causal, but otherwise arbitrary, mappings at each $k \in \mathbb{N}_0$. It follows from (C.37) that u^k can be stated as an arbitrary function, say N_k, of $(\eta_d^k, y^{k-h}, \eta_e^{k-h})$, i.e., $u^k = N_k(\eta_d^k, y^{k-h}, \eta_e^{k-h})$. Then from (C.36) and by induction, we can conclude that at each time instant $k \in \mathbb{N}_0$, $x(k)$ is a function of $(x(0), w^{k-1}, \eta_d^{k-1}, \eta_e^{k-1-h})$, $z(k)$ is a function of $(x(0), w^k, \eta_d^k, \eta_e^{k-h})$, and $y(k)$ is a function of $(x(0), w^k, \eta_d^{k-1}, \eta_e^{k-1-h})$.

In the second case, it is the link between the decoder-controller and the plant that induces the time delay. For such a setting, E_k, D_k, $\eta_e(k)$ and $\eta_d(k)$

yield a scheme with following dynamics:

$$\begin{aligned} y_q(k) &= E_k(y^k, \eta_e^k) \\ u_q(k) &= y_q(k) \\ u(k) &= D_{k-h}(u_q^{k-h}, \eta_d^{k-h}). \end{aligned} \tag{C.38}$$

It follows from (C.38) that in this case, u^k can be expressed as

$$u^k = M_k(y^{k-h}, {\eta_d}^{k-h}, \eta_e^{k-h}),$$

$\forall k \in \mathbb{N}_0$, where M_k is an arbitrary mapping which is specified by $\{E_i\}_{i=0}^{k-h}$ and $\{D_i\}_{i=0}^{k-h}$. Substituting such an expression into (C.36) an by induction, we can rederive $x(k)$, $z(k)$, and $y(k)$ as functions of $(x(0), w^{k-1}, \eta_d^{k-h-1}, \eta_e^{k-1-h})$, $(x(0), w^k, \eta_d^{k-h}, \eta_e^{k-h})$, and $(x(0), w^k, \eta_d^{k-h-1}, \eta_e^{k-h-1})$, respectively.

As the third case, we focus on a structure in which the delay is introduced by the path between the sensor and the encoder-controller. In this situation, the coding scheme is described by causal mappings E_k and D_k, and side informations $\eta_e(k)$ and $\eta_d(k)$, as follows:

$$\begin{aligned} y_q(k) &= E_k(y^{k-h}, \eta_e^k) \\ u_q(k) &= y_q(k) \\ u(k) &= D_k(u_q^k, \eta_d^k). \end{aligned}$$

Taking the same steps as for the previous cases, we derive $u^k = S_k(y^{k-h}, {\eta_d}^k, \eta_e^k)$, $\forall k \in \mathbb{N}_0$, where S_k is a causal mapping and a function of $\{E_i\}_{i=0}^k$ and $\{D_i\}_{i=0}^k$. Then considering (C.36) and based on induction, we come to the conclusion that for the closed-loop system considered in this case, $x(k)$ is a function of $(x(0), w^{k-1}, \eta_d^{k-1}, \eta_e^{k-1})$, $z(k)$ is a function of $(x(0), w^k, \eta_d^k, \eta_e^k)$, and $y(k)$ is a function of $(x(0), w^k, \eta_d^{k-1}, \eta_e^{k-1})$ for all $k \in \mathbb{N}_0$.

According to the above observations, comparing system states x, sensor output y, and the output z at each time instant indicates that such signals are not necessarily equal across the three cases studied above if the systems share the design (mappings for coding and control and side information) and have the same initial conditions and exogenous inputs. So values of each signal change by relocating the delay component in the NCS of Fig. C.4. However, it is straightforward to see from the structure of the variables describing processes x, z, and y that the equivalence over cases can be obtained under the condition that everything is the same across the cases except for side information which can be considered as decision variable.

References

[1] X. M. Zhang, Q. L. Han, and X. Yu, "Survey on recent advances in networked control systems," *IEEE Transactions on Industrial Informatics*, vol. 12, no. 5, pp. 1740–1752, Oct. 2016.

[2] G. N. Nair, F. Fagnani, S. Zampieri, and R. J. Evans, "Feedback control under data rate constraints: An overview," *Proceedings of the IEEE*, vol. 95, no. 1, pp. 108–137, Jan. 2007.

[3] L. Zhang, H. Gao, and O. Kaynak, "Network-induced constraints in networked control systems—a survey," *IEEE Transactions on Industrial Informatics*, vol. 9, no. 1, pp. 403–416, Feb. 2013.

[4] J. Baillieul and P. J. Antsaklis, "Control and communication challenges in networked real-time systems," *Proceedings of the IEEE*, vol. 95, no. 1, pp. 9–28, Jan. 2007.

[5] A. S. Matveev and A. V. Savkin, *Estimation and control over communication networks*. Springer Science & Business Media, 2009.

[6] N. C. Martins and M. A. Dahleh, "Feedback Control in the Presence of Noisy Channels: "Bode-Like" Fundamental Limitations of Performance," *IEEE Transactions on Automatic Control*, vol. 53, no. 7, pp. 1604–1615, Aug. 2008.

[7] N. C. Martins, M. A. Dahleh, and J. C. Doyle, "Fundamental limitations of disturbance attenuation in the presence of side information," *IEEE Transactions on Automatic Control*, vol. 52, no. 1, pp. 56–66, Jan. 2007.

[8] E. I. Silva, M. S. Derpich, and J. Østergaard, "A framework for control system design subject to average data-rate constraints," *IEEE Transactions on Automatic Control*, vol. 56, no. 8, pp. 1886–1899, Aug. 2011.

[9] ——, "An achievable data-rate region subject to a stationary performance constraint for LTI plants," *IEEE Transactions on Automatic Control*, vol. 56, no. 8, pp. 1968–1973, Aug. 2011.

[10] E. I. Silva, M. S. Derpich, J. Østergaard, and M. A. Encina, "A characterization of the minimal average data rate that guarantees a given closed-loop performance level," *IEEE Transactions on Automatic Control*, vol. 61, no. 8, pp. 2171–2186, Aug. 2016.

[11] T. Tanaka, P. M. Esfahani, and S. K. Mitter, "LQG control with minimum directed information: semidefinite programming approach," *IEEE Transactions on Automatic Control*, vol. 63, no. 1, pp. 37–52, Jan. 2018.

[12] P. Stavrou, J. Ostergaard, and C. D. Charalambous, "Zero-delay rate distortion via filtering for vector-valued Gaussian sources," *IEEE Journal of Selected Topics in Signal Processing*, pp. 1–1, 2018.

[13] V. Kostina and B. Hassibi, "Rate-cost tradeoffs in control," *arXiv preprint arXiv:1612.02126v2*, 2016.

[14] Z. Du, D. Yue, and S. Hu, "H-infinity stabilization for singular networked cascade control systems with state delay and disturbance," *IEEE Transactions on Industrial Informatics*, vol. 10, no. 2, pp. 882–894, May 2014.

[15] M. A. Khanesar, O. Kaynak, S. Yin, and H. Gao, "Adaptive indirect fuzzy sliding mode controller for networked control systems subject to time-varying network-induced time delay," *IEEE Transactions on Fuzzy Systems*, vol. 23, no. 1, pp. 205–214, Feb. 2015.

[16] R. Lu, H. Cheng, and J. Bai, "Fuzzy-model-based quantized guaranteed cost control of nonlinear networked systems," *IEEE Transactions on Fuzzy Systems*, vol. 23, no. 3, pp. 567–575, Jun. 2015.

[17] J. Xiong, J. Lam, Z. Shu, and X. Mao, "Stability analysis of continuous-time switched systems with a random switching signal," *IEEE Transactions on Automatic Control*, vol. 59, no. 1, pp. 180–186, Jan. 2014.

[18] L. Qiu, Y. Shi, F. Yao, G. Xu, and B. Xu, "Network-based robust H_2/H_∞ control for linear systems with two-channel random packet dropouts and time delays," *IEEE Transactions on Cybernetics*, vol. 45, no. 8, pp. 1450–1462, Aug. 2015.

[19] Z. Pang, G. Liu, D. Zhou, and M. Chen, "Output tracking control for networked systems: A model-based prediction approach," *IEEE Transactions on Industrial Electronics*, vol. 61, no. 9, pp. 4867–4877, Sept. 2014.

[20] H. Li and Y. Shi, "Network-based predictive control for constrained nonlinear systems with two-channel packet dropouts," *IEEE Transactions on Industrial Electronics*, vol. 61, no. 3, pp. 1574–1582, Mar. 2014.

[21] W. Yao, L. Jiang, J. Wen, Q. Wu, and S. Cheng, "Wide-area damping controller for power system interarea oscillations: A networked predictive control approach," *IEEE Transactions on Control Systems Technology*, vol. 23, no. 1, pp. 27–36, Jan. 2015.

[22] Y. Nakahira, "LQ vs. ℓ_∞ in controller design for systems with delay and quantization," in *Proceedings of the 55th IEEE Conference on Decision and Control (CDC)*, Dec. 2016, pp. 2382–2389.

[23] Q. Han, Y. Liu, and F. Yang, "Optimal communication network-based h_∞ quantized control with packet dropouts for a class of discrete-time neural networks with distributed time delay," *IEEE Transactions on Neural Networks and Learning Systems*, vol. 27, no. 2, pp. 426–434, Feb 2016.

[24] K. Liu, E. Fridman, K. H. Johansson, and Y. Xia, "Quantized control under round-robin communication protocol," *IEEE Transactions on Industrial Electronics*, vol. 63, no. 7, pp. 4461–4471, Jul. 2016.

[25] W. P. M. H. Heemels, A. R. Teel, N. van de Wouw, and D. Nešić, "Networked control systems with communication constraints: Tradeoffs between transmission intervals, delays and performance," *IEEE Transactions on Automatic Control*, vol. 55, no. 8, pp. 1781–1796, Aug. 2010.

[26] J. Zhang and C.-C. Wang, "On the rate-cost of Gaussian linear control systems with random communication delays," in *Proceedings of the 2018 IEEE International Symposium on Information Theory (ISIT)*, Jun. 2018, pp. 2441–2445.

[27] M. Barforooshan, J. Østergaard, and M. S. Derpich, "Interplay between transmission delay, average data rate, and performance in output feedback control over digital communication channels," in *Proceedings of the 2017 American Control Conference (ACC)*, May 2017, pp. 1691–1696.

[28] M. Barforooshan, J. Østergaard, and P. A. Stavrou, "Achievable performance of zero-delay variable-rate coding in rate-constrained networked control systems with channel delay," in *Proceedings of the IEEE 56th Annual Conference on Decision and Control (CDC)*, Dec. 2017, pp. 5991–5996.

[29] T. M. Cover and J. A. Thomas, *Elements of information theory*. John Wiley & Sons, 2012.

[30] M. S. Derpich, E. I. Silva, and J. Østergaard, "Fundamental inequalities and identities involving mutual and directed informations in closed-loop systems," *arXiv preprint arXiv:1301.6427*, 2013.

[31] K. Hashikura, "H^2/H^∞ controller design for input-delay and preview systems based on state decomposition approach," Ph.D. dissertation, Tokyo Metropolitan University, 2014.

[32] E. Johannesson, "Control and communication with signal-to-noise ratio constraints," Ph.D. dissertation, Lund University, 2011.

[33] K. J. Åström, *Introduction to stochastic control theory*. Courier Corporation, 2012.

[34] R. M. Gray, "Toeplitz and circulant matrices: A review," *Foundations and Trends in Communications and Information Theory*, vol. 2, no. 3, pp. 155–239, 2006.

[35] B. A. Francis, *A course in H_∞ control theory*. Berlin; New York: Springer-Verlag, 1987.

Paper D

Sparse Packetized Predictive Control Over Communication Networks with Packet Dropouts and Time Delays

Mohsen Barforooshan, Masaaki Nagahara, and Jan Østergaard

Technical report.

Abstract

This paper studies sparse packetized predictive control (PPC) for a feedback loop closed over a digital communication channel with time delay and bounded packet dropouts. In the considered networked control system (NCS), the channel is located between the controller and the actuator of a linear time-invariant (LTI) plant. We analyze the system under two PPC strategies. In one case, the controller computes each control packet by solving an sparsity-promoting unconstrained ℓ^1-ℓ^2 optimization problem. In the other case, the sparsity-promoting optimization based on which the controller performs is an ℓ^2-constrained ℓ^0 problem. We propose effective approaches for solving these optimization problems. Moreover, we establish practical and asymptotic stability conditions in terms of design parameters for unconstrained ℓ^1-ℓ^2 and ℓ^2-constrained ℓ^0 PPC, respectively, in the presence of constant channel delay. We show in both cases that to maintain stability while increasing the channel delay, the proposed sparse PPC strategies necessitate increasing the upper bound on overall size of the sequence of control packets generated at each time instant by the controller. We show, through simulation, that when the channel delay is higher, the controllers designed according to the proposed method can indeed bring the desired stability properties to the system but with lower performance.

1 Introduction

Networked control systems (NCSs) are feedback loops whose components (plants, sensors, controllers, actuators, etc.) are linked via communication channels. The imperfections associated with communication networks introduce new constraints to control problems [1, 2]. Non-ideal communications in data networks can be caused by quantization, data packet dropouts, and network-induced delays, to name a few, which bring challenges into the analysis and synthesis of NCSs [3, 4]. For instance, stability cannot be achieved if the rate of data transmission is lower than a minimal value [5], or if the probability of the packet loss or the value of transmission delay is greater than a specific upper bound [6, 7]. Similar trade-offs exist between communication imperfections and control performance in NCSs [8–10]. In general, designing control strategies that guarantee attaining certain performance levels despite the presence of communication constraints is one of the main goals in the theory and application of NCSs.

Minimizing the control effort is another goal in practical control design which is of high necessity. This is motivated by various environmental, economical and technical merits which control effort minimization brings about. For instance, it causes less energy consumption [11, 12], reduces the emission of polluters such as CO and CO_2 [13], attenuates noise and vibration [14], and

prevents system equipments from being saturated [15]. One way to minimize the control effort is maximizing the number of time intervals over which the control input is equal to zero [16]. This approach is pursued in maximum hands-off control [17, 18]. In fact, maximum hands-off control addresses the above environmental and economical concerns by prolonging the overall period of time for which the actuator is off [19, 20].

Sparse packetized predictive control (PPC) lies in the intersection of maximum hands-off control and networked control. To gain a grasp on this control strategy, we first need to explain PPC. In a PPC setup, the controller generates a packet containing tentative future control inputs and sends it over the channel to the actuator. The purpose of producing a control packet, instead of one single control command, is rendering the system robust against channel uncertainties such as data loss and transmission delay. The actuator stores each successfully received packet whose elements will be used, according to a selection logic, as control inputs in the upcoming time instants when no packet reaches the plant. In PPC, the control packets are computed based on a finite-horizon model predictive control (MPC) strategy [21–26]. Particularly, in the sparse PPC, the cost function associated with this MPC is a sparsity-promoting cost function [27, 28] which is commonly used in maximum hands-off control. So maximum hands-off control is of two favours when applied to NCSs. One is saving the fuel and energy by putting less control effort. The other is reducing the size of data transmitted over the channel in that vector symbols with many zero elements are easier to be compressed. In [29], the unconstrained ℓ^1-ℓ^2 and ℓ^2-constrained ℓ^0 problems are considered as sparsity-promoting optimization problems. The packetized predictive controllers proposed in [29] solve the unconstrained ℓ^1-ℓ^2 and ℓ^2-constrained ℓ^0 optimizations online by employing fast iterative shrinkage- thresholding algorithm (FISTA) and orthogonal matching pursuit (OMP) approaches, respectively. Moreover, the authors of [29] show the practical stability for unconstrained ℓ^1-ℓ^2 PPC and asymptotic stability for ℓ^2-constrained ℓ^0 PPC over a delay-free channel subject to bounded dropouts.

In this paper, we study sparse PPC for an NCS comprised of a fully observable discrete-time noiseless linear time-invariant (LTI) plant whose states are transmitted to the controller perfectly (no communication limitation in the measurement path). However, the control packets sent from the controller to the plant are subject to bounded dropouts and constant time delays. We analyze the system under two sparse PPC policies. One is unconstrained ℓ^1-ℓ^2 sparse PPC for which we derive conditions of practical stability. In the second case, every control packet is a solution to a finite-horizon sparsity-promoting ℓ^2-constrained ℓ^0 optimization problem at each time instant. In this case, we show that asymptotic stability is guaranteed under certain tuning conditions. The aforementioned notions of stability together with the delay imposed by the channel, say h steps, make us consider PPC strategies that instead of producing one packet at a time, generates a number of control packets each

based on a prediction of system states of h time steps later. Therefore, at each time instant, the controller uses the available current plant states and memory to make a number of predictions for the plant states at h time instant later. Then for each prediction, the controller solves the corresponding unconstrained ℓ^1-ℓ^2 or ℓ^2-constrained ℓ^0 optimization problem and gives a sequence of control packets. We show that the length of this sequence, which is equal to the number of predictions, is upper bounded by a finite value which is an exponential function of channel delay. Upon the arrival of a sequence on the other sider of the channel, the actuator selects the packet associated with the precise prediction of the current plant states. We utilize the methodology followed in [29] for stability analysis and solving the corresponding sparsity-promoting optimization problems in both cases of unconstrained ℓ^1-ℓ^2 sparse PPC and ℓ^2-constrained ℓ^0 sparse PPC. This is due to the advantages such as simplicity of the stability analysis and effectiveness (in sense of speed and convergence) of solving algorithm proposed in [29]. However, unlike [29], we consider a channel which induces a known constant delay on transmitted packets and accordingly, a different regime of control packet production. Therefore, as the first contribution, by deriving stability conditions, we propose how to design sparse ℓ^1-ℓ^2 and ℓ^2-constrained ℓ^0 PPC schemes that stabilize the system despite the existing channel delay. As the second contribution, we reveal insights to the trade-off between channel delay, size of the control packets and system stability and performance by showing that when the channel delay is larger, the upper bound on the number of packets to be sent over the channel will be higher and in the particular case of unconstrained ℓ^1-ℓ^2 sparse PPC for unstable plants, the upper bound on the ℓ^2-norm of system states at each time instant grows as channel delay increases. We verify, through a numerical example, that the proposed unconstrained ℓ^1-ℓ^2 and ℓ^2-constrained ℓ^0 sparse PPC schemes bring practical and asymptotic stability to the system, respectively, via sparse control commands. Moreover, simulation results illustrate that in the case of unstable plants, increasing the channel delay degrades system performance while it does not affect system stability.

The paper is organized as follows. Section 2 introduces the notation. Section 3 presents the problem formulation. Stability analysis is provided by Section 4. In Section 5, a numerical example is given. Finally, Section 6 concludes the paper.

2 Notation

We denote the set of natural numbers by $\mathbb{N}$ and define the set $\mathbb{N}_0$ as $\mathbb{N}_0 \triangleq \mathbb{N} \cup \{0\}$. An identity matrix with dimensions n is represented by $I_{n\times n}$ where $n \in \mathbb{N}$. Moreover, M^T symbolizes the transpose of the matrix (vector) M. Considering the vector $z = [z_1, \ldots, z_n]^T \in \mathbb{R}^n$, we define $\|z\|_1 \triangleq |z_1| + \cdots + |z_n|$,

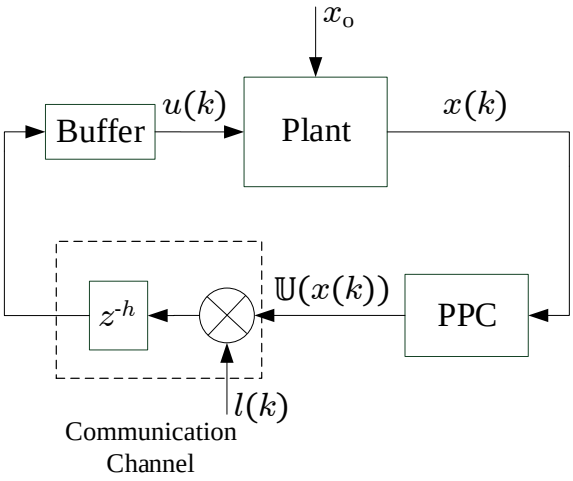

Fig. D.1: Considered PPC system

$\|z\|_2 \triangleq \sqrt{z^T z}$ and $\|z\|_\infty \triangleq \max\{|z_1|, \ldots, |z_n|\}$. Moreover, the positive definite matrix $W > 0$ defines $\|z\|_W$ as $\|z\|_W \triangleq \sqrt{z^T W z}$. By $supp(z) = \{i : z_i \neq 0\}$, we denote the support set of the vector z based on which the ℓ^0-norm of z is defined as $\|z\|_0 \triangleq |supp(z)|$ where $|supp(z)|$ is the cardinality of the set $supp(z)$. Therefore, ℓ^0-norm of a vector is the number of its non-zero elements. Minimum and maximum eigenvalue of the Hermitian matrix W is denoted by $\lambda_{\min}(W)$ and $\lambda_{\max}(W)$, respectively. Moreover, we define $\sigma_{\max}(W)$ as $\sigma_{\max}(W) \triangleq \lambda_{\max}(W^T W)$.

3 Problem Formulation

We consider a discrete-time LTI plant with the following state-space representation:

$$x(k+1) = Ax(k) + Bu(k), \qquad k \in \mathbb{N}_0, \tag{D.1}$$

where $x(k) \in \mathbb{R}^n$ and $u(k) \in \mathbb{R}$ represent the plant states and the control input, respectively. Moreover, A and B are time-invariant matrices of appropriate dimensions and assumed to be reachable.

The plant described through (D.1) is controlled in the feedback loop of Fig. D.1 where a digital communication channel connects the controller to the actuator. We assume that the channel imposes a known constant delay on transmitted data. Such a time delay is an integer multiplier of the system sampling period and denoted by $h \in \mathbb{N}_0$. Moreover, data packet dropouts occur across the channel. The binary random process $l(k)$ represents the packet loss.

If $l(k) = 0$, then the sequence of packets generated at time instant k will be dropped and if $l(k) = 1$, the packets will arrive at the actuator h steps later. Let assume that the packetized predictive controller in the NCS of Fig. D.1 is not aware of l^k at each time instant $k \in \mathbb{N}_0$. This controller generates a sequence of control packets, which is specified by

$$\mathbb{U}(x(k)) = [U(\hat{x}_1(k+h;k)) \dots U(\hat{x}_{s(k)}(k+h;k))]^T,$$

where $U(\hat{x}_i(k+h;k)) = [u_0(\hat{x}_i(k+h;k)) \dots u_{N-1}(\hat{x}_i(k+h;k))]^T$ denotes a packet containing tentative future control inputs generated based on the prediction $\hat{x}_i(k+h;k)$ of $x(k+h)$ for every $i \in \{1, \dots, s(k)\}$ and $k \in \mathbb{N}_0$. The controller makes use of $\{\mathbb{U}(x(i))\}_{i=0}^{k}$ and x^k to carry out such predictions and come up with possible values for $x(k+h)$. We show later on that for every $k \in \mathbb{N}_0$, $s(k)$ is a random integer less than 2^h. Then the controller forwards $\mathbb{U}(x(k))$ as a sequence of data packets over the channel. On the plant side, the actuator is connected to a buffer that stores each newly received packet sequence over its previous contents. Suppose that the time is k and $\mathbb{U}(x(k-h))$ arrives at the actuator. Then the buffer writes $\mathbb{U}(x(k-h))$ over whatever data is already available in it. For any $j \in \mathbb{N}_0$, let us denote by $\hat{x}_{p(j)}(j;j-h)$ the precise prediction of $x(j)$ made at time $j-h$, i.e., $\hat{x}_{p(j)}(j;j-h) = x(j)$, $p(j) \in \{1, \dots, s(j-h)\}$. The actuator selects the packet $U(\hat{x}_{p(k)}(k;k-h))$ and applies $u_0(\hat{x}_{p(k)}(k;k-h))$ to the plant as the control input. At the next time instant, if the packet sequence $\mathbb{U}(x(k-h+1))$ is received, then the buffer writes it over $\mathbb{U}(x(k-h))$ and applies $u_0(\hat{x}_{p(k+1)}(k+1;k+1-h))$ to the plant. Otherwise, the buffer selects $u_1(\hat{x}_{p(k)}(k;k-h))$ as the control input. Then until the successful arrival of the next packet sequence $\mathbb{U}(x(k+n-h))$, $n \geq 2$, the remaining elements of $\mathbb{U}(x(k-h))$ are applied in a successive manner to the plant as control inputs.

Assumption 3.1
In the NCS of Fig. D.1, the control input is zero at the first h time instants, i.e., $u(k) = 0$, $\forall k \in \{0, \dots, h-1\}$. Moreover the packet sequence $\mathbb{U}(x(0))$ reaches the buffer at time $k = h$. The number of consecutive packet dropouts is uniformly bounded from above by $N-1$. In other words, the buffer never becomes empty and at each time instant, there is a new control input to be applied to the plant.

It can be implied from boundedness of the number of consecutive packet dropouts mentioned in the above assumption that the sequence $\{l(i)\}_{i=1}^{\infty}$ cannot be i.i.d. In the following lemma, $l(k)$ having a binary distribution assists us to show that when it comes to predicting $x(k+h)$ at any $k \in \mathbb{N}_0$, the number of possible values is bounded form above by a constant value which is only a function of channel time delay.

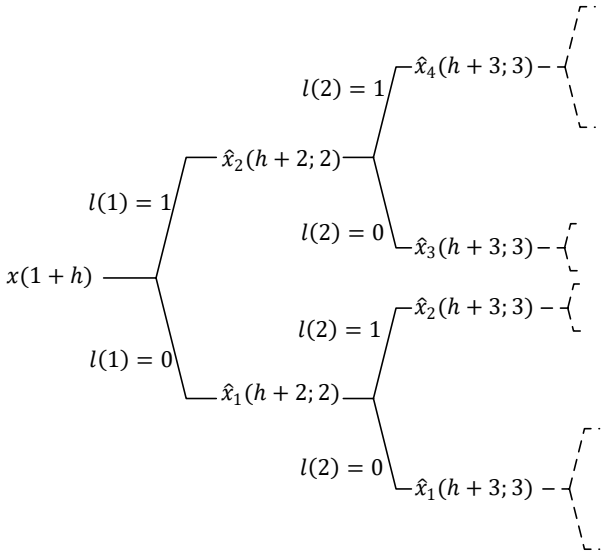

Fig. D.2: The tree structure showing the possible values for $x(k+h)$ at time k

Lemma 3.1
Consider the NCS of Fig. D.1 where Assumption 3.1 holds. Suppose that $N \geq 2$ and the controller has access to x^k and $\{\mathbb{U}(x(i))\}_{i=0}^{k}$ at each time instant $k \in \mathbb{N}_0$. Moreover, assume that the controller is to calculate all the possible values $\{\hat{x}_i(k+h;k)\}_{i=0}^{s(k)}$ for $x(k+h)$ at time k as pointed out above. Then $s(k) \leq 2^h$ at each time instant $k \in \mathbb{N}_0$.

Proof. According to Assumption 3.1, $u(k) = 0$, $\forall k \in \{0, \ldots, h-1\}$ and the packet sequence $\mathbb{U}(x(0))$ reaches the buffer at time $k = h$. So the controller knows $x(h-1)$ and $u(h-1)$ at $k = 0$ and $x(h)$ and $u(h)$ at time instant $k = 1$. Therefore, according to the dynamics of the plant in (D.1), there is no uncertainty in predicting the value of $x(h)$ and $x(h+1)$ at time $k = 0$ and $k = 1$, respectively. At time $k = 2$, the possible value of $x(2+h)$ depends on the value of $l(1)$ to which the controller does not have access. So according to the fact that $l(k)$ is a binary random variable at each $k \in \mathbb{N}_0$ and $N \geq 2$, $s(2) = 2$, i.e., $x(h+2) \in \{\hat{x}_1(2+h;2), \hat{x}_2(2+h;2)\}$. At time step $k = 3$, the controller can calculate the exact $x(h+3)$ bay knowing the values of $l(1)$ and $l(2)$. Again, since such knowledge is not provided, the controller can only calculates the potential values for $x(h+3)$ according ot all possible combinations of $l(1)$ and $l(2)$. However, it could be that the case $l(1) = l(2) = 0$ is impossible to happen due to the boundedness of consecutive packet dropouts. So $s(3)$ is either equal to 3 or 4. However, $s(3)$ certainly follows $s(3) \leq 2^2$. Assuming that the channel delay is large enough and by induction, we can conclude that the calculation of

the of possible values for $x(k+h)$ follows a tree structure as depicted in Fig. D.2 where $s(k) \leq 2^k - 1$ for every $k < h + 2$. From time $k = h + 2$, the controller has access to the exact value of the states for which it calculated the possible values h time steps later. For example, at time $h + 2$, the controller knows $x(h + 2)$. So based on the aforementioned tree structure, the upper bound on the number of potential values of $x(2h+2)$ becomes half of what was expected. There are at most $2^{h+1}/2$ possible values for $x(2h+2)$, i.e., $s(h+2) \leq 2^h$. The same occurs for all the future time instants and this completes the proof. □

The MPC strategy employed to generate the control packets in the NCS of Fig. D.1 is finite-horizon. So, the controller computes control packets by minimizing $s(k)$ finite-horizon cost functions at each time instant $k \in \mathbb{N}_0$. For every $x_j = \hat{x}_j(k + h; k)$, $j \in \{1, \ldots, s(k)\}$, the latter cost function is described by

$$J(x_j, u_j) = T(x_{Nj}^{'}) + \sum_{i=0}^{N-1} S(x_{ij}^{'}, u_{ij}), \tag{D.2}$$

in which N denotes the time horizon and $x_{ij}^{'}$ is calculated based on the recursion $x_{(i+1)j}^{'} = Ax_{ij}^{'} + Bu_{ij}$ for any $i \in \{0 \ldots N-1\}$ where $x_{0j}^{'} = \hat{x}_j(k + h; k)$. So, $x_{0j}^{'}$ represents the j-th candidate value for $x(k + h)$ and $x_{1j}^{'}, ..., x_{Nj}^{'}$ are predictions of future states $x(k+h+1), ..., x(k+h+N)$, respectively, based on $\hat{x}_j(k + h; k)$. Moreover, $\{u_{ij}\}_{i=0}^{N-1}$ denote tentative future control inputs that define u_j as $u_j \triangleq [u_{0j} \ldots u_{(N-1)j}]^T = [u_0(\hat{x}_j(k+h; k)) \ldots u_{N-1}(\hat{x}_j(k+h; k))]^T$, $j = 1, \ldots, s(k)$. Note that the controller has access to plant states $x(k)$ at each time step $k \in \mathbb{N}_0$. The functions S and T in (D.2) symbolize stage cost and terminal cost, respectively.

As already mentioned before, the aim is achieving robustness against network uncertainties while addressing fuel and data size concerns by designing a packetized predictive controller that generates only a few non-zero control inputs. Therefore, we set $J(x_j, u_j)$ together with some constraints in such a way that the optimization problem related to the above packetized predictive setup gives sparse control packets. To do so, we consider two different pairs of final and stage costs (S, T) that together with their corresponding constraints, define two types of sparsity-promoting optimization problems. One is called unconstrained ℓ^1-ℓ^2 optimization and the other is ℓ^2-constrained ℓ^0 optimization. We formalize these problems for the NCS of Fig. D.1 in the following subsection.

3.1 Unconstrained ℓ^1-ℓ^2 Optimization

In this case, the cost function has the general form of (D.2) where $S(x_{ij}^{'}, u_i j) = \|x_{ij}^{'}\|_Q^2 + \nu|u_i j|$ and $T(x_N^{'}) = \|x_{Nj}^{'}\|_P^2$. We assume that $\nu > 0$, and Q and P

are positive definite matrices. Since future state prediction is carried out based on $x^{'}_{(i+1)j} = Ax^{'}_{ij} + Bu_{ij}$ for $i = 0, ..., N-1$ and $j = 1, \ldots, s(k)$, then the cost function J can be rewritten as follows:

$$J(x_j, u_j) = \|Mu_j - Kx_j\|_2^2 + \|x_j\|_Q^2 + \nu\|u_j\|_1, \tag{D.3}$$

where $x_j = x^{'}_{0j}$ and $u_j = [u_{0j} \ldots u_{(N-1)j}]^T$. Additionally, we have

$$\Gamma = \begin{bmatrix} B & 0 & \ldots & 0 \\ AB & B & \ldots & 0 \\ \vdots & \vdots & \ddots & \vdots \\ A^{N-1}B & A^{N-2}B & \ldots & B \end{bmatrix}, \qquad \Lambda = \begin{bmatrix} A \\ A^2 \\ \vdots \\ A^N \end{bmatrix}$$

upon which M in (D.3) is defined as $M = \hat{Q}^{\frac{1}{2}}\Gamma$ and $K = -\hat{Q}^{\frac{1}{2}}\Lambda$, where $\hat{Q} = diag\{Q, \ldots, Q, P\}$. So the control packet associated with $\hat{x}_j(k+h;k)$ at each time instant $k \in \mathbb{N}_0$ is given by

$$u_j(x_j) = \arg\min_{u_j \in \mathbb{R}^N} \|Mu_j - Kx_j\|_2^2 + \|x - j\|_Q^2 + \nu\|u_j\|_1, \tag{D.4}$$

where $j \in \{1, \ldots, s(k)\}$. According to [30], the solution to the unconstrained ℓ^1-ℓ^2 optimization problem is a sparse vector that can be obtained through several methods. For such an optimization problem, simulation often gives a solution that is much sparser than the solution of ℓ^0 problem, which we address in the next subsection. However, if the plant is unstable, attaining asymptotic stability (converging $x(k)$ to zero as time goes to infinity) is never guaranteed for the closed-loop system in the case of sparse PPC with unconstrained ℓ^1-ℓ^2 optimization [29]. Instead, practical stability ($x(k)$ converging to a neighborhood of zero as time goes to infinity) can be attained in this case by choosing $Q > 0$, $P > 0$ and $\nu > 0$ appropriately; a result which we show in Section 4.1.

It should be emphasized that reexpressing $J(x_j, u_j)$ as in (D.3) is only based on the update rule of the state prediction $x^{'}_{(i+1)j} = Ax^{'}_{ij} + Bu_{ij}$ and has nothing to do with the channel delay or the way the actuator selects the control input.

3.2 ℓ^2-Constrained ℓ^0 Optimization

We formalize the cost function $J(x_j, u_j)$ for this case by setting T in (D.2) as $T(x^{'}_{Nj}) = 0$ and choosing S in such a way that $S(x^{'}_{ij}, u_{ij}) = 0$ if $u_{ij} = 0$ and $S(x^{'}_{ij}, u_{ij}) = 1$ if u_{ij} is non-zero. Furthermore, in this case, the controller solves a constrained optimization problem whose constraint is specified by the following set:

$$\upsilon(x_j) = \{u_j \in \mathbb{R}^N : \|x^{'}_{Nj}\|_P^2 + \sum_{i=0}^{N-1} \|x^{'}_{ij}\|_Q^2 \leq \|x_j\|_\Pi^2\}, \tag{D.5}$$

where weighting matrices P, Q, and Π are positive definite and selected in such away that for all $x_j \in \mathbb{R}^n$, $\upsilon(x_j)$ is non-empty . Moreover, $x_j = x_{0j}^{'}$ and $u_j = [u_{0j} \dots u_{(N-1)j}]^T$ as defined beforehand. The control packet pertaining to $\hat{x}_j(k+h;k)$ at each time instant $k \in \mathbb{N}_0$ in the ℓ^2-constrained ℓ^0 PPC is given by

$$\begin{aligned} u_j(x_j) &= \arg \min_{u_j \in \upsilon(x_j)} \|u_j\|_0 \\ \upsilon(x_j) &= \{u_j \in \mathbb{R}^N : \|Mu_j - Kx_j\|_2^2 \leq \|x_j\|_\Pi^2\} \end{aligned} \tag{D.6}$$

for $j = 1, \dots, s(k)$, where M and K are defined as in the previous case. Deriving $\upsilon(x_j)$ as in (D.6), which is a different presentation from (D.5), is based on the recursion $x_{(i+1)j}^{'} = Ax_{ij}^{'} + Bu_{ij}$ that predicts the future states $x(k+h+1), ..., x(k+h+N)$ by $x_{1j}^{'}, ..., x_{Nj}^{'}$.

To solve the NP hard ℓ^2-constrained ℓ^0 optimization problem [31], we use OMP approach. This is motivated by the fact that OMP has proven to be an efficient method for solving such problems as (D.6) with combinatorial nature [29, 32]. It should be noted that in the case of ℓ^2-constrained ℓ^0 PPC, the structure of the sparsity-promoting optimization is independent of the value of channel time delay or the selection mechanism of the actuator. More specifically, in the above setup, the optimization problem related to (D.6) is stated in the same way as a function of x_j, u_j, and weighting matrices for different values of channel time delay and different logics for the buffer.

4 Stability Analysis

In this section, we derive conditions under which the considered unconstrained ℓ^1-ℓ^2 and ℓ^2-constrained ℓ^0 sparse PPC strategies render the system of Fig. D.1 stable. We seek deterministic stability for both unconstrained ℓ^1-ℓ^2 PPC and ℓ^2-constrained ℓ^0 PPC, though the notion of convergence in each case is different from the other.

4.1 Stability of Unconstrained ℓ^1-ℓ^2 PPC

In this subsection, we present the stability analysis of the considered system in Fig. D.1 supposing that it is controlled according to (D.4). As already mentioned before, the unconstrained ℓ^1-ℓ^2 sparse PPC cannot bring asymptotic stability to the system if the plant has unstable poles. We start by showing where this result stems from in the following proposition.

Proposition 4.1
Suppose that for a $j \in \{1, \dots, s(k)\}$, x_j in (D.4) belongs to the set Γ_j where $\Gamma_j \triangleq \{x_j \in \mathbb{R}^n : \|M^T K x_j\|_\infty \leq \nu/2\}$. Then $u_j(x_j) = 0$.

Proof. See [33, Appendix B]. □

It can be implied from Proposition 4.1 that if at any time instant $k \in \mathbb{N}_0$, the exact prediction of $x(k+h)$, say x_p, satisfies $x_p \in \Gamma_p$, $l(k) = 1$ and A has eigenvalues outside the unit circle, then signals in the system of Fig. D.1 will start diverging from the origin. Since there is no constraint in (D.4) preventing any x_j from falling into Γ_j, then asymptotic stability is not guaranteed when using ℓ^1-ℓ^2 PPC. So we consider another notion of stability which can be assured for the NCS of Fig. D.1 in this case.

Definition 4.1
The feedback loop of Fig. D.1 is said to be practically stable if there exists $\varrho \in \mathbb{R}^+$ in such a way that $\lim_{k\to\infty} \|x(k)\|_2 \leq \varrho$.

To establish the conditions of practical stability, we investigate the value function V defined as

$$V(x_j) \triangleq \min_{u_j \in \mathbb{R}^N} J(x_j, u_j), \tag{D.7}$$

where $J(x_j, u_j)$ is as in (D.3). We first derive upper and lower bounds on $V(x_j)$ in the following theorem.

Lemma 4.1
The value function $V(x_j)$ is bounded as

$$\lambda_{\min}(Q)\|x_j\|_2^2 \leq V(x_j) \leq \tau(\|x_j\|_2) \tag{D.8}$$

for any $x_j \in \mathbb{R}^n$. In (D.8), $\tau(y) \triangleq \alpha y + (\beta + \lambda_{\max}(Q))y^2$, $\alpha = \nu\sqrt{n}\sigma_{\max}(M^\dagger K)$ and $\beta \triangleq \lambda_{\max}(\Pi^\star)$, where matrices $M^\dagger$ and $\Pi^\star$ are specified via

$$M^\dagger = (M^T M)^{-1} M^T, \qquad \Pi^\star = K^T(I - MM^\dagger)M. \tag{D.9}$$

Proof. The claim follows immediately from [29, Lemma 5] by noting that the cost function $J(x_j, u_j)$ in (D.7) is defined in the same way as for the case with delay-free channel studied in [29, Lemma 5]. □

According to the recursion $x'_{(i+1)j} = Ax'_{ij} + Bu_{ij}$, where $i = 0, \ldots, N-1$, $j = 1, \ldots, s(k)$ and $x'_{0j} = \hat{x}_j(k+h;k)$, every prediction x'_{fj} of $x(k+f+h)$, $1 \leq f \leq N$ based on $\hat{x}_j(k+h;k)$, can be stated as a function of $\hat{x}_j(k+h;k)$ and tentative control inputs at each time instant $k \in \mathbb{N}_0$. We denote the function associated with prediction x'_{fj} by $g^f(\hat{x}_j(k+h;k))$ and call it f-th iterated mapping with optimal vector $U(\hat{x}_j(k+h;k)) = [u_0(\hat{x}_j(k+h;k)) \ldots u_{N-1}(\hat{x}_j(k+h;k))]^T$. By induction and considering the logics of the buffer, for every $j \in \{1, \ldots, s(k)\}$ we have

$$g^f(\hat{x}_j(k+h;k)) = A^f \hat{x}_j(k+h;k) + \sum_{l=0}^{f-1} A^{f-1-l} B u_l(\hat{x}_j(k+h;k)), \tag{D.10}$$

where $f = 1, \ldots, N$. For the j associated with the exact prediction of $x(k+h)$ and where $l(k) = 1$, the difference equation in (D.10) describes the dynamics of the plant when the control packets are lost in the channel f times in a row after $k + h$. The following result determines the relationship between $V(x_j)$ and $V(g^f(x_j))$.

Lemma 4.2
Suppose that there exists $\zeta > 0$ defining $r = \mu^2 N/\zeta$ in such a way tha the following Riccati equation holds for $P \geq 0$:

$$P = A^T PA - A^T PB(B^T PB + r)^{-1} B^T PA + Q. \tag{D.11}$$

Then any $x_j \in \mathbb{R}^n$, $j \in \{1, \ldots, s(k)\}$ satisfies

$$V(g^f(x_j)) - V(x_j) \leq -\lambda_{\min}(Q)\|x_j\|_2^2 + \zeta, \tag{D.12}$$

where $f = 1, 2, \ldots, N$.

Proof. Based on the same definition for $J(x_j, u_j)$ and same recursions predicting the future states across the case with channel delay and the case with delay-free channel, we can deduce the claim immediately from [29, Lemma 7].□

The bounds derived in (D.8) and (D.12) are all functions of x_j. However, the above results will be used in the following Lemma to obtain a state-independent bound through introducing a contraction property for the optimal costs during periods of consecutive packet dropouts:

Lemma 4.3
If (D.11) holds for $P > 0$ with $r = \mu^2 N/\zeta$ and $\zeta > 0$, then there exists a real constant $\varphi \in (0, 1)$ in such a way that $V(g^f(x_j))$ satisfies

$$V(g^f(x_j)) \leq \varphi V(x_j) + \lambda_{\min}(Q)/4 + \zeta,$$

for every $x_j \in \mathbb{R}^n$, $j = 1, \ldots, s(k)$, and every f belonging to the set $\{1, 2, \ldots, N\}$.

Proof. The claim can be concluded immediately from [29, Lemma 8] based upon the fact that $J(x_j, u_j)$ and update rule for future states prediction are defined identically across cases of delay-free channel and channel with delay in the NCS of Fig. D.1. □

Utilizing the above results, we establish sufficient conditions for practical stability in the case where the considered system is controlled based on an unconstrained ℓ^1-ℓ^2 PPC strategy over a channel with known constant delay and dropouts. Such conditions are expressed in the following theorem.

Theorem 4.1
Consider the NCS of Fig. D.1 under the unconstrained ℓ^1-ℓ^2 sparse PPC (D.4) and suppose that Assumption 3.1 holds. Moreover, assume that $P > 0$ is chosen in such a way that (D.11) holds with $r = \mu^2 N/\zeta$, where $\zeta > 0$. Then at each time instant $k \in \mathbb{N}_0$, $\|x(k)\|_2$ is bounded. Moreover, the steady-state ℓ^2-norm of $x(k)$ is bounded from above as follows:

$$\lim_{k\to\infty} \|x(k)\|_2 \leq \Psi \triangleq \sqrt{\frac{1}{1-\varphi}\left(\frac{\zeta}{\lambda_{\min}(Q)} + \frac{1}{4}\right)}, \tag{D.13}$$

where φ is defined as

$$\varphi \triangleq 1 - \lambda_{\min}(Q)(\alpha + \beta\lambda_{\max}(Q))^{-1}.$$

Proof. let t_n represent the time instant when a packet is received by the actuator for the $n+1$-th time, i.e., $l(t_n - h) = 1$. The set comprising all such time steps is defined as follows:

$$\mathcal{T} \triangleq \{t_n\}_{n\in\mathbb{N}_0} \subseteq \mathbb{N}_0,$$

where $t_{n+1} > t_n, \forall n \in \mathbb{N}_0$. Moreover, let q_n specify the number of packet dropouts between t_n and t_{n+1}. Thus, q_n is given by

$$q_n = t_{n+1} - t_n - 1, \qquad \forall n \in \mathbb{N}_0. \tag{D.14}$$

It is clear that $q_n \geq 0$ with equality when there is no dropout between t_n and t_{n+1}. Suppose that the current time instant is t_n, $n \in \mathbb{N}_0$, and the packet sequence $\mathbb{U}(x(t_n - h))$ is received at the actuator. As already mentioned before, the actuator selects the packet generated based on the exact prediction of $x(t_n)$ at time $t_n - h$, i.e., $U(\hat{x}_{p(t_n)}(t_n; t_n - h)) = U(x(t_n))$ There will be q_n consecutive dropouts in the channel until the arrival of the next control packet at time t_{n+1}. Within the interval between t_n and t_{n+1}, the control inputs $u_0(x(t_n)), \ldots, u_{q_n}(x(t_n))$, produced based on the unconstrained ℓ^1-ℓ^2 PPC in the NCS of Fig.D.1, are applied to the plant in a successive manner and the states $x(t_n+1), \ldots, x(t_n+q_n+1)$ are generated. Based on Assumption 3.1, q_n satisfies $q_n \leq N-1$. Then according to the update rule for state predictions, plant dynamics (D.1) and Lemma 4.3, the value function of $x(k)$ is bounded as

$$V(x(k)) \leq \varphi V(x(t_n)) + \Theta \tag{D.15}$$

for all $k \in \{t_n+1, t_n+2, \ldots, t_n+q_n+1\}$ where Θ is defined as $\Theta \triangleq \lambda_{\min}(Q)/4 + \zeta$. It should be noted that since $u(k) = 0$ for $k = 0, 1, ..., h-1$, then $t_n \geq h$ holds for all $n \in \mathbb{N}_0$. It follows from $t_{n+1} = t_n + q_n + 1$ and (D.15) that

$$V(x(t_{n+1})) \leq \varphi V(x(t_n)) + \Theta. \tag{D.16}$$

applying induction to (D.16) and based on Assumption 3.1 where it is pointed out that $\mathbb{U}(x(0))$ reaches the actuator at time h, we can derive the following upper bound on the value function of $x(t_n)$:

$$V(x(t_n)) \leq \varphi^n V(x(h)) + (1 + \cdots + \varphi^{n-1})\Theta,$$

Then it follows from Lemma 4.1 that

$$V(x(t_n)) \leq \varphi^n \tau(\|x(h)\|_2) + (1-\varphi)^{-1}\Theta.$$

Now the inequality in (D.15) yields

$$V(x(k)) \leq \varphi^{n+1} \tau(\|x(h)\|_2) + (1-\varphi)^{-1}\Theta.$$

for any $k \in \{t_n + 1, \ldots, t_{n+1}\}$. We can use the lower bound on $V(x_j)$ in Lemma 4.1 to deduce

$$\|x(k)\|_2 \leq \sqrt{\frac{V(x(k))}{\lambda_{\min}(Q)}} \leq \left(\frac{\varphi^{n+1}\tau(\|x(h)\|_2)}{\lambda_{\min}(Q)} + \Psi^2\right)^{\frac{1}{2}}, \tag{D.17}$$

where Ψ is defined as in (D.13). The derivation in (D.17) together with the inequality $\sqrt{a+b} \leq \sqrt{a} + \sqrt{b}$, $\forall a, b \geq 0$, will give

$$\|x(k)\|_2 \leq \sqrt{\varphi^{n+1}} \sqrt{\frac{\tau(\|x(h)\|_2)}{\lambda_{\min}(Q)}} + \Psi. \tag{D.18}$$

Finally, since $k \to \infty$ implies $n \to \infty$ and $x(h)$ is finite for a finite h, the steady-state ℓ^2-norm of the states is bounded as follows:

$$\lim_{k\to\infty} \|x(k)\|_2 \leq \Psi,$$

which completes the proof of practical stability for the unconstrained ℓ^1-ℓ^2 sparse PPC. □

Remark 4.1

According to Assumption 3.1, the system runs with no control input at the first h time steps, i.e., $u(k) = 0$, $k = 0, \ldots, h-1$. So in the case where the plant is unstable, system states grows with respect to time over the interval $[0, h]$ which means $x(i+1) \geq x(i)$ for every $i \in \{0, \ldots, h-1\}$. This implies that increasing the channel delay h while keeping the initial states and every other component of the system intact will lead to a greater $x(h)$. Therefore, according to (D.18), the ℓ^2-norm of the states $\|x(k)\|_2$ is bounded by a larger value at each time instant $k \in \{\mathbb{N}_0\}$ if the channel delay is greater. However, since h is finite, increasing the delay will not affect the stability of the system, i.e., the system will be still practically stable for greater delays. So, in the unconstrained ℓ^1-ℓ^2

sparse PPC of certain LTI plants over channels with constant time delay, the practical stability can be achieved for greater delays but with the price of worst system performance.

4.2 Stability of ℓ^2-Constrained ℓ^0 PPC

Here, we establish conditions under which the asymptotic stability is guaranteed in the ℓ^2-constrained ℓ^0 PPC case. The corresponding optimization problem is formalized by (D.6). First, we investigate the feasibility of this problem in the following Lemma.

Lemma 4.4
Assume that for any $j \in \{1, \dots, s(k)\}$, $k \in \mathbb{N}_0$, $\upsilon^*(x_j)$ is defined as

$$\upsilon^*(x_j) \triangleq \{u_j \in \mathbb{R}^N : \|Mu_j - Kx_j\|_2^2 \leq \|x_j\|_{\Pi^*}^2\}.$$

in which Π^* is given by (D.9) and $x_j = \hat{x}_j(k+h;k)$. Then $\Pi \geq \Pi^*$ yields $\upsilon(x_j) \supseteq \upsilon^*(x_j)$ where $\upsilon(x_j)$ is defined as in (D.6). The feasible set $\upsilon(x_j)$ associated with any $\Pi \geq \Pi^*$ is closed, convex and non-empty over $\mathbb{R}^N$.

Proof. The set $\upsilon(x_j)$ (as a function of x_j) and matrices Π^* and Π are defined in the same way as $\mathcal{U}(x)$ (as a function of x), W and W^* in [29, Lemma 10] for the system with delay-free channel, respectively. Therefore, the claim immediately follows from [29, Lemma 10]. □

It stems from Lemma 4.4 that $\Pi^* > 0$ is the "smallest" Π which guarantees that finding the control packet sequence $\mathbb{U}$ based on (D.6) is feasible. Let denote the difference between Π and Π^* in the previous lemma by ξ. Hence, ξ is described by

$$\xi = \Pi - \Pi^* > 0. \tag{D.19}$$

In the following lemma, ξ is used to characterize feasible solutions for the optimization problem associated with (D.6).

Lemma 4.5
Any feasible solution to the optimization problem associated with (D.6), namely $u_j \in \upsilon(x_j)$, can be written as

$$u_j = u_j^* + \psi(x_j), \qquad \|M\psi(x_j)\|_2^2 \leq \|x_j\|_\xi^2,$$

for every $j \in \{1, \dots, s(k)\}$, $k \in \mathbb{N}_0$, where $\psi(x_j) \in \mathbb{R}^N$, $u_j^* \in \upsilon^*(x_j)$ and ξ is defined as in (D.19).

Proof. The claim follows immediately from [29, Lemma 11] by noting that the optimization problem in (D.6) comprises a cost function and a constraint each of which is defined identically to its counterpart in the delay-free sparsity-promoting ℓ^2-constrained ℓ^0 optimization in [29]. □

The next Lemma presents a derivation which is similar to the result stated in Lemma 4.3 but with two prominent differences. One is that instead of the value function, a quadratic candidate Lyapunov function defined as $V_P(x_j) \triangleq \|x_j\|_P^2$ is analyzed. The other difference is that the following result gives an upper bound which goes to zero as states converge to the origin.

Lemma 4.6
Consider $\Pi > 0$ and Π^* satisfying $\Pi > \Pi^*$ and ξ as in (D.19). For an arbitrary $Q > 0$, assume that $P > 0$ solves the Riccati equation (D.11) with $r = 0$. Then for any $x_j = \hat{x}_j(k+h;k)$, $j = 1, \ldots, s(k)$ and $k \in \mathbb{N}_0$, there exist constants $\varphi \in [0, 1)$ and $z > 0$ in such a way that

$$V_P(x_{ij}^{'}) \leq \varphi^i V_P(x_j) + z\|x_j\|_\xi^2, \qquad i = 1, 2, \ldots, N, \tag{D.20}$$

where $x_{(f+1)j}^{'} = Ax_{fj}^{'} + Bu_{fj}$, $f = 0, \ldots, N-1$, and $x_{0j}^{'} = x_j$. Moreover, $u_j = [u_{0j} \ldots u_{(N-1)j}]^T$ is the optimal control packet associated with x_j defined in (D.6).

Proof. The recursion related to the prediction of the future states and the structure of the optimization problem are specified identically across the ℓ^2-constrained ℓ^0 PPC analyzed here and the one studied in [29]. Therefore, we can conclude the claim immediately from [29, Lemma 13]. □

Now we can use the derived contraction property in (D.20) to show that under certain tuning conditions, the control signal given based on the ℓ^2-constrained ℓ^0 PPC strategy in (D.6) can render the considered system (with bounded dropouts and fixed finite delay) asymptotically stable. These conditions are presented in the following theorem:

Theorem 4.2
For an arbitrary $Q > 0$, let $P > 0$ solve the Riccati equation (D.11) with $r = 0$. Pick a ξ satisfying $0 \leq \xi \leq (1-\varphi)P/z$ where the constants $\varphi \in [0, 1)$ and $z > 0$ are calculated through (24), (25) and (26) in [29]. Suppose that Π^* and Π are set as $\Pi^* = P - Q$ and $\Pi = \Pi^* + \xi$, respectively. Then, the sparsity-promoting ℓ^2-constrained ℓ^0 optimization (D.6) solved by using these tuning parameters (P, Q, and Π) gives a control packet sequence $\mathbb{U}(x(k))$, at each time instant $k \in \mathbb{N}_0$, in such a way that $x(k) \to 0$ as $k \to \infty$.

Proof. Let t_n denote the time instant when a packet is received at the actuator successfully for the $n+1$-th time and q_n denote the number of dropouts between t_n and t_{n+1}, $n \in \mathbb{N}_0$. So q_n is defined as in (D.14). Consider a specific t_n and recall that $q_n \leq N-1$. Now it follows from selection logic of the actuator and Lemma 4.6 that

$$V_P(x(k)) \leq x(t_n)^T(\varphi P + z\xi)x(t_n) < V_P(x(t_n)), \tag{D.21}$$

where $k \in \{t_n + 1, \ldots, t_n + q_n + 1\}$. Since $t_n + q_n + 1 = t_{n+1}$, for the time step when $n + 2$-th packet is received successfully, the following inequality can be concluded:

$$V_P(x(t_{n+1})) < V_P(x(t_n)). \tag{D.22}$$

It follows from (D.22) that due to the positivity of $V_P(.)$, $x(t_n) \to 0$ as $n \to \infty$. Then based on (D.21), we can conclude that the states converge to the origin as time goes to infinity, i.e. $x(k) \to 0$ as $k \to \infty$. It means that the system is asymptotically stable, and therefore, the proof is complete. □

5 Numerical Example

We consider the model of an inverted pendulum on a cart taken from [34] as the plant model in the NCS of Fig. D.1. The state matrix A and input vector B associated with this state-space model are specified as follows:

$$A = \begin{bmatrix} 1.000 & 0.0498 & 0.0028 & 0.0001 \\ 0.000 & 0.9913 & 0.1116 & 0.0028 \\ 0.000 & -0.0005 & 1.0327 & 0.0508 \\ 0.000 & -0.0189 & 1.3062 & 1.0327 \end{bmatrix}, \qquad B = \begin{bmatrix} 0.0098 \\ 0.3908 \\ 0.0212 \\ 0.8485 \end{bmatrix}. \tag{D.23}$$

It is straightforward to verify that the pair (A, B) is reachable. We simulate the feedback loop of Fig. D.1 where the plant is modelled based on (D.23) for both unconstrained ℓ^1-ℓ^2 PPC and ℓ^2-constrained ℓ^0 PPC. To do so, we set the horizon length as $N = 10$. Furthermore, we set the process $l(k)$ in such a way that the number of consecutive packet dropouts is distributed uniformly over $[0, 1, .., N-1]$. In both cases, the weighting matrix Q is chosen as $Q = I$. Each element of the initial states x_0 is drawn from the standard normal distribution and is independent from other elements. The performance of the PPC strategies proposed through (D.4) and (D.6) is examined over three different values of channel delay, $h \in \{0, 10, 20\}$. For the unconstrained ℓ^1-ℓ^2 PPC, we select the parameters ν and r as $\nu = 15$ and $r = 2$. We solve the corresponding sparsity-promoting optimization problem in (D.4) by using FISTA. For the case of ℓ^2-constrained ℓ^0 PPC, we calculate Π and ξ according to the procedure suggested in Theorem 4.2. For instance, we set ξ as $\xi = (1 - \varphi)P/2z$ so that it is smaller than $(1 - \varphi)P/z$.

Utilizing the above parameters, we simulate the NCS of Fig. D.1. Figures D.3 and D.4 demonstrate the results which are average over 200 number of 300-sample-long simulations. The ℓ^2-norm of the states $x(k)$ in the case of unconstrained ℓ^1-ℓ^2 PPC is illustrated by Fig. D.3 (top). The curves in Fig. D.3 (top) show the boundedness of $\|x(k)\|_2$ over the considered time interval. This implies that the controller designed based on the ℓ^1-ℓ^2 PPC strategy renders the system practically stable. Secondly, in Fig. D.3 (top), the values of

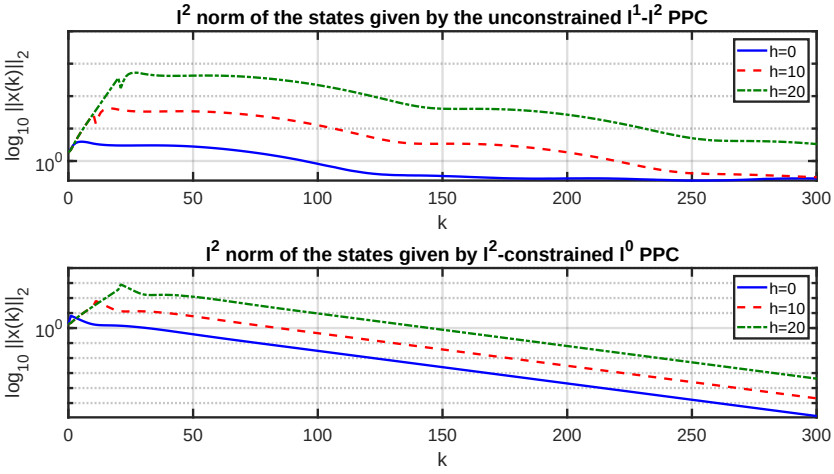

Fig. D.3: Average ℓ^2 norm of the state $x(k)$ in the unconstrained ℓ^1-ℓ^2 PPC (top) and ℓ^2-constrained ℓ^0 PPC (bottom)

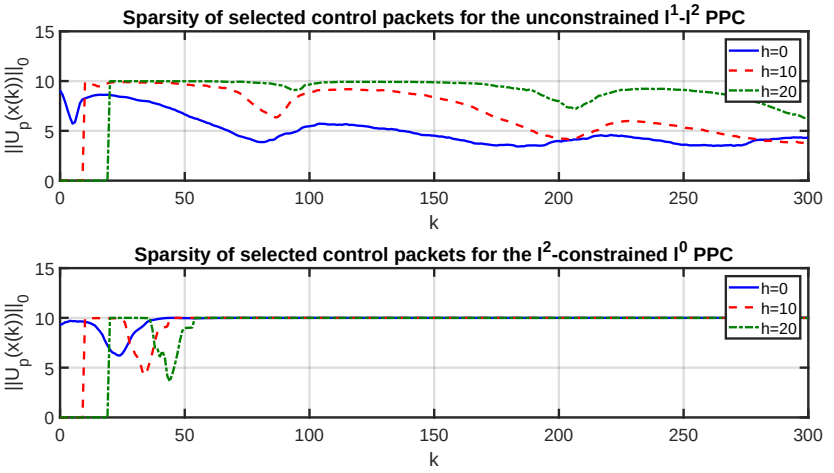

Fig. D.4: Average ℓ^0 norm of the control packet $U_h(x(k))$ in the unconstrained ℓ^1-ℓ^2 PPC (top) and ℓ^2-constrained ℓ^0 PPC (bottom)

curves associated with higher channel delays are larger while they all converge to the same value as time proceeds. This is in accordance with the observation pointed out in Remark 4.1. For the ℓ^2-constrained ℓ^0 PPC setting, the asymptotic stability of the resulted system is verified according to the curves in Fig. D.3 (bottom) which demonstrate the ℓ^2-norm of $\|x(k)\|_2$. As depicted in Fig. D.3, the stability in each case holds regardless of the channel delay value. However, it can be observed that increasing the channel delay degrades the performance of the system in both cases. The ℓ^0-norm of the selected control packet $U_p(x)$ is demonstrated by Fig. D.4. The curves in Fig. D.4 show that for a fixed channel time delay, unconstrained ℓ^1-ℓ^2 PPC generates sparser control commands than ℓ^2-constrained ℓ^0 PPC. This is of course caused by our choice of ν. According to (D.3), making the parameter ν smaller will reduce the sparsity of the obtained control vector. Clearly, enlarging ν will give solutions with more zero elements to the sparsity-promoting unconstrained ℓ^1-ℓ^2 problem. However, such improved sparsity comes with the cost of control performance degradation.

6 Conclusions

In this paper, PPC over digital communication channels subject to time delays and data packet dropouts has been studied. In the considered NCS, the communication channel is located in the actuation path between the controller and a discrete-time LTI plant. We have analyzed the stability of the overall closed-loop system under two different sparsity-promoting control policies; unconstrained ℓ^1-ℓ^2 PPC and ℓ^2-constrained ℓ^0 PPC. We have shown that under certain conditions, the unconstrained ℓ^1-ℓ^2 PPC will bring practical stability to the system. Moreover, we have derived conditions guaranteeing asymptotic stability in the case of utilizing ℓ^2-constrained ℓ^0 PPC. For both cases, we have shown that the number of packets generated by the controller at each time instant is bounded from above by a fixed value which becomes larger as channel time delay grows. We have demonstrated, through simulation, that in each case of unconstrained ℓ^1-ℓ^2 PPC or ℓ^2-constrained ℓ^0 PPC, the optimization problem giving the stabilizing control inputs has sparse solution. Moreover, the simulation results show that increasing the channel-induced delay worsens the system performance, though such an increase in the value of the delay has no effect on system stability.

Future research will focus on disturbed plants with model uncertainties, random channel delays, finding tighter upper bound on $\|x(k)\|_2$ in stability analysis of unconstrained ℓ^1-ℓ^2 PPC, and analyzing the effect of quantization.

References

[1] X. M. Zhang, Q. L. Han, and X. Yu, "Survey on recent advances in networked control systems," *IEEE Transactions on Industrial Informatics*, vol. 12, no. 5, pp. 1740–1752, Oct. 2016.

[2] G. N. Nair, F. Fagnani, S. Zampieri, and R. J. Evans, "Feedback control under data rate constraints: An overview," *Proceedings of the IEEE*, vol. 95, no. 1, pp. 108–137, Jan. 2007.

[3] J. Baillieul and P. J. Antsaklis, "Control and communication challenges in networked real-time systems," *Proceedings of the IEEE*, vol. 95, no. 1, pp. 9–28, Jan. 2007.

[4] L. Zhang, H. Gao, and O. Kaynak, "Network-induced constraints in networked control systems—a survey," *IEEE Transactions on Industrial Informatics*, vol. 9, no. 1, pp. 403–416, Feb. 2013.

[5] S. Wen and G. Guo, "Minimum data rate for exponential stability of networked control systems with medium access constraints," *International Journal of Control, Automation and Systems*, vol. 16, no. 2, pp. 717–725, 2018.

[6] K. Okano and H. Ishii, "Stabilization of uncertain systems with finite data rates and markovian packet losses," *IEEE Transactions on Control of Network Systems*, vol. 1, no. 4, pp. 298–307, Dec. 2014.

[7] C. Tan and H. Zhang, "Necessary and sufficient stabilizing conditions for networked control systems with simultaneous transmission delay and packet dropout," *IEEE Transactions on Automatic Control*, vol. 62, no. 8, pp. 4011–4016, Aug. 2017.

[8] E. I. Silva, M. S. Derpich, J. Østergaard, and M. A. Encina, "A characterization of the minimal average data rate that guarantees a given closed-loop performance level," *IEEE Transactions on Automatic Control*, vol. 61, no. 8, pp. 2171–2186, Aug. 2016.

[9] W. P. M. H. Heemels, A. R. Teel, N. van de Wouw, and D. Nešić, "Networked control systems with communication constraints: Tradeoffs between transmission intervals, delays and performance," *IEEE Transactions on Automatic Control*, vol. 55, no. 8, pp. 1781–1796, Aug. 2010.

[10] E. G. Peters, D. Marelli, D. E. Quevedo, and M. Fu, "Controller design for networked control systems affected by correlated packet losses," *IFAC-PapersOnLine*, vol. 50, no. 1, pp. 2555 – 2560, 2017, 20th IFAC World Congress.

[11] M. Athans, "Minimum-fuel feedback control systems: second-order case," *IEEE Transactions on Applications and Industry*, vol. 82, no. 65, pp. 8–17, Mar. 1963.

[12] R. R. Liu and I. M. Golovitcher, "Energy-efficient operation of rail vehicles," *Transportation Research Part A: Policy and Practice*, vol. 37, no. 10, pp. 917 – 932, 2003.

[13] B. Dunham, "Automatic on/off switching gives 10-percent gas saving," *Popular Science*, vol. 205, no. 4, p. 170, 1974.

[14] C. C. Chan, "The state of the art of electric, hybrid, and fuel cell vehicles," *Proceedings of the IEEE*, vol. 95, no. 4, pp. 704–718, Apr. 2007.

[15] B. D. Anderson and J. B. Moore, *Optimal control: Linear quadratic methods*. Courier Corporation, 2007.

[16] M. Nagahara, D. E. Quevedo, and D. Nesic, "Hands-off control as green control," *arXiv preprint arXiv:1407.2377*, 2014.

[17] M. Nagahara, D. E. Quevedo, and D. Nešić, "Maximum hands-off control: a paradigm of control effort minimization," *IEEE Transactions on Automatic Control*, vol. 61, no. 3, pp. 735–747, Mar. 2016.

[18] ——, "Maximum hands-off control and L^1 optimality," in *Proceedings of the 52nd IEEE Conference on Decision and Control (CDC)*, Dec. 2013, pp. 3825–3830.

[19] M. Nagahara, J. Østergaard, and D. E. Quevedo, "Discrete-time hands-off control by sparse optimization," *EURASIP Journal on Advances in Signal Processing*, vol. 2016, no. 1, p. 76, Jun. 2016.

[20] T. Ikeda and M. Nagahara, "Value function in maximum hands-off control for linear systems," *Automatica*, vol. 64, pp. 190 – 195, 2016.

[21] D. E. Quevedo and D. Nešić, "Input-to-state stability of packetized predictive control over unreliable networks affected by packet-dropouts," *IEEE Transactions on Automatic Control*, vol. 56, no. 2, pp. 370–375, Feb. 2011.

[22] D. E. Quevedo, J. Østergaard, and D. Nešić, "Packetized predictive control of stochastic systems over bit-rate limited channels with packet loss," *IEEE Transactions on Automatic Control*, vol. 56, no. 12, pp. 2854–2868, Dec. 2011.

[23] P. L. Tang and C. W. de Silva, "Compensation for transmission delays in an ethernet-based control network using variable-horizon predictive control," *IEEE Transactions on Control Systems Technology*, vol. 14, no. 4, pp. 707–718, Jul. 2006.

[24] G. P. Liu, Y. Xia, J. Chen, D. Rees, and W. Hu, "Networked predictive control of systems with random network delays in both forward and feedback channels," *IEEE Transactions on Industrial Electronics*, vol. 54, no. 3, pp. 1282–1297, Jun. 2007.

[25] J. Østergaard and D. Quevedo, "Multiple descriptions for packetized predictive control," *EURASIP Journal on Advances in Signal Processing*, vol. 2016, no. 1, p. 45, Apr. 2016.

[26] E. G. W. Peters, D. E. Quevedo, and J. Østergaard, "Shaped Gaussian dictionaries for quantized networked control systems with correlated dropouts," *IEEE Transactions on Signal Processing*, vol. 64, no. 1, pp. 203–213, Jan. 2016.

[27] M. Nagahara and D. E. Quevedo, "Sparse representations for packetized predictive networked control," *IFAC Proceedings Volumes*, vol. 44, no. 1, pp. 84 – 89, 2011, 18th IFAC World Congress.

[28] M. Nagahara, D. E. Quevedo, and J. Østergaard, "Packetized predictive control for rate-limited networks via sparse representation," in *Proceedings of the 51st IEEE Conference on Decision and Control (CDC)*, Dec. 2012, pp. 1362–1367.

[29] ——, "Sparse packetized predictive control for networked control over erasure channels," *IEEE Transactions on Automatic Control*, vol. 59, no. 7, pp. 1899–1905, Jul. 2014.

[30] K. Hayashi, M. Nagahara, and T. Tanaka, "A user's guide to compressed sensing for communications systems," *IEICE transactions on communications*, vol. 96, no. 3, pp. 685–712, 2013.

[31] B. K. Natarajan, "Sparse approximate solutions to linear systems," *SIAM journal on computing*, vol. 24, no. 2, pp. 227–234, 1995.

[32] Y. C. Pati, R. Rezaiifar, and P. S. Krishnaprasad, "Orthogonal matching pursuit: Recursive function approximation with applications to wavelet decomposition," in *Proceedings of the 27th Asilomar Conference on Signals, Systems and Computers (ACSSC)*, vol. 1, Nov. 1993, pp. 40–44.

[33] J. . Fuchs, "On the application of the global matched filter to doa estimation with uniform circular arrays," *IEEE Transactions on Signal Processing*, vol. 49, no. 4, pp. 702–709, Apr. 2001.

[34] T. Tanaka, K. H. Johansson, and M. Skoglund, "Optimal block length for data-rate minimization in networked lqg control," *IFAC-PapersOnLine*, vol. 49, no. 22, pp. 133 – 138, 2016, 6th IFAC Workshop on Distributed Estimation and Control in Networked Systems (NECSYS).

Paper E

Hands-off Control for Discrete-time Linear Systems subject to Polytopic Uncertainties

Masako Kishida, Mohsen Barforooshan, and Masaaki Nagahara

The paper has been published in the proceedings of the
7th IFAC Workshop on Distributed Estimation and Control in Networked Systems, 2018.

The layout has been revised.

Abstract

This paper develops approaches to the hands-off control problem subject to performance constraints for discrete-time linear systems. The approaches minimize the l_1-norm of the control input to acquire the hands-off property, while satisfying the performance constraints that are given in terms of the quadratic cost of states and inputs with respect to the optimal solution to the finite-horizon linear quadratic regulator problem. We consider three kinds of the input and state matrices for the system; 1) known, 2) uncertain but contained in a known discrete set, and 3) uncertain but contained in a known polytopic uncertainty set. For the first two cases, we show that each problem is formulated as an l_1 optimization that is expressed as a second-order cone programming. We also show that the last case leads to a second-order cone programming after relaxations. A numerical example is included to illustrate the validity of the proposed approach.

keywords

Robust control, Uncertainty, Linear optimal control, Convex programming, Discrete-time systems

1 Introduction

Control effort minimization is a fundamental requirement in practical control systems for saving fuel/electricity consumption and reducing noise and vibration [1, 2]. For such problems, sparse control which takes input value mostly zero is effective. Thus, a novel design method called *maximum hands-off control* that produces a control input with the minimum support per unit of time has been proposed [3].

The maximum hands-off control problem is initially formulated as an L^0 optimal control for continuous-time systems to bring an arbitrary state to the origin. Although the L^0 minimization problem is difficult to solve due to the non-convexity and the non-smoothness of the problem, it is proved that the set of L^0 optimal solutions is equivalent to that of L^1 optimal solutions under a uniqueness assumption called normality [3]. This property is important in view of computation; L^1 optimal control problem can be formulated as a convex optimization problem, which is easily solved by numerical methods [4]. For discrete-time systems, the equivalence between l_0 and l_1 sparsity-promoting problems is also investigated in [5]. Here, we note that even though the equivalence does not hold always, we may still obtain a hands-off control that has a short support per unit of time by minimizing l_1-norm because it was shown

that the l_1-norm is the convex envelope of the l_0-norm [6] and l_1-minimization is known to lead to sparse solutions.

Robustness against uncertainty is a critical requirement in a lot of practical real-world control systems. Thus, robust control has been one of the most appealing approaches in the realm of control theory over 30 years. One of the most well-known approaches in robust control is H_∞ control, in which the uncertain system is modeled as a set of systems. It finds a control that achieves a control objective for all possible systems in the set; see [7] for example.

In this paper, we consider the hands-off control problem that minimizes the l_1 norm of the control input subject to uncertainties with performance constraint. The considered uncertainty takes the form of polytopic uncertainty, which is modeled by the convex hull of multiple possible systems [8, 9]. On the other hand, the considered performance constraint is obtained by relaxing the optimal cost of the finite-horizon linear quadratic regulator (LQR) problem. For such problem, the robust control design is formulated in terms of linear matrix inequalities (LMIs) [10], which represents a convex optimization problem and can be solved numerically by optimization softwares such as `YALMIP` in `MATLAB` [11–13].

The main contribution of this paper is twofold. (i) the inclusion of a design parameter that allows us to specify the degree of possible cost relaxation under which the input sparsity is sought for, (ii) the consideration of uncertainties in the system model. This is achieved by adopting a relaxed constraint for the terminal state, instead of forcing the terminal state to be zero as in [3].

The remainder of this paper is organized as follows: Section 2 provides the notation and an overview of linear quadratic regulator problem, followed by a presentation of the basic problem formulation for the nominal system in Section 3. Section 4 is the main part of this paper, which considers the hands-off control for uncertain systems. Following to some remarks in Section 5, Section 6 presents a numerical example. Finally, Section 7 concludes the paper.

2 Mathematical Preliminaries

2.1 Notation

The set of real numbers is denoted by $\mathbb{R}$. The set of vectors with length n is denoted by $\mathbb{R}^n$, and the set of matrices of size $n \times m$ is denoted by $\mathbb{R}^{n\times m}$. The vector of ones whose length is n is denoted by $\mathbf{1}_n$. The identity matrix of size n is denoted by I_n. The subscript n is dropped when the size is clear. For matrices M and N, $M \otimes N$ indicates the Kronecker product.

2.2 A review of linear-quadratic regulator problem

This subsection provides a brief overview on the finite-horizon LQR problem [14], based on which this paper proposes approaches to hands-off control problems.

Consider a discrete-time linear system

$$x[t+1] = Ax[t] + Bu[t],\ x[0] = x_0, \tag{E.1}$$

where $A \in \mathbb{R}^{n_x \times n_x}$ and $B \in \mathbb{R}^{n_x \times n_u}$ form a controllable pair, $x[t] \in \mathbb{R}^{n_x}$ represents the system state, and $u[t] \in \mathbb{R}^{n_u}$ represents the control input.

The objective of the finite-horizon LQR problem is to find a sequence of control inputs that minimizes the following quadratic cost function:

$$J(u) = x^T[T_f]Q_f x[T_f] + \sum_{t=0}^{T_f-1} x^T[t]Qx[t] + u^T[t]Ru[t],$$
$$Q = Q^T > 0,\ Q_f = Q_f^T > 0,\ R = R^T > 0,$$

where T_f is the time horizon. Generally, Q and Q_f are required to be positive semidefinite. However, we restrict our attention to positive definite weight matrices for convenience. For such a problem, it is well-known that the optimal control input is [15]

$$\begin{aligned} u^*[t] &= -F[t]x[t],\ t = 0, 1, \cdots, T_f - 1, \\ F[t] &= \left(B^T P[t+1]B + R\right)^{-1} B^T P[t+1]A, \end{aligned} \tag{E.2}$$

where $P[t]$ is the solution to

$$\begin{aligned} P[t] &= A^T P[t+1]A + Q \\ &- A^T P[t+1]B \left(B^T P[t+1]B + R\right)^{-1} B^T P[t+1]A, \\ P[T_f] &= Q_f. \end{aligned}$$

Moreover, the corresponding optimal cost is given by

$$J_{\mathrm{LQR}} := J(u^*[t]). \tag{E.3}$$

2.3 Some matrix inequalities

To treat polytopic uncertainties efficiently in Section 4, the following relaxations will be used:

Lemma 2.1 ([16])
Let $M_i = M_i^T > 0$ and $\lambda_i \geq 0$ for $i = 1, 2, \cdots, p$ satisfy $\sum_{i=1}^p \lambda_i = 1$. Then

$$\left(\sum_{i=1}^p \lambda_i N_i\right)^T \left(\sum_{i=1}^p \lambda_i M_i\right)^{-1} \left(\sum_{i=1}^p \lambda_i N_i\right) \leq \sum_{i=1}^p \lambda_i N_i^T M_i^{-1} N_i$$

The equality holds if and only if $N_1^T M_1^{-1} = \cdots = N_p^T M_p^{-1}$.

It should be emphasized that N_i is not required to be symmetric or square. In addition, according to the original reference, the results of Lemma 2.1 holds under the assumption that $\lambda_i > 0$. However, we can trivially include the case with $\lambda_i = 0$.

Corollary 2.1
Let $M_i = M_i^T > 0$ and $\lambda_i \geq 0$ for $i = 1, 2, \cdots, p$ satisfy $\sum_{i=1}^{p} \lambda_i = 1$. Then

$$\left(\sum_{i=1}^{p} \lambda_i M_i \right)^{-1} \leq \sum_{i=1}^{p} \lambda_i M_i^{-1}.$$

The equality holds if and only if $M_1 = M_2 = \cdots = M_p$.

Proof. Let $N_i = I$ for all i in Lemma 2.1. □

Corollary 2.2
Let $L = L^T > 0$ and $\lambda_i \geq 0$ for $i = 1, 2, \cdots, p$ satisfy $\sum_{i=1}^{p} \lambda_i = 1$. Then

$$\left(\sum_{i=1}^{p} \lambda_i N_i \right)^T L \left(\sum_{i=1}^{p} \lambda_i N_i \right) \leq \sum_{i=1}^{p} \lambda_i N_i^T L N_i.$$

The equality holds if and only if $N_1 = N_2 = \cdots = N_p$.

Proof. Let $M_i = L^{-1}$ for all i in Lemma 2.1. □

3 Hands-off Control Problem for Known System

Using the results in Section 2.2, this section proposes the hands-off control problem for the system (E.1) with a known controllable pair of A and B. More specifically, the problem is set up so as to minimize the l_1-norm of the control input while satisfying the control performance condition that specifies the degree of relaxation compared with the optimal cost of the LQR problem in (E.3).

Problem 3.1
(Hands-off Control Problem with Performance Constraint cf. [3]):
For the linear system

$$x[t+1] = Ax[t] + Bu[t], \quad x[0] = x_0, \quad t = 0, 1, \cdots, T_f - 1,$$

with the controllable pair of (A, B), find a sequence of control inputs $u[t]$ that minimizes the l_1-norm of the control input

$$\sum_{t=0}^{T_f-1} \sum_{i=1}^{n_u} |u_i[t]|, \tag{E.4}$$

where $|\cdot|$ denotes the element-wise absolute value, subject to

$$J(u) := x^T[T_f]Q_f x[T_f] + \sum_{t=0}^{T_f-1} x^T[t]Qx[t] + u^T[t]Ru[t] \leq J^*, \tag{E.5}$$

where

$$J^* := \gamma J_{\mathrm{LQR}},\ \gamma \geq 1. \tag{E.6}$$

In (E.6), J_{LQR} is defined as in (E.3) and specifies the control performance condition.

Remark 3.1
The parameter γ is used to make a balance between the sparsity of the control input and the deviation from the optimal cost (E.3). If $\gamma = 1$, then there is no freedom to minimize the norm of the control inputs, and the solution to the problem coincides with (E.2). As γ becomes larger, the l_1-norm of the hands-off control inputs may become smaller, but the performance degrades more and more compared with (E.3).

To solve Problem 3.1, let us first simplify the expressions in (E.4)-(E.5) by defining

$$\begin{aligned}
&\bar{x} := \begin{bmatrix} x[0] \\ x[1] \\ \vdots \\ x[T_f] \end{bmatrix},\ \bar{u} := \begin{bmatrix} u[0] \\ u[1] \\ \vdots \\ u[T_f-1] \end{bmatrix}, \\
&\hat{A} := \begin{bmatrix} I_{n_x} & 0 & \cdots & 0 \\ A & & & 0 \\ \vdots & \vdots & \ddots & \\ A^{T_f-1} & A^{T_f-2} & \cdots & I_{n_x} \end{bmatrix}, \\
&\bar{A} := \begin{bmatrix} 0_{n_x \times n_x T_f} \\ \hat{A} \end{bmatrix},\ \bar{B} := I_{T_f} \otimes B,\ A_0 := \begin{bmatrix} A \\ 0_{(n_x-1)T_f \times n_x} \end{bmatrix}, \\
&\hat{Q} := \mathrm{diag}[I_{T_f-1} \otimes Q, Q_f],\ \bar{Q} := \mathrm{diag}[Q, \hat{Q}],\ \bar{R} := I_{T_f} \otimes R, \\
&G_1 := \bar{A}\bar{B},\ G_2 := \begin{bmatrix} I_{n_x} \\ \hat{A}A_0 \end{bmatrix}.
\end{aligned} \tag{E.7}$$

Then, the cost (E.4) can be rewritten as

$$\sum_{t=0}^{T_f-1} \sum_{i=1}^{n_u} |u_i[t]| = \mathbf{1}_{n_u T_f}^T |\bar{u}|. \tag{E.8}$$

Also, the vector of the states is expressed as

$$\bar{x} = G_1 \bar{u} + G_2 x_0,$$

and thus $J(u)$ in (E.5) can be expressed as

$$J(u) = \bar{x}^T \bar{Q} \bar{x} + \bar{u}^T \bar{R} \bar{u} = \begin{bmatrix} \bar{u} \\ x_0 \end{bmatrix}^T \begin{bmatrix} G_1^T \bar{Q} G_1 + \bar{R} & G_1^T \bar{Q} G_2 \\ G_2^T \bar{Q} G_1 & G_2^T \bar{Q} G_2 \end{bmatrix} \begin{bmatrix} \bar{u} \\ x_0 \end{bmatrix}. \quad \text{(E.9)}$$

Based upon (E.8)-(E.9), Problem 3.1 can be reformulated as a second-order cone programming as follows:

$$\begin{aligned} &\min_{w} \; q_0^T w \\ &\text{s.t. } \; w^T P_1 w + q_1^T w + r_1 \leq 0, \\ &\quad\; q_2^T w \leq 0, \; q_3^T w \leq 0, \end{aligned} \quad \text{(E.10)}$$

where

$$\begin{aligned} &w := \begin{bmatrix} \bar{u} \\ v \end{bmatrix}, \; q_0 := \begin{bmatrix} 0_{n_u T_f} \\ \mathbf{1}_{n_u T_f} \end{bmatrix}, \\ &P_1 := \begin{bmatrix} G_1^T \bar{Q} G_1 + \bar{R} & 0 \\ 0 & 0 \end{bmatrix}, \; q_1 := \begin{bmatrix} 2 G_1^T \bar{Q} G_2 x_0 \\ 0 \end{bmatrix}, \\ &r_1 := x_0^T G_2^T \bar{Q} G_2 x_0 - J^*, \\ &q_2 := \begin{bmatrix} I_{n_u T_f} \\ -I_{n_u T_f} \end{bmatrix}, \; q_3 := \begin{bmatrix} -I_{n_u T_f} \\ -I_{n_u T_f} \end{bmatrix}. \end{aligned} \quad \text{(E.11)}$$

This second-order cone programming (E.10)-(E.11) can be solved using existing numerical softwares such as `YALMIP` on `MATLAB` [11–13]. Here, the constraint $w^T P_1 w + q_1^T w + r_1 \leq 0$ corresponds to (E.5) and guarantees the satisfaction of the performance condition, while the other two constraints, $q_2^T w \leq 0$ and $q_3^T w \leq 0$, determine the bounds on the absolute value of $u[t]$.

Remark 3.2
Unlike the original paper [3], where a continuous-time setup is considered, it is not necessary to impose the constraint $\max_i |u_i[t]| \leq 1$ in a discrete-time setup. This is because without such a constraint, a continuous-time setup produces an optimal control input of a Dirac delta function, while a discrete-time setup guarantees the boundedness of $|u_i[t]|$ as long as (E.8) is bounded.

4 Hands-off Control Problem for Uncertain Systems

This section considers the hands-off control problem for the system (E.1) but with uncertainties in the state matrix A and input matrix B. As in the previous section, we impose the control performance condition that specifies the degree of relaxation compared with the optimal cost of the LQR problem.

4.1 Discrete Uncertainties

Let us start with the system (E.1) where the pair (A, B) is uncertain but contained in a known discrete set, i.e.,

$$(A, B) \in \mathcal{S}_d := \{(A, B) = (A_j, B_j),\ j = 1, \cdots, n\}, \tag{E.12}$$

where n is the number of scenarios and (A_j, B_j) are controllable pairs for all $j = 1, \cdots, n$. For such systems, the performance condition is specified using the following upper bound

$$J_d^* := \max_{j=1,\cdots,n} \gamma_j J_{\mathrm{LQR},j},\ \gamma_j \geq 1, \tag{E.13}$$

in place of (E.6), where $J_{\mathrm{LQR},j}$ is the optimal cost (E.3) corresponding to the scenario (A_j, B_j) in (E.12), and γ_j specifies the degree of relaxation for each scenario. In this way, the existence of the control input satisfying the performance condition is guaranteed, and the parameter γ can be used to balance between the sparsity of the input and the deviation from the optimal cost in the worst-case scenario.

The constraint of performance condition (E.5) needs to be satisfied in any of the n scenarios, thus the second-order cone programming of this problem replaces the first constraint of (E.10) by n constraints, each of which corresponds to one of n scenarios. Therefore, the following second-order cone programming provides the solution to the hands-off control problem subject to discrete uncertainties.

$$\begin{aligned} &\min_{w}\ q_0^T w \\ \text{s.t. }\ &w^T P_{1j} w + q_{1j}^T w + r_{1j} \leq 0,\ j = 1, \cdots, n, \\ &q_2^T w \leq 0,\ q_3^T w \leq 0, \end{aligned} \tag{E.14}$$

where w, q_0, q_2 and q_3 are defined as in (E.11), and

$$\begin{aligned} &P_{1j} = \begin{bmatrix} G_{1,j}^T \bar{Q} G_{1,j} + \bar{R} & 0 \\ 0 & 0 \end{bmatrix},\ q_{1j} = \begin{bmatrix} 2G_{1,j}^T \bar{Q} G_{2,j} x_0 \\ 0 \end{bmatrix}, \\ &r_{1j} = x_0^T G_{2,j}^T \bar{Q} G_{2,j} x_0 - J_d^*, \end{aligned} \tag{E.15}$$

and $G_{1,j}$ and $G_{2,j}$ are defined as in (E.7) for the each scenario j of the pair (A_j, B_j). Thus, we have n quadratic constraints and $4n_{u_x}T_f$ linear constraints. The formulation in (E.14)-(E.15) minimizes the l_1-norm of the control input while guaranteeing the performance condition satisfaction for any of the n scenarios in (E.12).

Remark 4.1
It is known that the set of these n constraints in (E.14) is equivalent to

$$w^T P_1 w + q_1^T w + r_1 \leq 0,\ \forall (P_1, q_1, r_1) \in \mathcal{S}_p,$$

where

$$\mathcal{S}_p = \left\{ (P_1, q_1, r_1) | (P_1, q_1, r_1) = \sum_{j=1}^{n} \lambda_j (P_{1j}, q_{1j}, r_{1j}) \lambda_j \geq 0,\ \sum_{j=1}^{n} \lambda_j = 1 \right\}.$$

We will use this equivalence in the following subsection.

4.2 Polytopic Uncertainties

This subsection considers the case where the pair (A, B) contains polytopic uncertainties, i.e.,

$$\begin{aligned} &[A\ B] \in \Omega_p, \\ &\Omega_p := \left\{ [A(\lambda)\ B(\lambda)] = \sum_{i=1}^{p} \lambda_i [A_i\ B_i], \sum_{i=1}^{p} \lambda_i = 1,\ \lambda_i \geq 0 \right\}, \end{aligned} \tag{E.16}$$

where A_i and B_i are constant matrices satisfying the controllability of (A_i, B_i) for all i, and λ_is are time-invariant uncertainties.

Unlike the case of discrete uncertainties, systems with polytopic uncertainties have infinite number of scenarios that replaces (E.5). Thus, to treat polytopic uncertainties efficiently, the constraint (E.5) is relaxed using an upper bound on the cost function (E.9) that is easy to compute. For this purpose, first notice that from the definitions in (E.7), it holds that

$$\begin{aligned} G_1^T \bar{Q} G_1 =& \bar{B}^T \bar{A}^T \bar{Q} \bar{A} \bar{B} = \bar{B}^T \hat{A}^T \hat{Q} \hat{A} \bar{B}, \\ G_2^T \bar{Q} G_1 =& (\hat{A} A_0)^T \hat{Q} \hat{A} \bar{B} = A_0^T \hat{A}^T \hat{Q} \hat{A} \bar{B}, \\ G_2^T \bar{Q} G_2 =& A_0^T \hat{A}^T \hat{Q} \hat{A} A_0 + Q. \end{aligned}$$

Accordingly, the matrix characterizing $J(u)$ in (E.9) can be expressed as

$$\begin{aligned} &\begin{bmatrix} G_1^T \bar{Q} G_1 + \bar{R} & G_1^T \bar{Q} G_2 \\ G_2^T \bar{Q} G_1 & G_2^T \bar{Q} G_2 \end{bmatrix} \\ &= \begin{bmatrix} \bar{B} & \\ & A_0 \end{bmatrix}^T \begin{bmatrix} \hat{A}^T \hat{Q} \hat{A} & \hat{A}^T \hat{Q} \hat{A} \\ \hat{A}^T \hat{Q} \hat{A} & \hat{A}^T \hat{Q} \hat{A} \end{bmatrix} \begin{bmatrix} \bar{B} & \\ & A_0 \end{bmatrix} + \begin{bmatrix} \bar{R} & \\ & Q \end{bmatrix}. \end{aligned}$$

Next, define

$$\begin{aligned} &\tilde{A} := I - \begin{bmatrix} 0 & 0 \\ I_{T_f - 1} \otimes A & 0 \end{bmatrix},\ \tilde{A}_i := I - \begin{bmatrix} 0 & 0 \\ I_{T_f - 1} \otimes A_i & 0 \end{bmatrix}, \\ &\hat{A}_i := \begin{bmatrix} I & 0 & \cdots & 0 \\ A_i & & & 0 \\ \vdots & \vdots & \ddots & \\ A_i^{T_f - 1} & A_i^{T_f - 2} & \cdots & I \end{bmatrix},\ A_{0,i} := \begin{bmatrix} A_i \\ 0_{(n_x - 1) T_f \times n_x} \end{bmatrix}. \end{aligned} \tag{E.17}$$

Then, it follows that

$$\hat{A} = \tilde{A}^{-1} = \left(\sum_{i=1}^{p} \lambda_i \tilde{A}_i \right)^{-1}, \ \hat{A}_i = \tilde{A}_i^{-1}, \ A_0 = \sum_{i=1}^{p} \lambda_i A_{0,i}. \tag{E.18}$$

Moreover, define

$$\bar{B}_i := I_{T_f} \otimes B_i. \tag{E.19}$$

Then, (E.16), (E.17) and (E.19) yield

$$\begin{bmatrix} \bar{B} & 0 \\ 0 & A_0 \end{bmatrix} = \sum_{i=1}^{p} \lambda_i \begin{bmatrix} \bar{B}_i & 0 \\ 0 & A_{0i} \end{bmatrix}. \tag{E.20}$$

On the other hand, from Corollary 2.1 and (E.18), it holds that

$$\begin{aligned} \hat{A}^T \hat{Q} \hat{A} = \tilde{A}^{-T} \hat{Q} \tilde{A}^{-1} &= \left(\sum_{i=1}^{p} \sum_{j=1}^{p} \lambda_i \lambda_j \tilde{A}_i^T \hat{Q}^{-1} \tilde{A}_j \right)^{-1} \\ \leq \sum_{i=1}^{p} \sum_{j=1}^{p} \lambda_i \lambda_j \left(\tilde{A}_i^T \hat{Q}^{-1} \tilde{A}_j \right)^{-1} &= \sum_{i=1}^{p} \sum_{j=1}^{p} \lambda_i \lambda_j \hat{A}_j^T \hat{Q} \hat{A}_i. \end{aligned} \tag{E.21}$$

From (E.21), it follows that

$$\begin{bmatrix} \hat{A}^T \hat{Q} \hat{A} & \hat{A}^T \hat{Q} \hat{A} \\ \hat{A}^T \hat{Q} \hat{A} & \hat{A}^T \hat{Q} \hat{A} \end{bmatrix} \leq \sum_{i=1}^{p} \sum_{j=1}^{p} \lambda_i \lambda_j \begin{bmatrix} \hat{A}_j^T \hat{Q} \hat{A}_i & \hat{A}_j^T \hat{Q} \hat{A}_i \\ \hat{A}_j^T \hat{Q} \hat{A}_i & \hat{A}_j^T \hat{Q} \hat{A}_i \end{bmatrix}. \tag{E.22}$$

Due to the fact that $\mathbf{1}^T \mathbf{1}$ and $M = M^T$ are both positive semidefinite, $(\mathbf{1}^T \mathbf{1}) \otimes M$ is positive semidefinite. Hence, based on Corollary 2.2 together with (E.20) and (E.22), we can deduce

$$\begin{aligned} &\begin{bmatrix} \bar{B} & 0 \\ 0 & A_0 \end{bmatrix}^T \begin{bmatrix} \hat{A}^T \hat{Q} \hat{A} & \hat{A}^T \hat{Q} \hat{A} \\ \hat{A}^T \hat{Q} \hat{A} & \hat{A}^T \hat{Q} \hat{A} \end{bmatrix} \begin{bmatrix} \bar{B} & 0 \\ 0 & A_0 \end{bmatrix} \\ \leq &\sum_{i=1}^{p} \sum_{j=1}^{p} \sum_{k=1}^{p} \lambda_i \lambda_j \lambda_k \begin{bmatrix} \bar{B}_k^T \hat{A}_j^T \hat{Q} \hat{A}_i \bar{B}_k & \bar{B}_k^T \hat{A}_j^T \hat{Q} \hat{A}_i A_{0,k} \\ A_{0,k}^T \hat{A}_j^T \hat{Q} \hat{A}_i \bar{B}_k & A_{0,k}^T \hat{A}_j^T \hat{Q} \hat{A}_i A_{0,k} \end{bmatrix}. \end{aligned}$$

Thus, an upper bound on the cost function $J(\bar{u})$ is obtained as a function of the control input:

$$J(\bar{u}) \leq \sum_{i=1}^{p} \sum_{j=1}^{p} \sum_{k=1}^{p} \lambda_i \lambda_j \lambda_k J_{ijk}(\bar{u}),$$

where

$$\begin{aligned} J_{ijk}(\bar{u}) =& \bar{u}^T \left(\bar{B}_k^T \hat{A}_j^T \hat{Q} \hat{A}_i \bar{B}_k + \bar{R} \right) \bar{u} \\ &+ 2x_0^T \left(A_{0,k}^T \hat{A}_j^T \hat{Q} \hat{A}_i \bar{B}_k \right) \bar{u} \\ &+ x_0^T \left(A_{0,k}^T \hat{A}_j^T \hat{Q} \hat{A}_i A_{0,k} + Q \right) x_0. \end{aligned}$$

So the constraint (E.5) is relaxed as

$$\sum_{i=1}^{p} \sum_{j=1}^{p} \sum_{k=1}^{p} \lambda_i \lambda_j \lambda_k J_{ijk}(\bar{u}) \leq J_p^*.$$

Here, it is assumed that J_p^*, which characterizes the trade-off between the sparsity of control input and systems' performance, is given. The selection of the performance parameter J_p^* is discussed in Section 5.

The corresponding second-order cone programming formulation of (E.10) replaces P_1, q_1 and r_1 by

$$\begin{aligned} P_1 &= \sum_{i=1}^{p} \sum_{j=1}^{p} \sum_{k=1}^{p} \lambda_i \lambda_j \lambda_k P_{1ijk}, \ q_1 = \sum_{i=1}^{p} \sum_{j=1}^{p} \sum_{k=1}^{p} \lambda_i \lambda_j \lambda_k q_{1ijk}, \\ r_1 &= \sum_{i=1}^{p} \sum_{j=1}^{p} \sum_{k=1}^{p} \lambda_i \lambda_j \lambda_k r_{1ijk}, \end{aligned} \tag{E.23}$$

where

$$\begin{aligned} P_{1ijk} &= \begin{bmatrix} \bar{B}_k^T \hat{A}_j^T \hat{Q} \hat{A}_i \bar{B}_k + \bar{R} & 0 \\ 0 & 0 \end{bmatrix}, \\ q_{1ijk} &= \begin{bmatrix} 2\bar{B}_k^T \hat{A}_i^T \hat{Q} \hat{A}_j A_{0,k} x_0 \\ 0 \end{bmatrix}, \\ r_{1ijk} &= x_0^T \left(A_{0,k}^T \hat{A}_j^T \hat{Q} \hat{A}_i A_{0,k} + Q \right) x_0 - J_p^*. \end{aligned}$$

Using (E.23) with Remark 4.1, the second-order cone programming formulation for the hands-off control for polytopic uncertainties is

$$\begin{aligned} &\min_{w} q_0^T w \\ &\text{s.t. } w^T P_{1ijk} w + q_{1ijk}^T w + r_{1ijk} \leq 0, \ i,j,k = 1, \cdots, p, \\ &\quad q_2^T w \leq 0, \ q_3^T w \leq 0, \end{aligned} \tag{E.24}$$

where w, q_0, q_2 and q_3 are defined as in (E.11). This optimization problem has p^3 quadratic constraints and $4n_{u_x}T_f$ linear constraints.

Remark 4.2
It is straightforward to show that the number of quadratic constraints in (E.24) can be reduced from p^3 to $p^2(p+1)/2$ by using the symmetry of i and j in P_{1ijk}, q_{1ijk} and r_{1ijk}.

5 Discussions

This section briefly discusses the computational cost and some concerns regarding the performance condition of the proposed approach.

5.1 Computational Cost

As we have seen, the computational cost of (E.24) increases quadratically with respect to the number of vertices of polytopic uncertainty. However, this computational cost of (E.24) can be reduced by further relaxing the constraints. An approach is to find a pair $(\bar{P}_1, \bar{q}_1, \bar{r}_1)$ such that $\forall w$,

$$\begin{aligned} & w^T \bar{P}_1 w + \bar{q}_1^T w + \bar{r}_1 \leq 0 \\ \Rightarrow & w^T P_{1ijk} w + q_{1ijk}^T w + r_{1ijk} \leq 0, \ \forall i, j, k = 1, \cdots, p. \end{aligned}$$

If such a pair is found, then the number of quadratic constraints is reduced from p^3 to one. To find such $(\bar{P}_1, \bar{q}_1, \bar{r}_1)$, an inner Dikin ellipsoid, an inner Löwner John ellipsoid [17], or other inner approximations for the intersection of ellipsoids $(P_{1ijk}, q_{1ijk}, r_{1ijk})$ [10] can be used.

5.2 Performance Condition

As in the case with discrete uncertainties, it is possible to choose the performance condition J_p^* using the exact upper bound on $\sum_i \lambda_i J_i(\bar{u})$ by solving a minimax constrained problem. However, Section 4.2 proposes to relax the constraint in Problem 3.1 by using the upper bound of quadratic cost instead of the quadratic cost itself. Thus, there is no reason to use the exact upper bound on $\sum_i \lambda_i J_i(\bar{u})$.

One option is to choose J_p^* sufficiently large. For example, we may compare the performance with the nominal by using J_{LQR} corresponding to the nominal system (e.g., $A = \sum_{i=1}^p A_i/p$ and $B = \sum_{i=1}^p B_i/p$) and then setting $J_p^* = \gamma J_{\mathrm{LQR}}$ with a relatively large γ. Note that such J_p^* may lead to infeasible programming, if selected γ is not sufficiently large. In this case, increase the value of γ.

One other method for choosing J_p^* is setting it in such a way that the existence of a feasible control input is guaranteed. For example, if both A and B are subject to polytopic uncertainty as in (E.16), then we may compute $\bar{u}$ that minimizes $J_{ijk}(\bar{u})$ for each i, j, and k and let

$$J_p^* = \gamma \max_{i,j,k} J_{ijk}(\bar{u}_{\mathrm{approx}}), \ \gamma \geq 1$$

where $\bar{u}_{\mathrm{approx}} = \arg\max_{i,j,k} J_{ijk}^*(\bar{u})$. Then it is guaranteed that there exists a

control input $\bar{u} = \bar{u}_{\text{approx}}$ that satisfies

$$\sum_{i=1}^{p}\sum_{j=1}^{p}\sum_{k=1}^{p}\lambda_i\lambda_j\lambda_k J_{ijk}(\bar{u}) \leq J_p^*.$$

Alternatively, we could evaluate how much control effort is needed to improve the performance compared with the worst case of uncertainties without control inputs by setting J_p^* as follows:

$$J_p^* = \eta J(0),\ \eta \leq 1,\ J(0) = \max_{A} x_0^T G_2^T \bar{Q} G_2 x_0.$$

6 Numerical Example

In this section, we apply the results obtained in Section 4.2. to a discrete-time linear system subject to polytopic uncertainties. The example is taken from [18], which considers the model of a continuous stirred tank reactor for an exothermic, irreversible reaction. The polytope representing uncertainties of the considered plant is characterized by 4 vertices as follows:

$$A_1 = \begin{bmatrix} 0.8227 & -0.00168 \\ 6.1233 & 0.9367 \end{bmatrix},\ A_2 = \begin{bmatrix} 0.9654 & -0.00182 \\ -0.6759 & 0.9433 \end{bmatrix},$$
$$A_3 = \begin{bmatrix} 0.8895 & -0.00294 \\ 0.9447 & 0.9968 \end{bmatrix},\ A_4 = \begin{bmatrix} 0.8930 & -0.00062 \\ 2.7738 & 0.8864 \end{bmatrix},$$

$$B_1 = \begin{bmatrix} -0.000092 & 0.1014 \end{bmatrix}^T,\ B_2 = \begin{bmatrix} -0.000097 & 0.1016 \end{bmatrix}^T,$$
$$B_3 = \begin{bmatrix} -0.000157 & 0.1045 \end{bmatrix}^T,\ B_4 = \begin{bmatrix} -0.000034 & 0.0986 \end{bmatrix}^T,$$

where each pair (A_i, B_i) is controllable. The initial state of the plant is a 2-dimensional random vector whose elements are selected from a uniform distribution over $(0, 1)$. The horizon length T_f is set to 50. Weighting matrices are selected as $Q = I$, $Q_f = I$, and $R = 1$. We set the constant γ in (E.13) to 1.5. For the true system, we set $\lambda_1 = 0.1$, $\lambda_2 = 0.2$, $\lambda_3 = 0.3$, and $\lambda_4 = 0.4$.

The optimization is set up based on (E.23) and (E.24) and solved using `YALMIP` with solver option of `fmincon` on `MATLAB` [11–13]. The optimal control input is illustrated in Fig. E.1. In this figure, we also plot the standard finite-horizon LQR control as in (E.2). Compared with the standard LQR control, the hands-off control is sufficiently sparse.

Moreover, we apply the obtained control input to the considered plant in order to assess the behavior of state trajectories. The state trajectories generated by the standard LQR control and the hands-off control are shown in Fig. E.2. According to this figure, the proposed hands-off control, which is much sparser than the LQR control, leads to a comparable performance with the LQR control. One can obtain different sparsity and robustness properties by manipulating γ and weighting matrices.

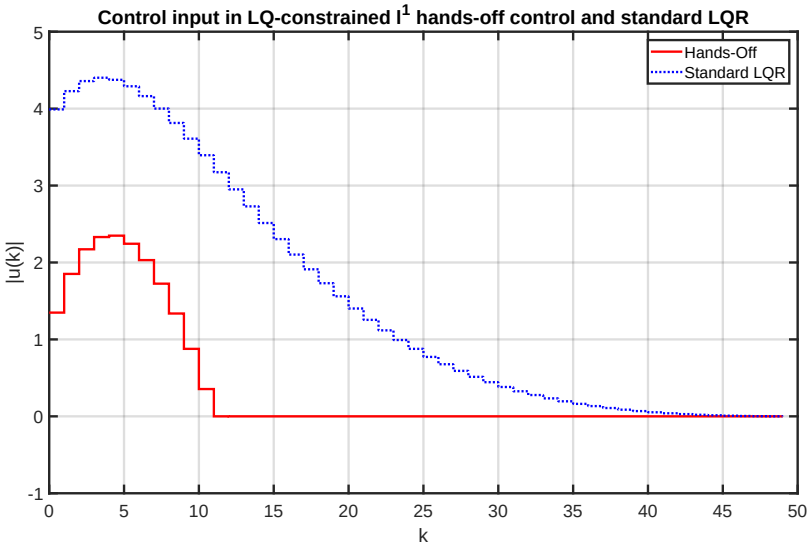

Fig. E.1: Control input $u[t]$: hands-off control (real line) and standard LQR (dotted line)

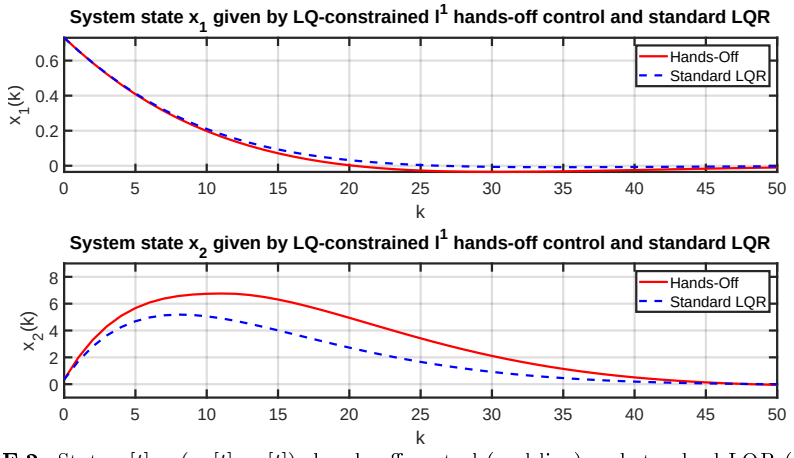

Fig. E.2: State $x[t] = (x_1[t], x_2[t])$: hands-off control (real line) and standard LQR (dotted line)

7 Conclusions

This paper has proposed approaches to constrained hands-off control problem for discrete-time linear systems for three different scenarios. Such a problem has been formulated as minimization of the l_1-norm of the control input that satisfies given performance conditions. It has been shown that this optimization problem is simplified to second-order cone programing. Moreover, it has been illustrated through a numerical example that the proposed approach gives a sparse control input while the system performance is fairly close to the standard finite-horizon LQR performance as desired.

References

[1] C. C. Chan, "The state of the art of electric, hybrid, and fuel cell vehicles," *Proceedings of the IEEE*, vol. 95, no. 4, pp. 704–718, Apr. 2007.

[2] B. Dunham, "Automatic on/off switching gives 10-percent gas saving," *Popular Science*, vol. 205, no. 4, p. 170, 1974.

[3] M. Nagahara, D. E. Quevedo, and D. Nešić, "Maximum hands-off control: a paradigm of control effort minimization," *IEEE Transactions on Automatic Control*, vol. 61, no. 3, pp. 735–747, Mar. 2016.

[4] S. Boyd and L. Vandenberghe, *Convex Optimization*. Cambridge University Press, 2004.

[5] M. Nagahara, J. Østergaard, and D. E. Quevedo, "Discrete-time hands-off control by sparse optimization," *EURASIP Journal on Advances in Signal Processing*, vol. 2016, no. 1, p. 76, Jun. 2016.

[6] M. Fazel, "Matrix rank minimization with applications," Ph.D. dissertation, Stanford University, 2002.

[7] K. Zhou, J. C. Doyle, and K. Glover, *Robust and Optimal Control*. Prentice Hall, 1996.

[8] T. A. Badgwell, "Robust model predictive control of stable linear systems," *International Journal of Control*, vol. 68, no. 4, pp. 797–818, 1997.

[9] A. Bemporad and M. Morari, "Robust model predictive control: A survey," in *Robustness in identification and control*. Springer, 1999, pp. 207–226.

[10] S. Boyd, L. El Ghaoui, E. Feron, and V. Balakrishnan, *Linear matrix inequalities in system and control theory*. SIAM, 1994.

[11] J. Löfberg, "YALMIP : a toolbox for modeling and optimization in matlab," in *Proccedings of the 2004 IEEE International Conference on Robotics and Automation (ICRA)*, Sept. 2004, pp. 284–289.

[12] J. Löfberg, "Automatic robust convex programming," *Optimization methods and software*, vol. 27, no. 1, pp. 115–129, 2012.

[13] J. Löfberg, "Pre- and post-processing sum-of-squares programs in practice," *IEEE Transactions on Automatic Control*, vol. 54, no. 5, pp. 1007–1011, May 2009.

[14] S. Boyd, "Linear quadratic regulator: Discrete-time finite horizon, lecture notes," 2008, https://stanford.edu/class/ee363/lectures/dlqr.pdf.

[15] G. C. Chow *et al.*, *Analysis and Control of Dynamic Economic Systems*. Wiley, 1975.

[16] J. Kiefer, "Optimum experimental designs," *Journal of the Royal Statistical Society. Series B*, vol. 21, no. 2, pp. 272–319, 1959.

[17] D. Henrion, S. Tarbouriech, and D. Arzelier, "LMI approximations for the radius of the intersection of ellipsoids: Survey," *Journal of Optimization Theory and Applications*, vol. 108, no. 1, pp. 1–28, 2001.

[18] B. Ding and X. Ping, "Dynamic output feedback robust model predictive control with guaranteed quadratic boundedness under redefined bounds on the unknown true state for the system with polytopic uncertainty and bounded disturbance," in *Proceedings of the 32nd Chinese Control Conference*, Jul. 2013, pp. 4137–4142.

ISSN (online): 2446-1628
ISBN (online): 978-87-7210-257-3

AALBORG UNIVERSITY PRESS